1 General

Fatigue failure is one of the primary damage modes of offshore structures. The report is on the fatigue strength assessment of the Liuhua FPS, in which fatigue life of the key structural nodes of the platform are given. The fatigue analysis is completed with the fatigue strength direct computing method based on spectral analysis. According to the result of analysis, some conclusions and suggestions are given.

1.1 General Situation of the Platform Structure

The LiuHua Floating Production System (FPS) is a semi-submersible mobile offshore drilling unit. It consists of two lower hulls (pontoons) which are connected by one cross pontoon at each end. From the lower hulls four corner column/sponsons and four intermediate columns rise up to support the rectangular main deck. Transverse trusses and braces are arranged between the four pairs of columns and the main deck transverse girders.

1.1.1 Principal Dimension and Other Parameters

The principal dimensions and parameters of Liuhua FPS are described in Table1.1.

Table 1.1 Principal characteristics of LuiHua FPS

Dimensions		Units/m	Units/ft
Main deck	Length molded	90.221	296
	Breadth molded	73.4568	241
	Height molded	39.624	130
Lower hull	Length molded	89.926	295
	Breadth molded	15.240	50
	height molded	6.401	21
Cross pontoon	Breadth molded	6.401	21
	Height molded	3.658	12
Corner column	Diameter	9.144	30
Intermediate column	Diameter	5.486	18
Operating draft		22.860	75

*Drafts are all from the base line.

Where, the lower hull is spaced 195'apart, center to center. All stability columns are spaced 75' apart in longitudinal direction, which have a constant diameter when extending from the top of lower hull at 21' level to the main deck at 130' level.

1.1.2 **General Situation of the Structure**

The major structure is composed by main deck, derrick, column and sponsons, intermediate columns, chords and lower pontoons. The basic frame is shown in Fig.1.1.

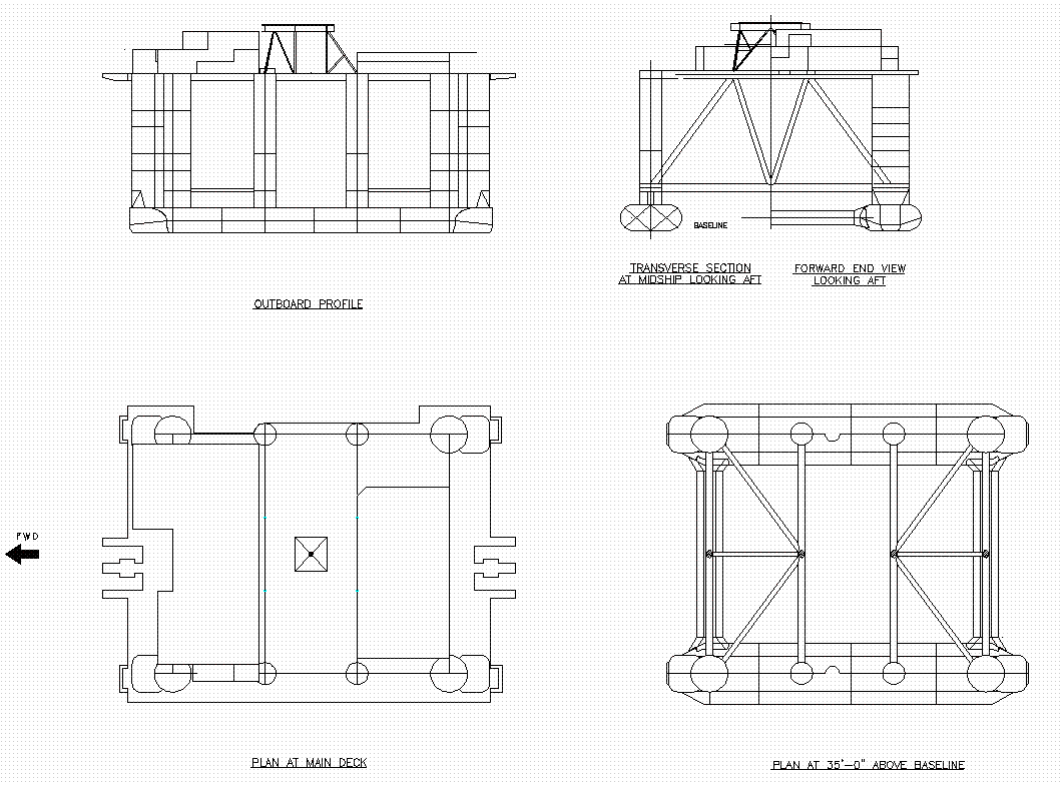

Fig.1-1 basic frame of the calculated FPS

1.2 **Data Source**

The basic data used in the modeling, calculations and analysis come from the following resources:

[1] BH10101-BH10110. LOWER HULL MODIFICATIONS

[2] BH10201-BH10204. STABILITY COLUMN MODIFICATIONS-SPONSONS

[3] BH10301-BH10302. MAIN TRUSS MODIFICATIONS TUBULARS

[4]BH10401-BH10405.MAIN DECK FRAMING PLAN (ELEV. & SECTS. & DETAIL)

[5] BH10501-BH10507. CONSTRUCTION PLAN COLUMN TOPS FOR CHAIN JACKS-DETAILS

[6] BH10601-BH10602. MAIN TRUSS MODIFICATIONS JOINTS

[7] BH10701-BH10707. MAIN & INTERM GIRDER MODS -KEY PLAN & SECT.

[8] BH10801-BH10804. CHAIN FAIRLEAD SUPPORT

[9] BH10901. PORT/AFT 30'-0" COLUMN 111'-9" DECK

[10] BD00101-BD01202. GENERAL ARRANGEMENT

[11] BD01401-BD01402. CAPACITY PLAN

[12] BD01501-BD01504. ALLOWABLE DECK LOAD PLAN

[13] D01601A,B,E. INCLINING EXPERIMENT AGENDA AND PROCEDURE

[14] D01901. DOCKING PLAN

[15] D03101A,D,E,F. CONTRACTOR'S WEIGHT ESTIMATE

[16] COLUMN-D1(30FT) SITE CHECK

[17] 1971 Drawings

[18] FPS Nan Hai Tiao Zhan Specialist Inspection Survey of Column

[19] FPS Nan Hai Tiao Zhan Specialist Inspection Survey of Substructure Beam under Drilling Derrick and Main Deck

[20] Ultrasonic Wall Thickness Survey (July 2006)

[21] ABS, Rules for the Construction and Classification of Mobile Offshore Units

[22] ABS, Rules for the building and Classing Mobile Offshore drilling Units(2006)

[23] ABS, GUIDE FOR THE ASSESSMENT OF OFFSHORE STRUCTURE

2 Calculation Programs

The FEM was modeled by software MSC.Patran. The fatigue loads of the FPS in regular waves calculated with 3-D linear wave load calculation program. The powerful FEM software MSC/NASTRAN is utilized in FEM analysis.

The 3-D linear wave load calculation program was developed by the laboratory and used in numbers of ships' wave load calculation, and the results were much closed to the results calculated by the software SESAM.

2.1 Theory of Wave Loads on Floating Structure

2.1.1 The Coordinate Systems

For describing incident waves, floating structure motions, velocity potential of flow as well as sectional wave loads of the floating structure, 3 coordinate systems are built as follows.

Coordinate system 1: (See Fig. 2.1)

The spacial fixed coordinate system $O-X_1Y_1Z_1$, the origin is located on the undisturbed water surface;

Coordinate system 2: (See Fig. 2.1)

The translatory coordinate system $o-xyz$ fixed on the mean position of the floating structure, the xoy plane is located on the undisturbed water surface, with positive z vertically upwards through the center of gravity of the floating structure in mean position. On the assumption that the floating structure advances along OX-axis, and the waves propagate at the inverse direction of OX, the incident wave angle is β (for head waves, $\beta = 0^\circ$).

Coordinate system 3: (See Fig. 2.1)

The coordinate system $G-x_by_bz_b$ fixed n the floating structure, the origin is G (the center of gravity of the floating structure). The vertical coordinate of the point G is z_G in Coordinate system 2.

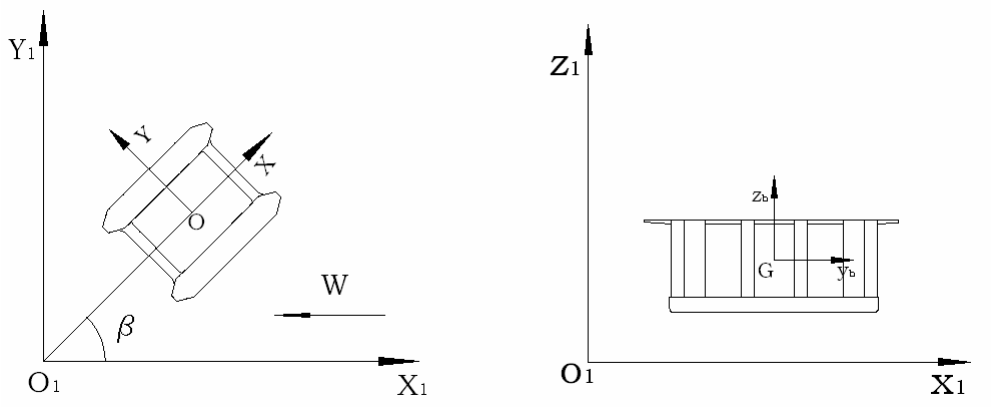

Figure 2.1 Coordinate system

2.1.2 The 3-D Hydrodynamic Forces on Floating Structures

According to the linear potential flow theory, the total velocity potential $\Phi(x,y,z,t)$ of the flow field corresponding to the steady-state solution of the floating structure motions in regular waves can be expressed as follows in the coordinate system $o-xyz$,

$$\Phi(x,y,z,t)=\left[-Ux+\Phi_s(x,y,z)\right]+\mathrm{Re}\left\{\phi_T(x,y,z)e^{i\omega t}\right\} \tag{2.1}$$

where U is the forward transit speed of the floating structure, $\left[-Ux+\Phi_s(x,y,z)\right]$ describes the steady flow including the steady wave pattern created around the floating structure, $\mathrm{Re}\left[\phi_T(x,y,z)e^{i\omega t}\right]$ is the unsteady potential, the spacial part of which can be decomposed into incident wave potential, radiation potential and diffraction potential, i.e.,

$$\phi_T(x,y,z)=\phi_I(x,y,z)+\phi_D(x,y,z)+\phi_R(x,y,z) \tag{2.2}$$

and,

$$\phi_I(x,y,z)=\zeta_a\phi_0(x,y,z) \tag{2.3}$$

$$\phi_R(x,y,z)=\sum_{j=1}^{6}\left[i\omega\eta_j\cdot\phi_j(x,y,z)\right] \tag{2.4}$$

$$\phi_D(x,y,z)=\zeta_a\phi_7(x,y,z) \tag{2.5}$$

Where, ζ_a is the amplitude of the regular wave, ϕ_0, ϕ_j and ϕ_7 are respectively unit incident wave potential, unit radiation potential and unit diffraction potential. The unit

incident wave potential is presented as follows:

$$\phi_0(x,y,z)=\frac{ig}{\omega_0}\cdot\frac{ch[k_0(z+h)]}{ch(k_0h)}\cdot e^{ik_0(x\cos\beta-y\sin\beta)} \qquad \text{For finite water depth} \qquad (2.6)$$

$$\phi_0(x,y,z)=\frac{ig}{\omega_0}\cdot e^{k_0z}\cdot e^{ik_0(x\cos\beta-y\sin\beta)} \qquad \text{For infinite water depth} \qquad (2.7)$$

Where, k_0 is the wave number.

According to the wetted body surface condition, ϕ_j can be decomposed into the sum of ϕ_j^0 and ϕ_j^u, i.e.,

$$\phi_j=\phi_j^0+\frac{U}{i\omega}\phi_j^u \qquad (2.8)$$

The unit diffraction potential ϕ_7 and the radiation potential ϕ_j^0, ϕ_j^u satisfy the boundary conditions for floating structure with a forward transit speed. It is very complicated to solve the problem of complete solution with a forward speed, and some hypotheses are applied for simplifying the calculation.

If neglecting the steady perturbation potential Φ_s, we have

$$\begin{cases}\phi_j^u=0 \quad (j=1\sim 4)\\ \phi_5^u=\phi_3^0\\ \phi_6^u=-\phi_2^0\end{cases} \qquad (2.9)$$

On the assumption that the wave frequency is not low and the forward speed is not high, we have

$$\omega >> U\frac{\partial}{\partial x} \qquad (2.10)$$

And,

$$\left(i\omega-U\frac{\partial}{\partial x}\right)^2\approx-\omega^2 \qquad (2.11)$$

The unit radiation potential ϕ_j^0 and unit diffraction potential ϕ_7^0 satisfy the following equations:

for conditions in the fluid domain [*L*],

$$\nabla^2\phi_j^0=0 \quad (j=1,2,\cdots,7) \qquad (2.12)$$

For linearized free surface condition [*F*],

$$g\frac{\partial \phi_j^0}{\partial z} - \omega^2 \phi_j^0 = 0 \quad (z = 0,\ j = 1, 2, \cdots, 7) \tag{2.13}$$

For body surface condition [S],

$$\begin{cases} \dfrac{\partial}{\partial n}\phi_7^0 = -\dfrac{\partial}{\partial n}\phi_0 \\ \dfrac{\partial}{\partial n}\phi_j^0 = n_j \quad (j = 1, 2, \cdots, 6) \end{cases} \tag{2.14}$$

For bottom condition [B],

$$\frac{\partial}{\partial z}\phi_j^0 = 0 \quad (z = -h,\ j = 1,2,\ \cdots,7) \qquad \text{For definite water depth} \tag{2.15}$$

$$\nabla\phi_j \to 0 \quad (z \to -\infty,\ j = 1,2,\ \cdots,7) \qquad \text{For indefinite water depth} \tag{2.16}$$

For radiation condition [R]:

$$\lim_{R\to\infty}\sqrt{R}\left(\frac{\partial \phi_j^0}{\partial R} - ik_0\phi_j^0\right) = 0 \quad (j = 1, 2, \cdots, 7) \tag{2.17}$$

It is shown that the above boundary conditions are completely in the same form except that the natural circular frequency ω_0 of wave is substituted by the circular frequency of encounter ω for floating structures of zero forward speed.

The solution for ϕ_j^0 can be obtained by distributive source technique. The velocity potential ϕ_j^0 is expressed in the form of the distributed source on the body surface, as

$$\phi_j^0(p) = \iint_S \sigma^{(j)}(q)G(p,q)dS_q \tag{2.18}$$

Where, $\sigma^{(j)}(q)$ is the strength of source, $G(p,q)$ is Green's Function satisfying all the boundary conditions but that of body surface.

According to the body surface condition of the velocity potential ϕ_j^0, the strength of source $\sigma^{(j)}(q)$ satisfies the following integral equation,

$$2\pi\sigma^{(j)}(p) + \iint_S \sigma^{(j)}(q)\frac{\partial}{\partial n_p}G(p,q)dS_q = \begin{cases} -\dfrac{\partial}{\partial n^{(p)}}\phi_0 \\ n_j^{(p)} \end{cases} \tag{2.19}$$

(p is on body surface)

Corresponding to the incident wave potential (for infinite or finite water depth), the tree-dimensional Green's Function in frequency domain for zero forward speed is applied. The above integral equation can be transformed into linear algebra equations by using the panel element method, and the equations can be solved. Then the diffraction potential and radiation potential can be obtained.

Because the water depth where LiuHua_FPS operates is far beyond the wavelength, the infinite water depth is adopted in this computation. When the platform is under operational or survival conditions, the forward speed U is taken as zero.

2.1.3 The Equations of Floating Structure Motions

According to the dynamics of rigid body, the equations of the floating structure motions with the center of gravity G being the center of moment can be expressed as,

$$[M]\cdot\{\ddot{\eta}(t)\} = \{F(t)\} = \{F\}\cdot e^{i\omega t} \tag{2.20}$$

where $[M]$ is the generalized mass matrix of the floating structure, $\{F(t)\}$ is the vector of fluid loads on the floating structure, which exclude the still water buoyant force in balance with the gravity of the floating structure.

The fluid loads acting on the floating structure can be divided into the hydrostatic restoring loads $\{F^S(t)\}$ induced by the displacement of the floating structure from the mean position, the hydrodynamic loads $\{F^D(t)\}$ depending on the waves and floating structure motions, namely

$$\{F(t)\} = \{F^S(t)\} + \{F^D(t)\} \tag{2.21}$$

The hydrostatic restoring loads can be obtained by static of the floating structure,

$$\{F^S(t)\} = -[C]\{\eta(t)\} \tag{2.22}$$

Where, $[C]$ is the matrix of hydrostatic restoring force coefficients.

The hydrodynamic loads can be obtained by integrating the hydrodynamic pressures on the wet surface of the floating structure. According to the division of the velocity potential of flow, the hydrodynamic loads can be decomposed into incident wave force, diffraction wave force and radiation force, i.e.,

$$\{F^D(t)\} = \{F_I(t)\} + \{F_D(t)\} + \{F_R(t)\} \tag{2.23}$$

The incident wave force and diffraction wave force can be combined as the so-called wave excitation loads,

$$\{f(t)\} = \{F_I(t)\} + \{F_D(t)\} \tag{2.24}$$

The radiation force can be expressed as,

$$\{F_R(t)\} = -[A]\{\ddot{\eta}(t)\} - [B]\{\dot{\eta}(t)\} \tag{2.25}$$

Where, $[A]$ and $[B]$ are the matrix of three-dimensional hydrodynamic coefficients.

Eq.(2.20) representing the equations of floating structure motions in regular waves can be written as, by taken into consideration of above forces and moments,

$$([M]+[A])\cdot\{\ddot{\eta}(t)\} + [B]\{\dot{\eta}(t)\} + [C]\{\eta(t)\} = \{f(t)\} = \{f\}e^{i\omega t} \tag{2.26}$$

2.1.4 The Fluid Dynamic Pressure and Sectional Loads on The Floating Structures

Once the solution of velocity potential ϕ_j $(j = 1, 2, \cdots, 7)$ and the steady-state solution η_j $(j = 1, 2, \cdots, 6)$ of the floating structure motion responses in regular waves have been obtained, the radiation potential ϕ_R and the diffraction potential ϕ_D can be determined by Eq.(3) and Eq.(4). By including the contribution of the hydrostatic restoring force, the total fluid dynamic pressure can be obtained by linearized Bernoulli's Equation,

$$\left.\begin{aligned} P(x,y,z,t) &= \mathrm{Re}\left[p(x,y,z)e^{i\omega t}\right] \\ p(x,y,z) &= p_S(x,y,z) - \rho\cdot i\omega\cdot[\phi_I(x,y,z) \\ &\qquad + \phi_D(x,y,z) + \phi_R(x,y,z)] \end{aligned}\right\} \tag{2.27}$$

Where, $p_S(x,y,z) = -\rho g(\eta_3 + y\eta_4 - x\eta_5)$.

Thus, the fluid dynamic pressure on the controlling point of each panel element can be obtained, and the fluid dynamic pressure distribution on the floating structure hull can be given.

When the floating structure motions and the fluid dynamic pressure loads are given,

the wave-induced forces and moments in the sections of floating structure hull can be calculated by using D'Alembert's Principle, which include the vertical and horizontal shear forces and moments as well as torsional moments.

2.1.5 The Mesh Grid of LiuHua_FPS

The number of wet surface grid of LiuHua_FPS for hydrodynamic computation is 1348 as shown in Fig.4.2 the braces are neglected because their dimensions are much smaller compared with the critical wave length.

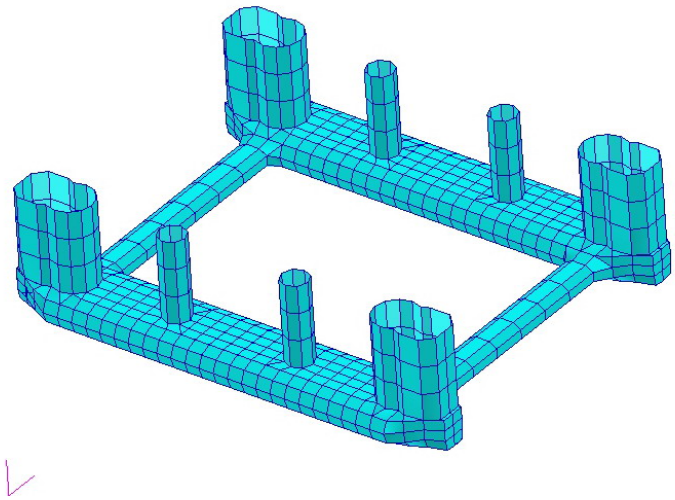

Fig.2.2 the Mesh Grid of LiuHua_FPS

3 Structural Simulation

3.1 Materials

All the deck plating are made of ABS grade A steel, and the rest structures of the unit such as girder plates, stiffeners column shell etc. are made of ABS AH32 steel, the properties of which are as follows:

Yield stress (σ_Y) =235MPa; （ABS grade A）

Yield stress (σ_Y) =315MPa; （ABS AH32）

Young's modulus(E) = 2.1×10^5 MPa,

Poisson rate (ν) =0.3

Density (ρ) =7.8×10^3Kg/m^3

3.2 The Global FE Model

The space plate-beam combined structure is adopted in the global structural FE model.

Where, flat plate components such as outer shell, bulkheads, deck/flat structures and the web plate of main girders, etc. are simulated with 4-node and 3-node shell element. The platform framework including longitudinal girders, stiffeners, transverse frames and the faceplate of transverse frames, etc. are simulated with 2-node beam element. All the scaling and thickness are derived from the plans and the thickness report(The plates and stiffeners have been eroded since last examination and service about 10 years ago, so the less one was adopted in modeling between the design thickness and the thickness from report). A total of 151086 nodes, 260838elements and 905756 free degrees are used in the global FE model of the unit.

The origin of the global coordinate system locates in the symmetrical center of the two pontoon bottoms. The X-axis is located along the longitudinal direction of the platform and aft body is its positive direction; while the Y-axis is located along the direction from the port to the starboard of the platform; the Z-axis is located along the direction of vertical upwards. The overall FE model and various detailed parts of the platform are shown in Figures 3.1~3.11

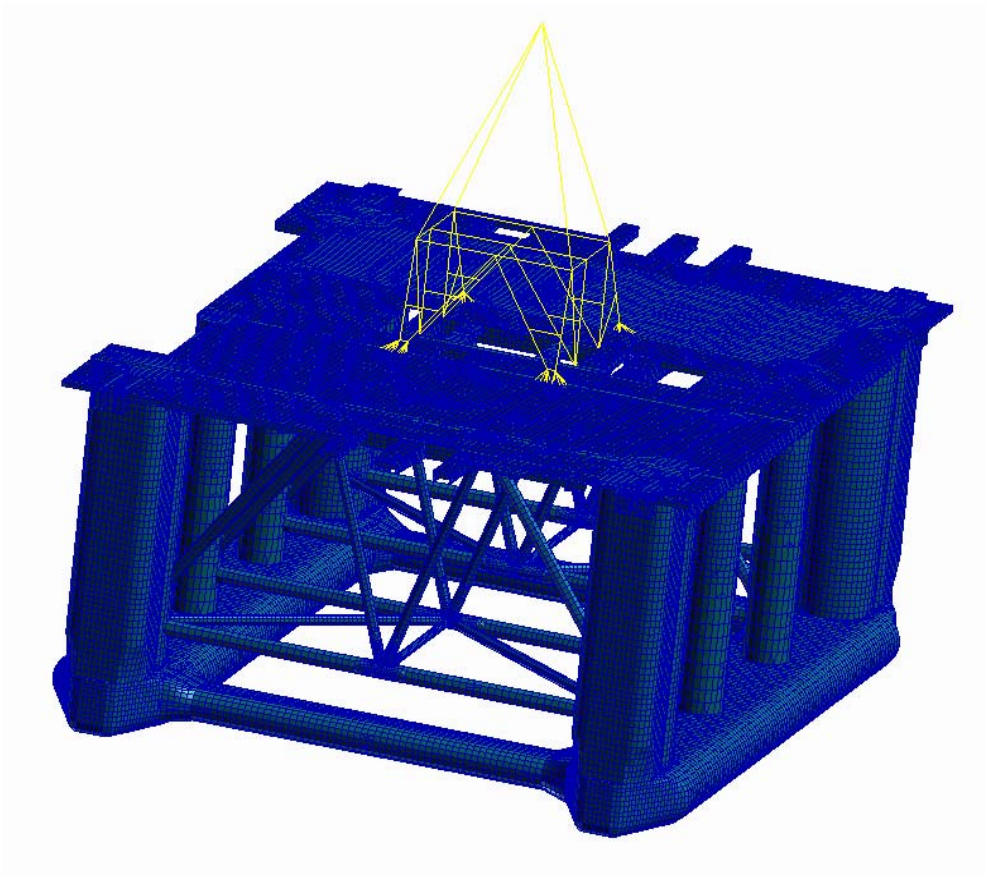

Figure 3.1 Global finite element model of the platform

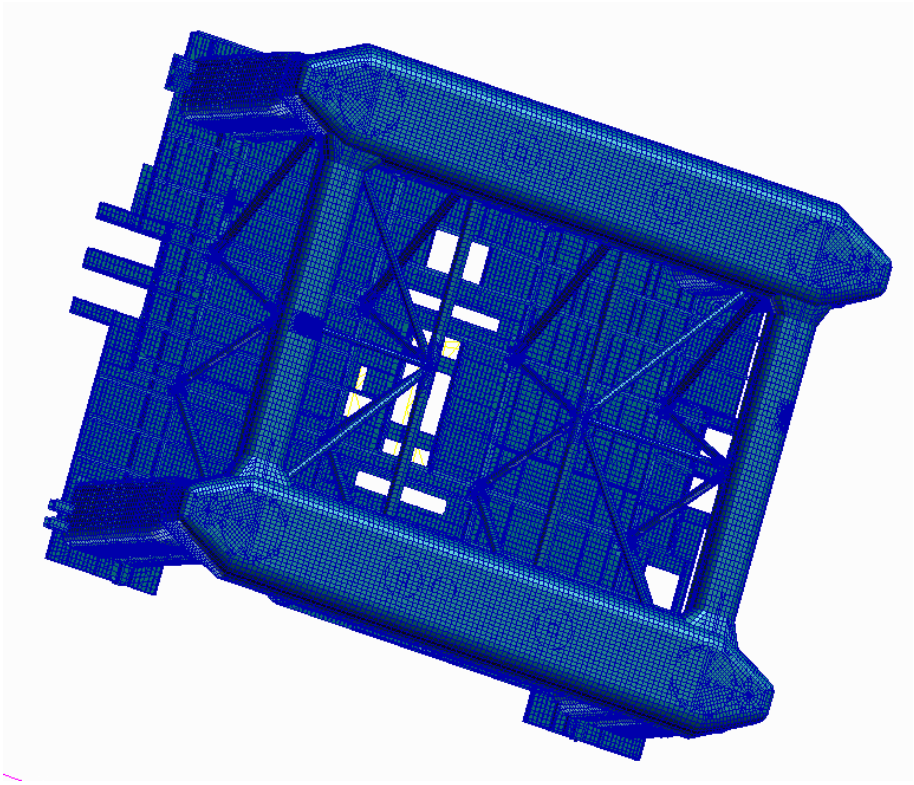

Figure 3.2 Global finite element model of the platform (from bottom)

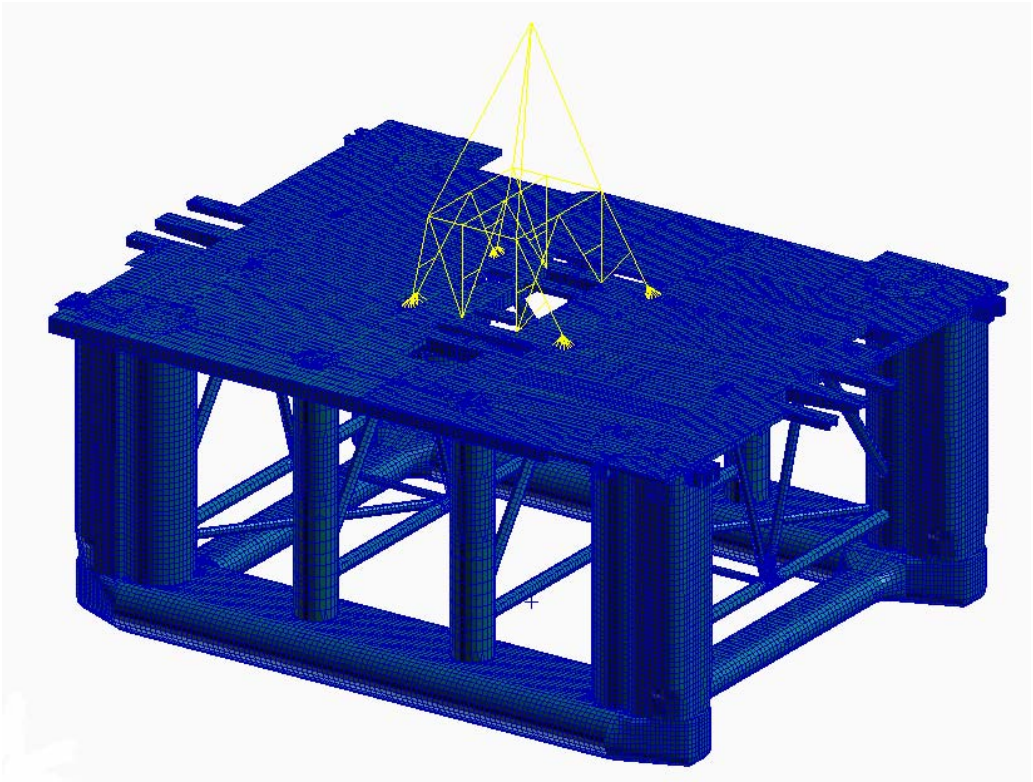

Figure 3.3 Global finite element model of the platform

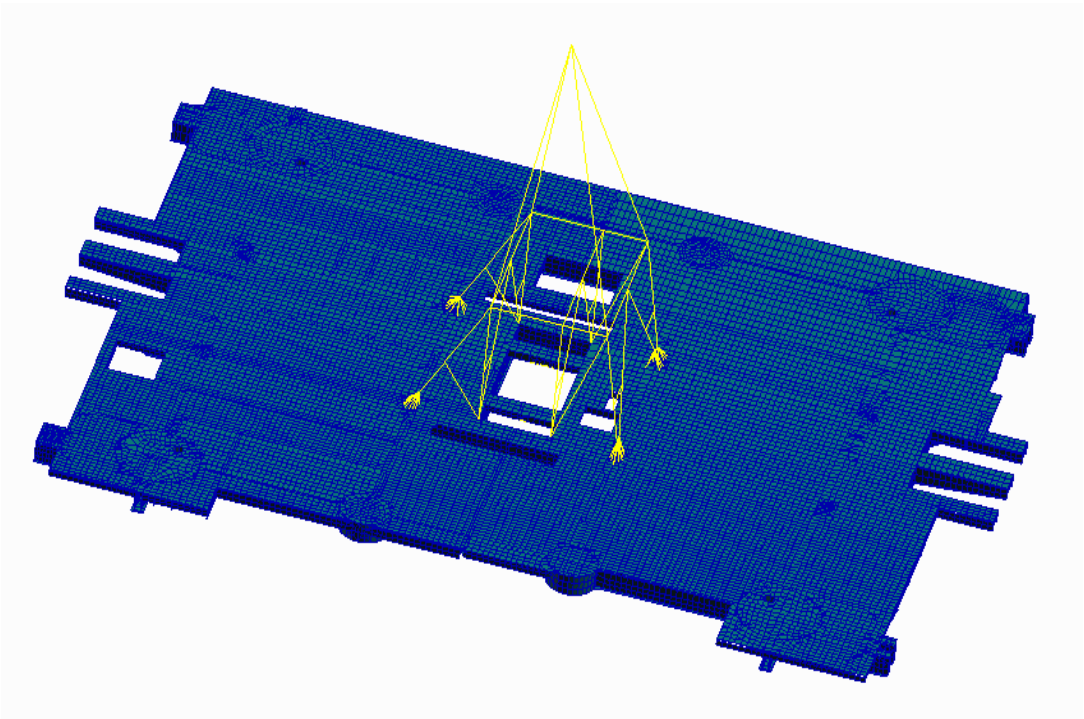

Figure 3.4 Global finite element Model of the main deck and derrick

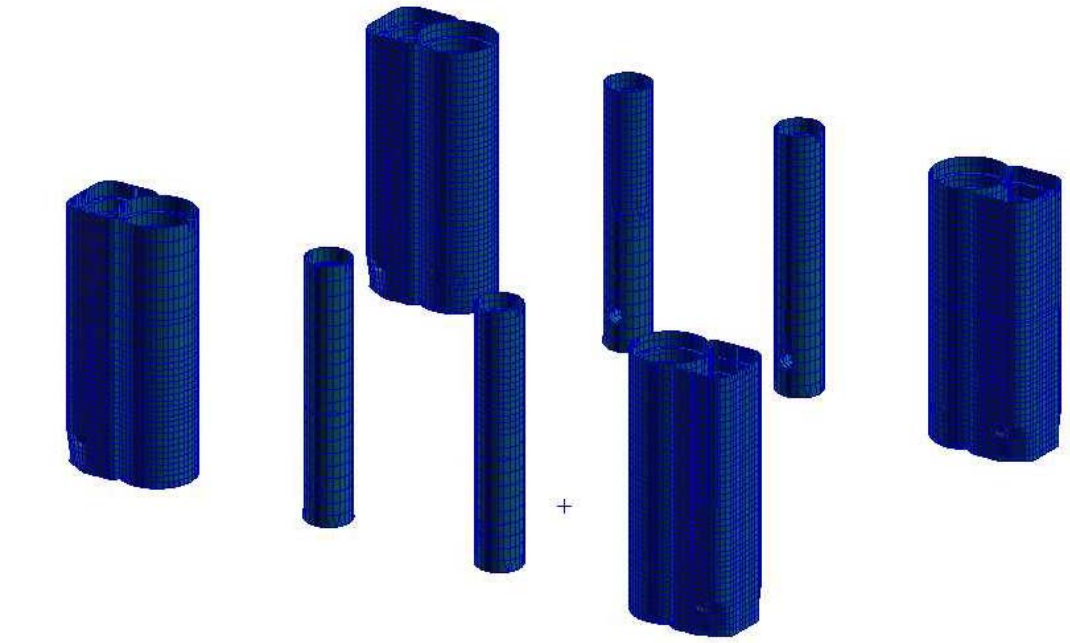

Figure 3.5 finite element model of the stability columns and sponsons

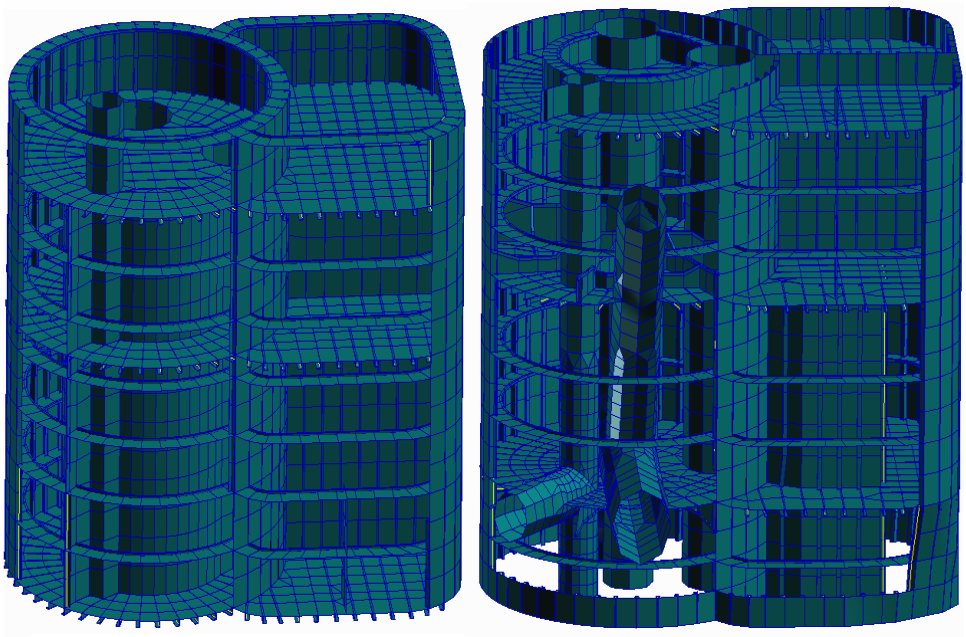

Figure 3.6 finite element model of the inner structure of the column and sponson

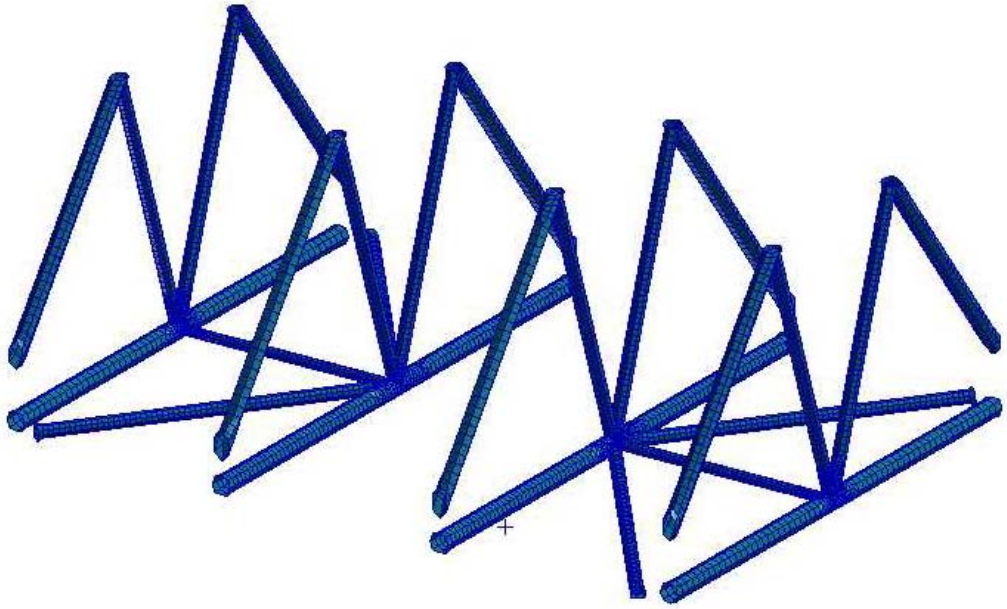

Figure 3.7 finite element model of the brace

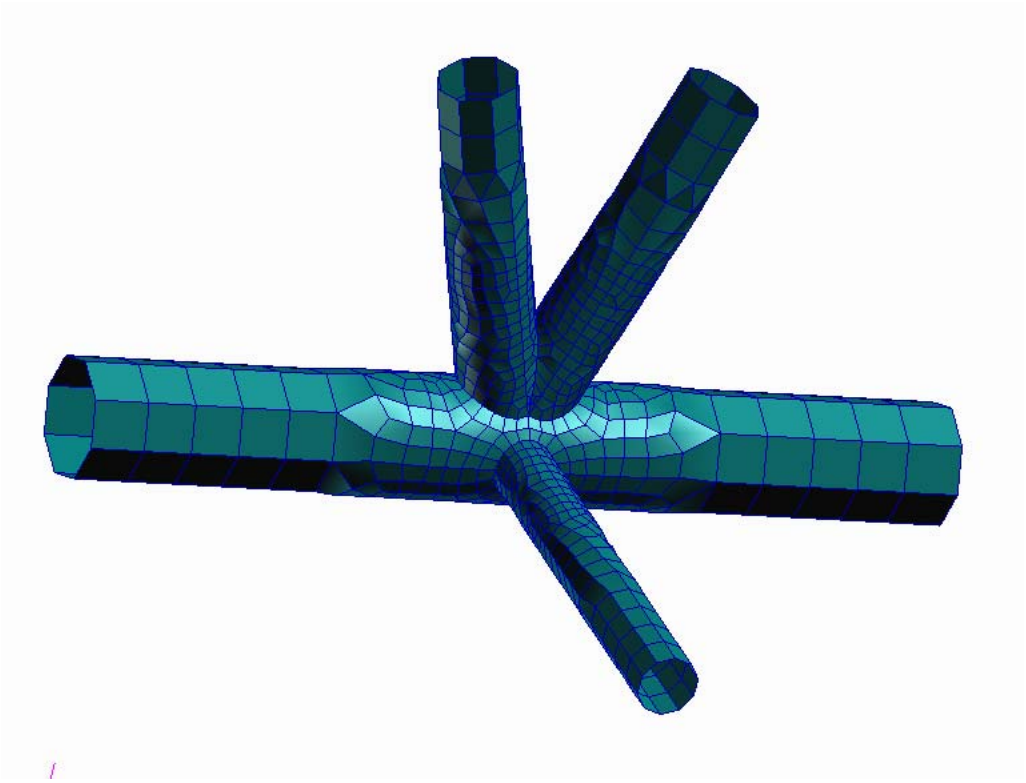

Figure 3.8 local model of the joint

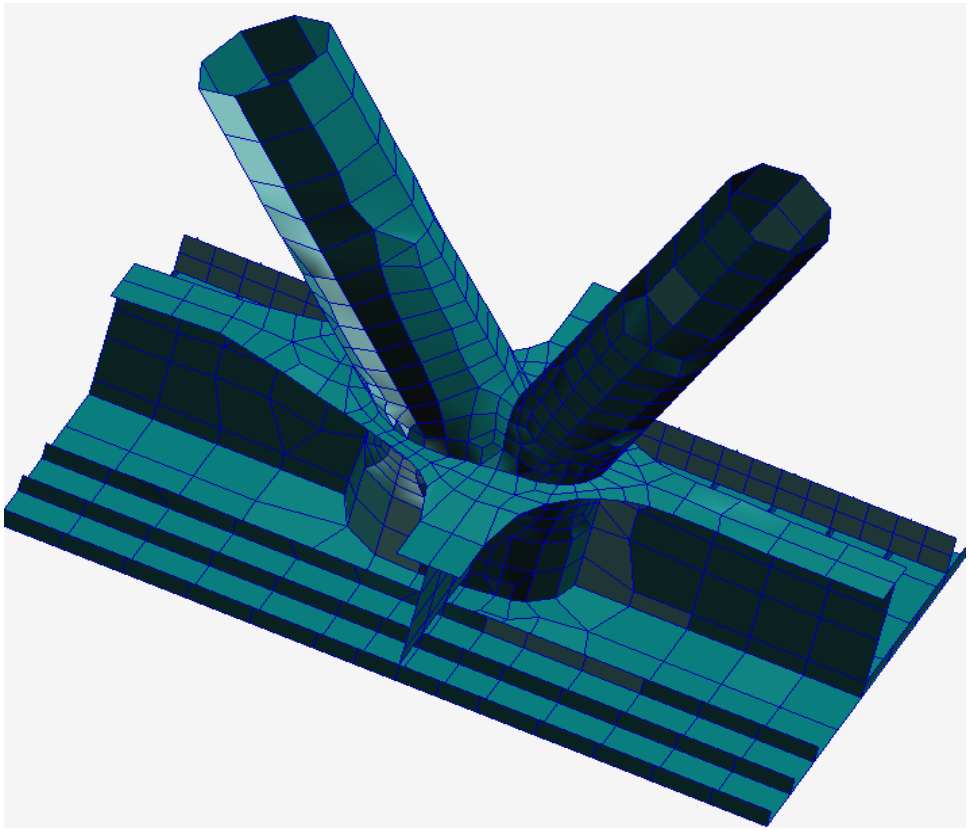

Figure 3.9 local model of the K_joint in main deck

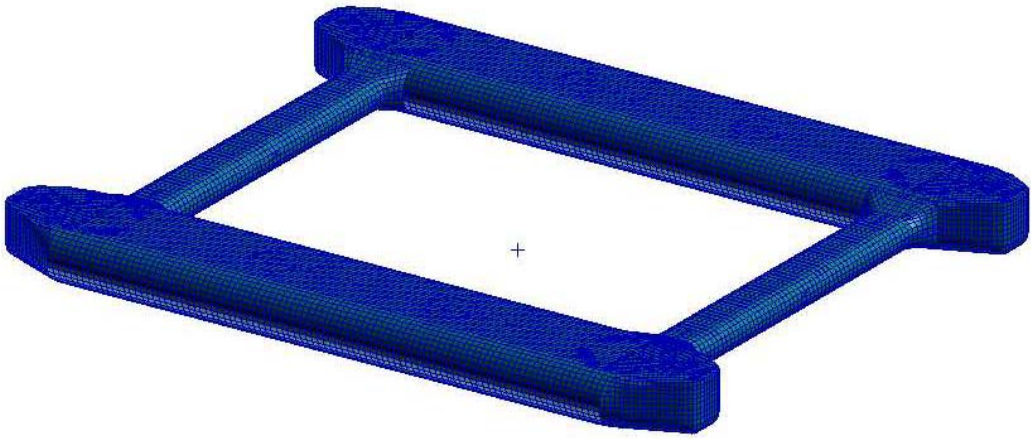

Figure 3.10 finite element model of pontoon

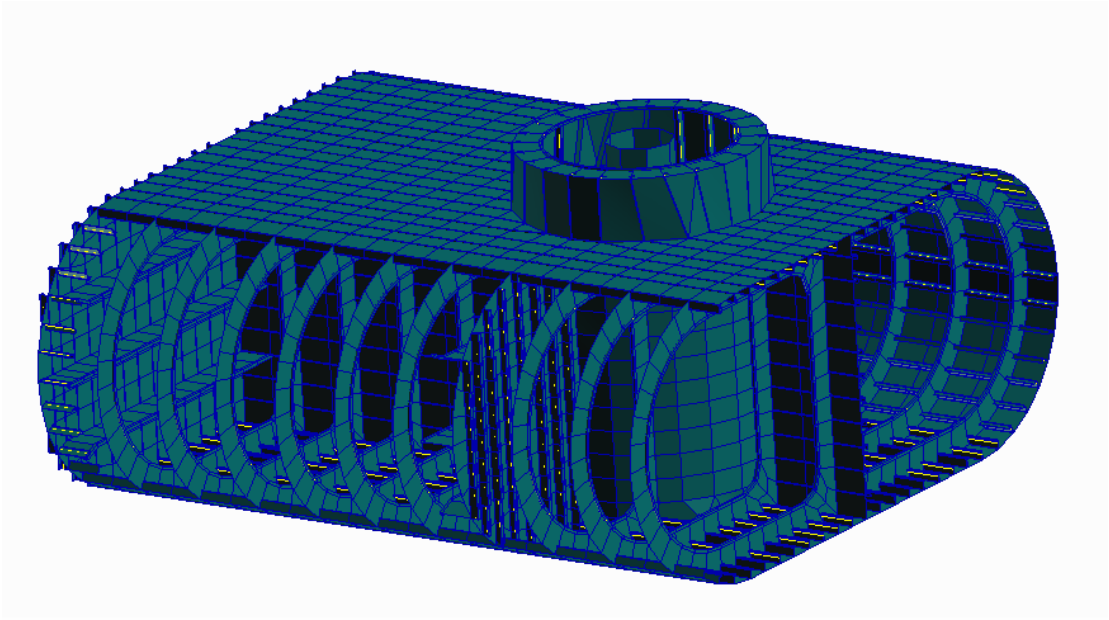

Figure 3.11 finite element model of the inner structure of pontoon

3.3 The Adjust of Weight Distribution and Boundary Condition

In order to simulate the real statement of the structures, the weight of superstructures and equipments needs to be taken into account. The one-node elements with mass are adopted here.

After the balance of gravity of buoyancy was adjusted, the inertial relief method (a function of MSC.NASTRAN) is adopted to deal with the boundary condition. In this function, the program computes the acceleration of every node. The law of inertia is adopted in order to form an equation. By this way the displacement of every node can be computed.

Table 3.1 Weight of LiuHua_FPS（Operating condition）

N	DETAILS	WEIGHT (kips)	x (ft)	y (ft)	z (ft)
10～29	Lightship	34591	-7.51	-0.43	88.35
30	Bulk Storage	1213	78.75	63.75	126.75
31	Liquid Mud	924	75.00	0.00	126.75
32	Piperack	949	75.00	0.00	126.75
33	Drilling Equipment	264	0.00	63.75	126.75
34	Workover	50	-37.50	59.25	126.75
35	Subsea	221	25.25	30.00	126.75
36	Jumper	268	45.16	50.82	126.75
37	ROV	234	7.69	2.73	126.75
38	ESP	95	0.00	0.00	126.75
39	Wells Functional	1915	-0.32	-0.25	151.66
40	Mooring System	20	-150.00	0.00	126.75
41	Main Deck Tanks	696	-26.67	-49.90	126.75
42	Msc.-Deck	250	-75.00	30.00	126.75
43	Column Consumable	450	-112.50	97.50	126.75
44	Marine Growth	1158	0.00	0.00	48.00
45	Pontoon Consumable	9364	11.10	12.14	10.50
46	Ballast	5867	-1.47	-21.52	10.50
47A	Mooring Tension	2750	00.00	00.00	75.00
47B	Mooring Chain	996	00.00	00.00	55.00
	TOTAL MASS	62276	00.00	00.00	72.85

4 Fatigue loads

4.1 Environmental data

The spectral-based fatigue assessment is conducted according to the ABS rules. The wave states were derived from data measured at the Liuhua site. The occurrence probability of each wave state which is represented by the Hs(m) and Tp(s), as described in Table 4.1～4.8.

Table 4.1 Occurrence probability of Wave States (From North）

Hs/Tp	4	6	8	10	12	14
0.5	0	0.1	0.1	0.05	0.05	0
1.5	0	0.2	0.2	0.1	0.1	0
3	0	0	0.7	0.5	0.3	0
5	0	0	0	0.5	0.3	0
7	0	0	0	0	0	0
9	0	0	0	0	0	0

Table 4.2 Occurrence probability of Wave States (From Northeast）

Hs/Tp	4	6	8	10	12	14
0.5	0	2	1	0.4	0	0.1
1.5	0	7	4	2	0	0.6
3	0	0	15	10	6	3.7
5	0	0	2	1	0.5	0.3
7	0	0	0	0.4	0.2	0
9	0	0	0	0	0.05	0.05

Table 4.3 Occurrence probability of Wave States (From East)

Hs/Tp	4	6	8	10	12	14
0.5	0	2.5	3	0	0	0.4
1.5	0	3	2	1.5	0	1.2
3	0	0	2	1.5	1	0.3
5	0	0	0.05	0.05	0.05	0.05
7	0	0	0	0.1	0.1	0
9	0	0	0	0	0	0

Table4.4 Occurrence probability of Wave States (From Southeast)

Hs/Tp	4	6	8	10	12	14
0.5	0	1	0.6	0.4	0.2	0
1.5	0	0.2	0.2	0.1	0.1	0
3	0	0.3	0.3	0.2	0.1	0
5	0	0	0	0	0	0
7	0	0	0	0	0	0
9	0	0	0	0	0	0

Table4.5 Occurrence probability of Wave States (From South)

Hs/Tp	4	6	8	10	12	14
0.5	0	1	0.5	0.5	0.4	0
1.5	0	2	1	0.4	0.2	0
3	0	0.8	0.4	0.3	0.2	0
5	0	0	0.05	0.1	0.05	0
7	0	0	0	0	0	0
9	0	0	0	0	0	0

Table4.6 Occurrence probability of Wave States (From Southwest)

Hs/Tp	4	6	8	10	12	14
0.5	0	2	0.7	0.4	0.2	0
1.5	0	2.5	1	0.6	0.4	0
3	0	0.2	0.2	0.1	0.1	0
5	0	0	0	0	0	0
7	0	0	0	0	0	0
9	0	0	0	0	0	0

Table4.7 Occurrence probability of Wave States (From West)

Hs/Tp	4	6	8	10	12	14
0.5	0.4	0.3	0.2	0.1	0	0
1.5	0.1	0.1	0.05	0.05	0	0
3	0	0	0	0	0	0
5	0	0	0	0	0	0
7	0	0	0	0	0	0
9	0	0	0	0	0	0

Table4.8 Occurrence probability of Wave States (From Northwest)

Hs/Tp	4	6	8	10	12	14
0.5	0.05	0.05	0.1	0	0	0
1.5	0.05	0.05	0.05	0.05	0	0
3	0	0	0	0	0	0
5	0	0	0	0	0	0
7	0	0	0	0	0	0
9	0	0	0	0	0	0

4.2 The Parameters for the Calculation of Fatigue Loads

4.2.1 Wave Directions

Eight wave directions are chosen when computing the fatigue loads. Fig 3.1 shows the position of the platform and wave directions. The occurrence of each wave direction is given in table 4.9.

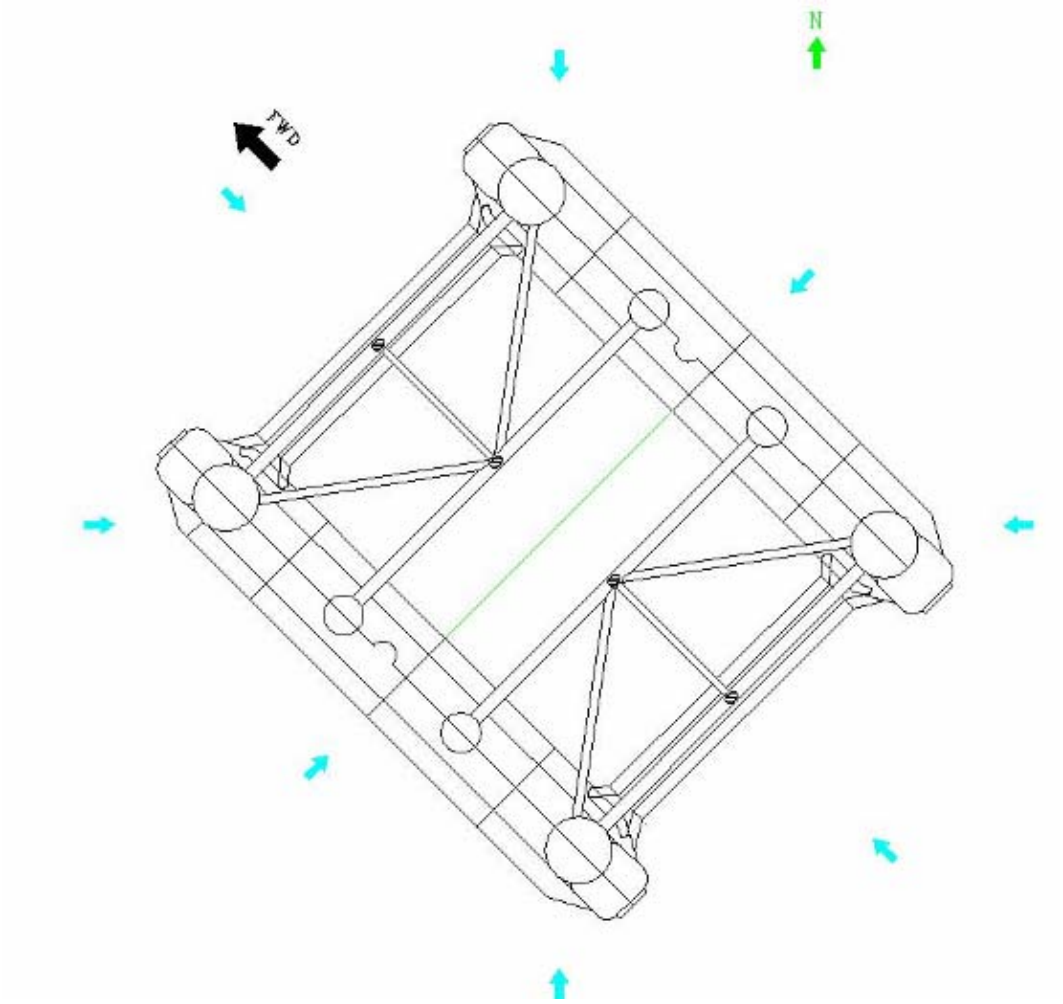

Fig.4.1 The selection of wave directions

Table 4.9 Environmental Data (%)

Direction	N	NE	E	SE	S	SW	W	NW
Angle	-45	-90	-135	180	135	90	45	0
Occurr.	3.2	56.3	18.8	3.7	7.9	8.4	1.3	0.4

4.2.2 The division of the wave frequency

The character of the regular wave can be described by some parameters. The parameters and their relation are given as follows,

$$k = \frac{\omega^2}{g} = \frac{2\pi}{\lambda} \tag{4.1}$$

$$\omega^2 = \frac{2\pi g}{\lambda} \tag{4.2}$$

Where， k —Wave number；

λ —Wave length；

ω —Circular frequency of the wave；

g —Acceleration of the gravity（=9.81m/s^2）。

Then, according to the range of the obtained wave frequency, fifteen frequencies for the calculation of the fatigue loads are taken from 0.20 to 1.8 with unequal spacing. According to the above-mentioned principle, the basic parameters for the calculation of the fatigue loads can be determined, as shown in table 4.10

Table 4.10 Basic parameters for the calculation of the fatigue loads

Items	Unit	Data
Wave circular frequency ω （$n_w = 15$）	Rad/S	0.20， 0.40，0.5， 0.60， 0.70，0.80，0.90，1.00，1.10，1.20，1.30 1.40，1.60，1.80, 2.0

4.3 The calculation of the fatigue loads

The fatigue loads of the FPS in regular waves can be computed with the 3-D linear wave load calculation program. The hydrodynamic pressure on the wet hull is turned into pressure field and added on the finite element model.

5 Selections of the Joints for Fatigue Assessment

5.1 Selection of the Joint Structures for Fatigue Assessment

According to the ABS rules, GUIDE FOR THE FATIGUE ASSESSMENT OF OFFSHORE STRUCTURES, 1791 critical joints were selected in the global spectrum fatigue analysis using coarse mesh FE model. It includes all kinds of fatigable joints such as the connection between stiffeners and main girders, deck and columns, pontoons and columns, little stiffeners and strings in the pontoon and columns etc. nominal stress method was adopted in dealing with the fatigue assessment. After transforming the fatigue damage into fatigue life, the joints whose fatigue life was less than 300 years were selected to be meshed fine in order to calculate their fatigue life exactly and the hot spot stress method was used in calculation. The location and the number of the joints were list following（the whole joints were list in **Appendix A**）

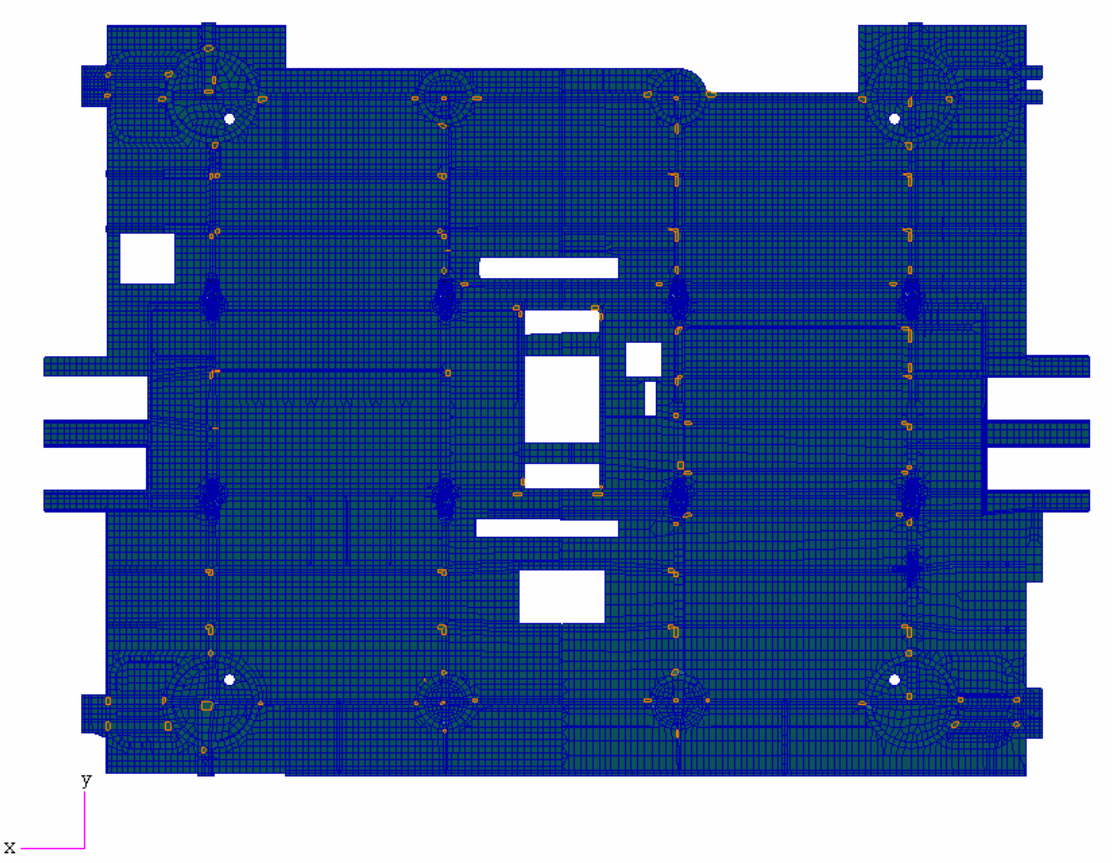

Figure 5.1 the numbers of connection between girders

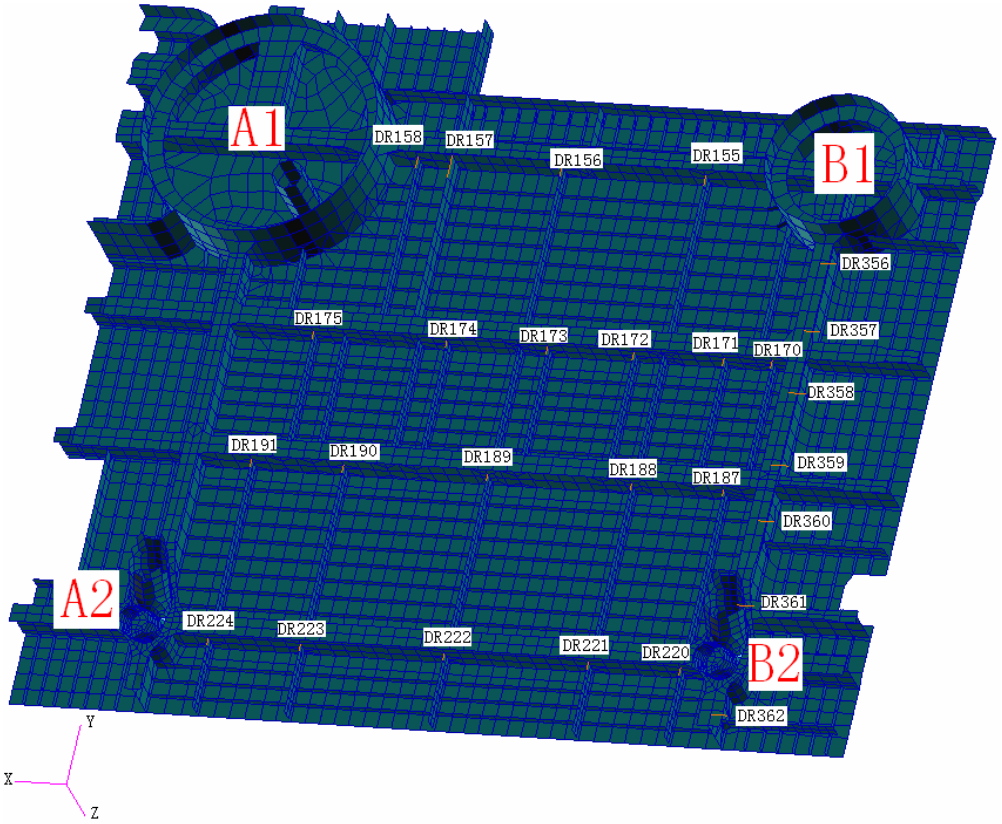

Figure 5.2 the serial number of calculated joints on main deck (partial)

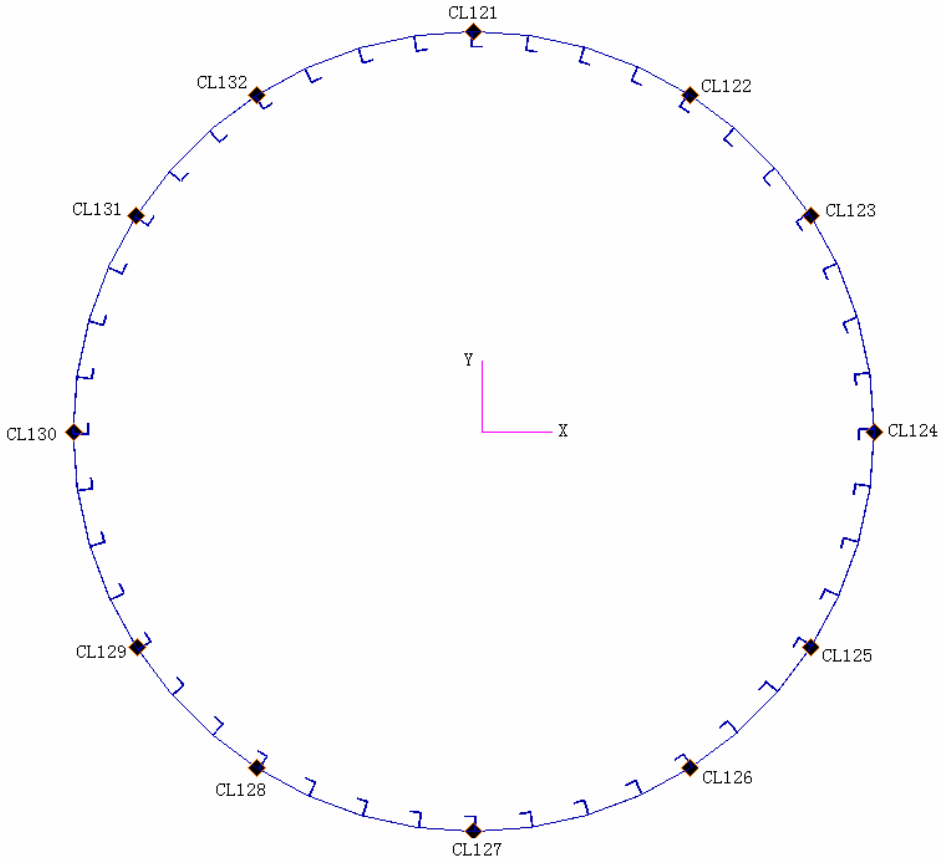

Figure 5.3 the serial number of calculated joints in A4 column (65’ ft)

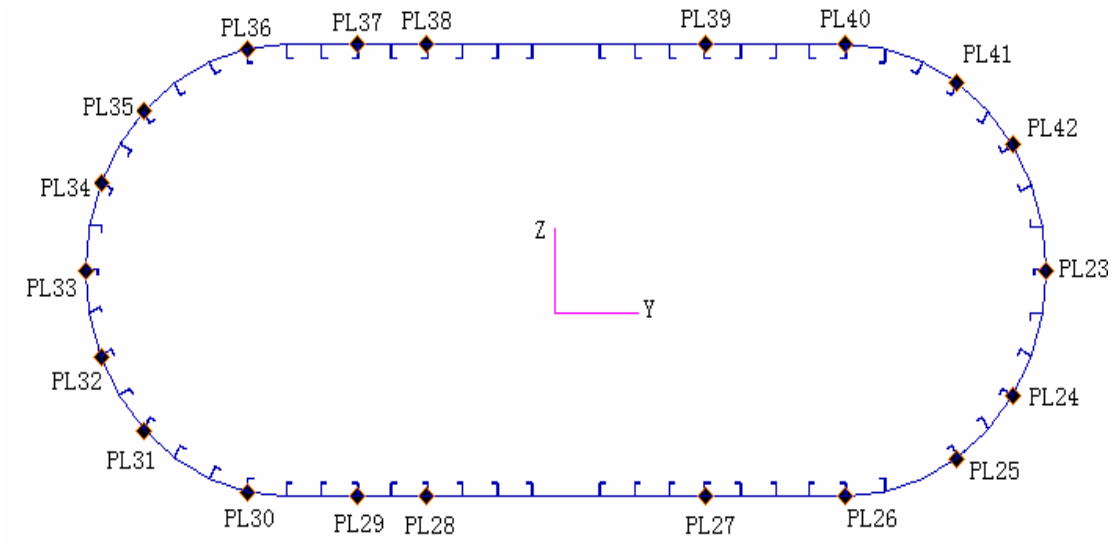

Figure 5.4 the serial number of calculated joints in pontoon (24#)

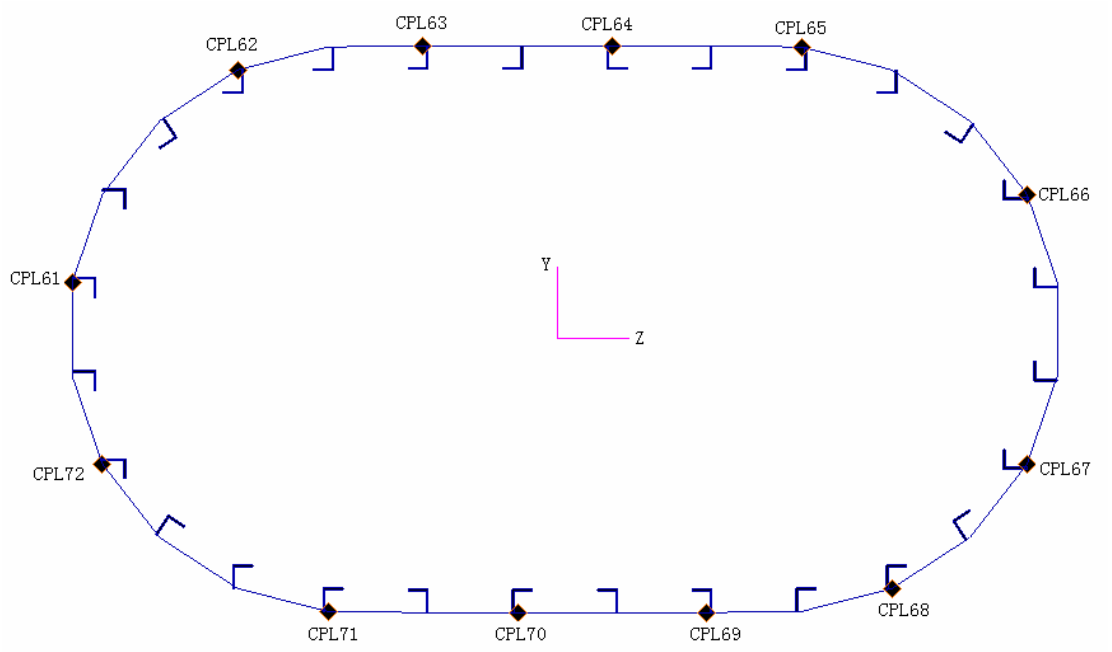

Figure 5.5 the serial number of calculated joints in cross pontoon

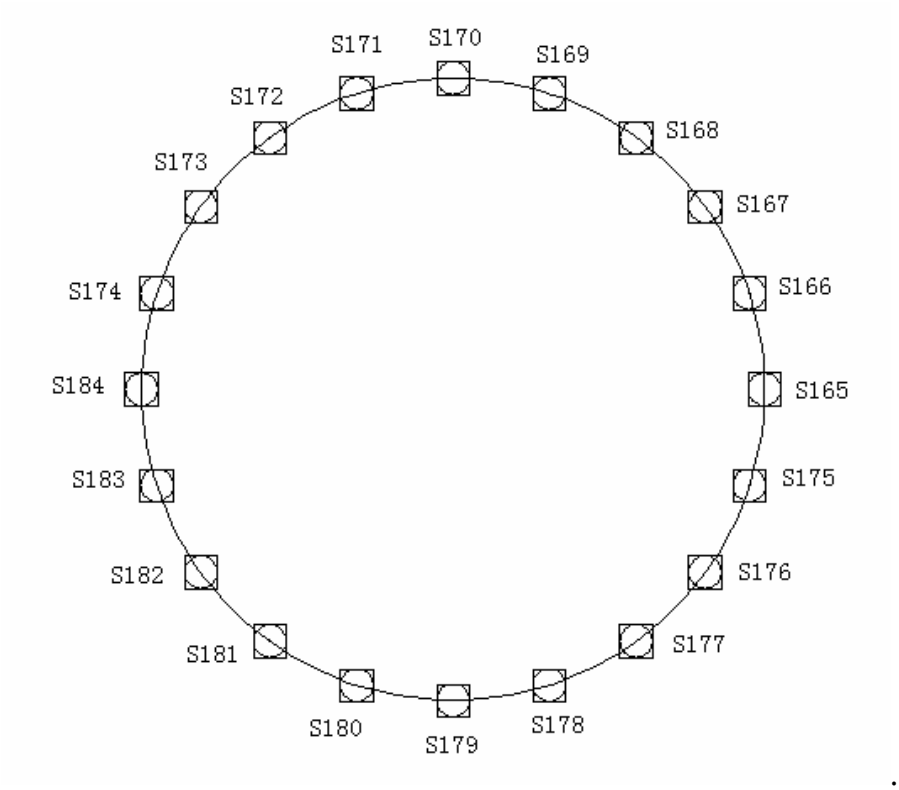

Figure 5.6 the serial number of calculated joints for joint

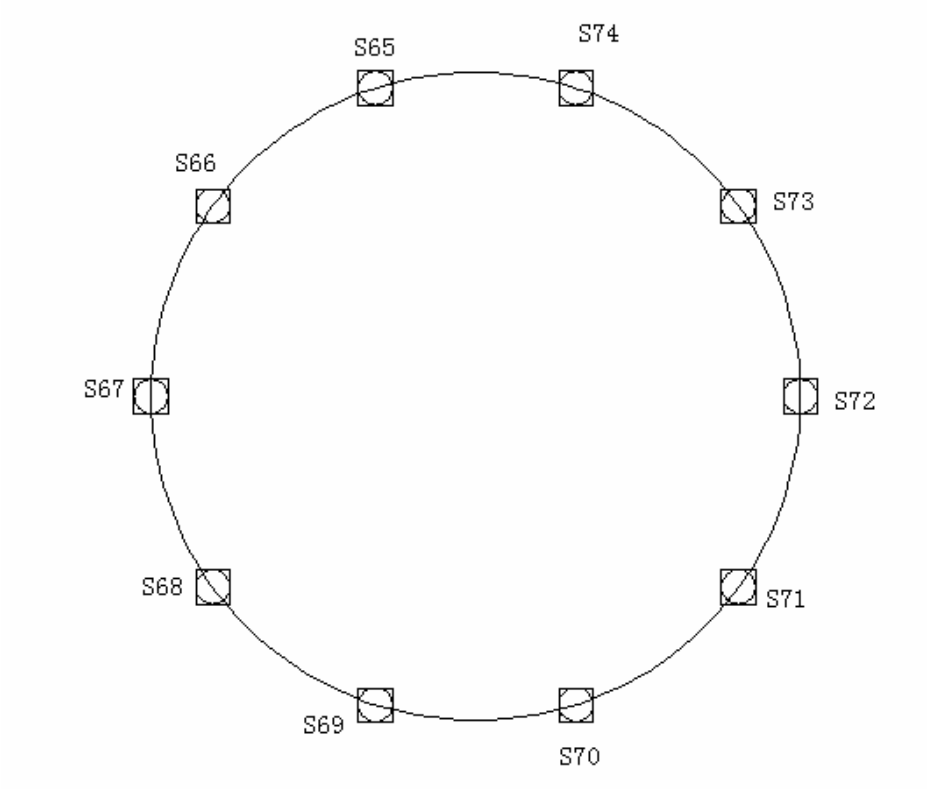

Figure 5.7 the serial number of joints in the connection between A1column and brace

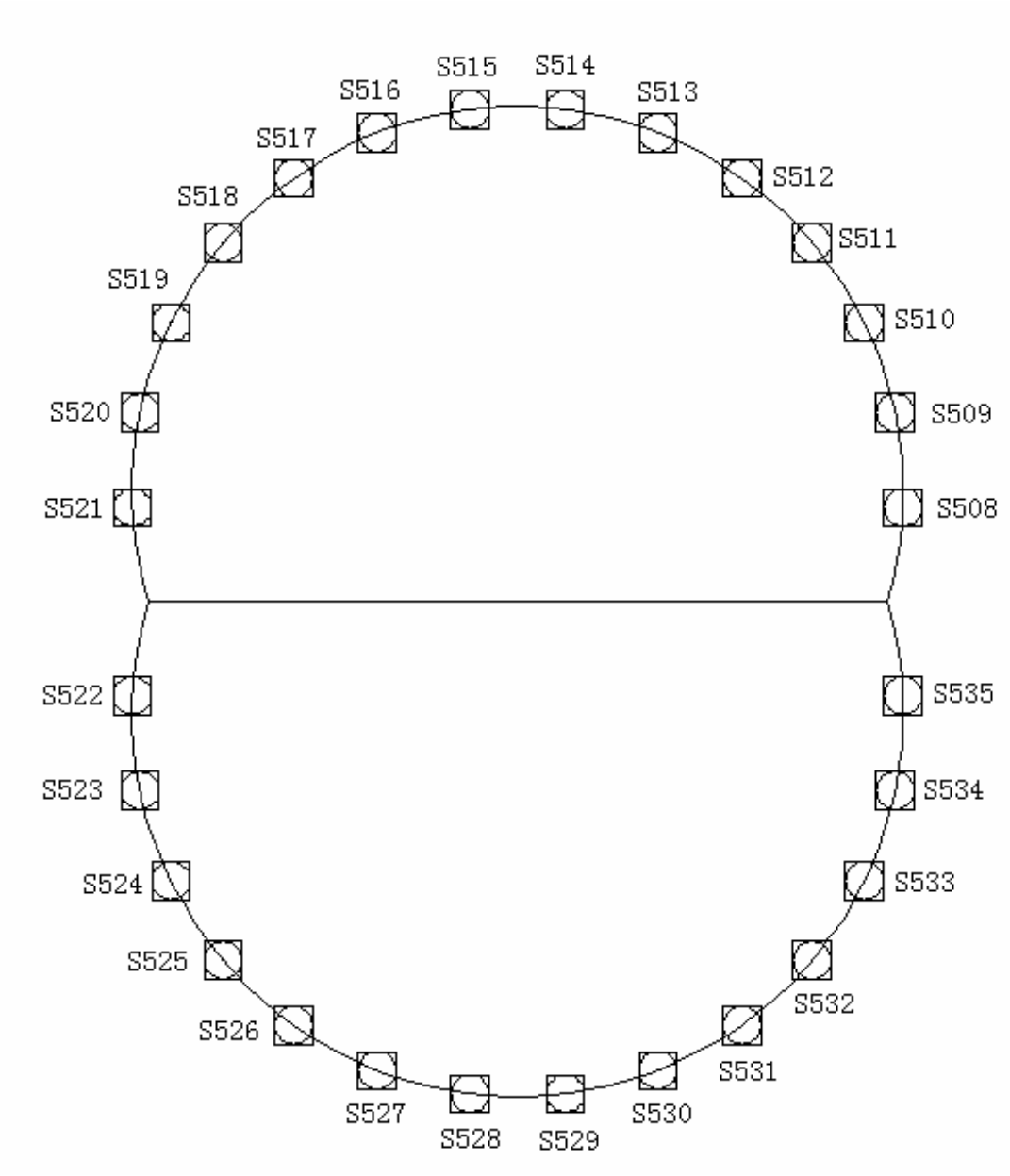

Figure 5.8 the serial number of calculated joints in the K_joint between B1column and B4column

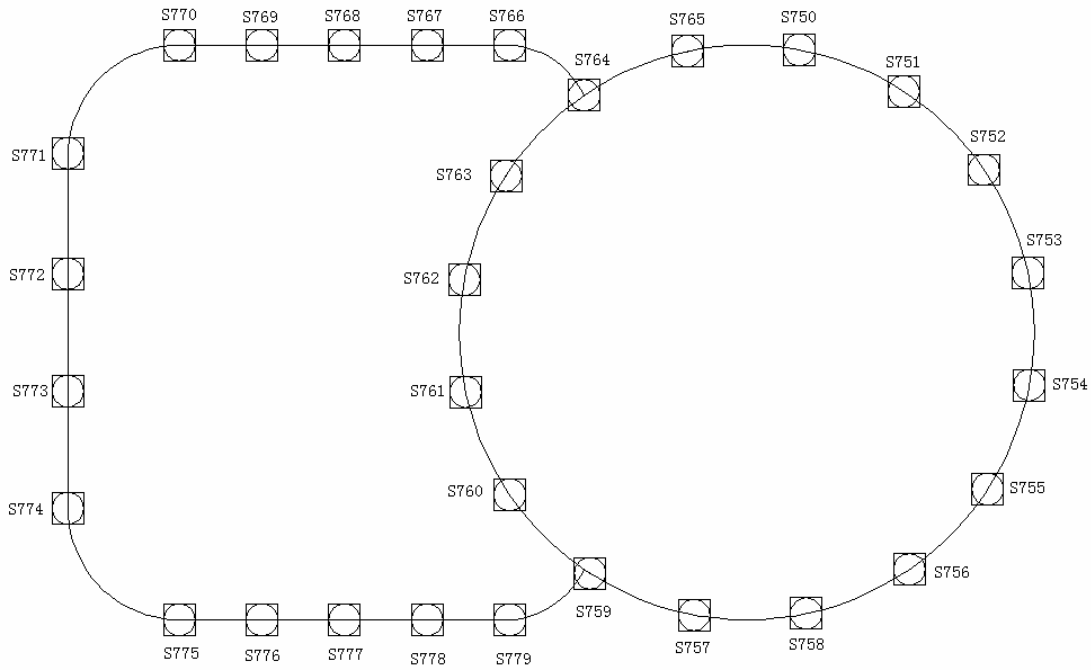

Figure 5.9 the serial number of calculated joints in the connection between column and pontoon

6 Fatigue Assessment in Coarse Mesh

The nominal stress method was adopted in dealing with the fatigue assessment of the 1791 joints in coarse mesh.

6.1 The calculation of the fatigue stress

For the linear system, the amplitude of the responses can be calculated by combination of the sine component and cosine component of the responses. The principle will be described as below,

$$[M]\{\ddot{\eta}(t)\} = \{F(t)\} = \{F\}e^{i\varpi_e t} \tag{6.1}$$

$$\{\ddot{\eta}(t)\} = -\omega_e{}^2\{\eta\}e^{i\omega_e t} \tag{6.2}$$

Where,

$\{\eta\}$—column vector in complex, denote the amplitude of each motion component,;

$\{F\}$—column vector in complex, denote the amplitude of each force component;

$[M]$—mass matrix;

ω_e— the encounter frequency of waves;

For the question here, the force is the resultant of the hydrodynamic pressure acted on the wetted surface of FPS. The following formula is derived from (6.1) and (6.2)

$$-\omega_e{}^2[M]\{\eta\} = \{F(t)\} = \iint_S p(x,y,z)\{n\}ds \tag{6.3}$$

The left part of the equation is the inertial load of the structure, and the right part is the integration of the hydrodynamic pressure along the wetted surface o the FPS.

If the motion component $\{\eta\}$ and pressure $p(x,y,z)$ is expressed in complex，then

$$\{\eta\} = \{\eta_C\} + i\{\eta_S\} \tag{6.4}$$

$$p(x,y,z) = p_C(x,y,z) + ip_S(x,y,z) \tag{6.5}$$

Substituting Eq(6.4) and Eq(6.5) into Eq(6.3), we get two equations,

$$-\omega_e{}^2[M]\{\eta_C\} = \iint_S p_C(x,y,z)\{n\}ds \tag{6.6}$$

$$-\omega_e^2[M]\{\eta_S\} = \iint_S p_S(x,y,z)\{n\}ds \tag{6.7}$$

For the linear system of wave and FPS, the response of stress is linear. So, the cosine component of the stress is obtained with Eq(6.6), and sine component with Eq(6.7). The resultant stress may be expressed as $\sigma = \sigma_c + i\sigma_s$ in complex, consequently, the amplitude of the stress can be calculated by $\sigma_A = \sqrt{\sigma_c^2 + \sigma_s^2}$.

In order to get the corresponding stress response σ_c and σ_s, the above process is carried out at different frequency by applying the real and imaginary component of the loads induced by unit height wave. And then, the amplitude of the stress σ_A is calculated. Because the calculation is done relative to wave direction and frequency, the transfer function of the stress can be expressed as:

$$H_\sigma(\omega_e,\theta) = \sigma_A(\omega_e,\theta) \tag{6.8}$$

According to the previous discussion, the total number of the calculation is 1（loading condition number）×8（sea direction number）×15（frequency number）×2（sine component and cosine component）=240.

6.2 Thickness Adjustment

According to the ABS rules, the basic design S-N cures are applicable to the thickness that do not exceed the reference thickness t_R=22 mm(7/8 inch). For the members with greater thickness, the thickness correction is to be considered for fatigue strength assessment of welded joint. The following formula applies:

$$S_f = S \cdot (\frac{t}{t_R})^{-q} \tag{6.9}$$

Where, S ——unmodified stress range in the S-N curve

t ——plate thickness of the member under assessment

t_R——reference thickness (=22mm)

q ——thickness exponent factor (=0.25)

6.3 The calculation of the cumulative fatigue damage

6.3.1 The principle of the cumulative fatigue damage calculation

6.3.1.1 The short-term stress-range distribution

The long-term distribution of the sea waves is generally regarded as the combination of many short-term distributions of the sea waves in shipbuilding and marine engineering. For each short-term sea state, the wave can be treated as a steady normal random process, and so do the stress response at the sea state. According to the statistic property of the steady normal random process, the short-term stress range distribution for each short-term sea state may be described in continuous probability density function

In practice, the cyclic stress process for each sea state and sea direction θ is considered as a steady narrow-banded random process with zero-expectation and the Rayleigh probability density function can be used to describe the distribution of the stress amplitude:

$$f_Y(y) = \frac{y}{\sigma_X^2}\exp\left(-\frac{y^2}{2\sigma_X^2}\right) \qquad 0 \le y < +\infty \tag{6.10}$$

Where

y —Stress amplitude

σ_X —Root-mean-square value of y

Assume the stress energy spectrum at sea direction θ is $G_{XX}(\omega_e,\theta)$, it can be obtained by scaling the wave energy spectrum in the following manner:

$$G_{XX}(\omega_e,\theta) = \left|H_\sigma(\omega_e,\theta)\right|^2 \cdot G_{\eta\eta}(\omega_e,\theta) \tag{6.11}$$

Where

$H_\sigma(\omega_e,\theta)$ —The stress transfer function

ω_e —The encounter frequency of waves，

θ —Wave direction，

$G_{\eta\eta}(\omega_e,\theta)$ —The spectrum described by encounter frequency, expressed in the following formula (6.12),

$$G_{\eta\eta}(\omega_e,\theta)=\frac{G_{\eta\eta}(\omega)}{1+\frac{2\omega U}{g}\cos\theta} \tag{6.12}$$

Where,

$G_{\eta\eta}(\omega)$ —The Pierson-Moskowitz spectrum described by significant wave height H_S and the zero crossing period T_Z, as expressed in Eq(6.13)

$$G_{\eta\eta}(\omega)=\frac{{H_S}^2}{4\pi}\left(\frac{2\pi}{T_Z}\right)^4\omega^{-5}\exp\left(-\frac{1}{\pi}\left(\frac{2\pi}{T_Z}\right)^4\omega^{-4}\right) \tag{6.13}$$

$$T_Z=0.772T_P \tag{6.14}$$

T_P—amplitude period

The 0-th m_0 and second order m_2 spectral moments are calculated as follows:

$$m_n=\int_0^{+\infty}{\omega_e}^n G_{XX}(\omega_e,\theta)d\omega_e \qquad (\text{n= 0, 2}) \tag{6.15}$$

The root-mean-square value of the cyclic stress process can be achieved in the following formula,

$$\sigma_X=\sqrt{\int_0^{+\infty}G_{XX}(\omega)d\omega}=\sqrt{m_0} \tag{6.16}$$

In addition, to get the number of the stress cycles in a certain time, the zero-up crossing frequency needs to be calculated as follows,

$$f_0=\frac{1}{2\pi}\sqrt{\frac{m_2}{m_0}} \tag{6.17}$$

When the cyclic stress process is a narrow-banded process, the stress range S and the stress amplitude y can be expressed as follows:

$$S=2y \quad \text{or} \quad y=S/2 \tag{6.18}$$

Hence, the probability density function of the stress range is derived from Eq(6.10) and Eq(6.17) in the following formula:

$$f_S(S)=\frac{S}{4\sigma_X^2}\exp\left(-\frac{S^2}{8\sigma_X^2}\right) \qquad 0\le S<+\infty \tag{6.19}$$

6.3.1.2 The calculation of the cumulative fatigue damage

When the fatigue load spectrum is expressed in continuous probability density

function, the cumulative fatigue damage can be calculated as follows:

$$D = \int_L \frac{dn}{N} = \int_0^{+\infty} \frac{N_L f_S(S) dS}{N} = N_L \int_0^{+\infty} \frac{f_S(S)}{N} dS \tag{6.20}$$

Where

S— Stress range，

$f_S(S)$ — Probability density function of the stress range distribution，

N— Average number of loading cycles to failure under constant amplitude loading at that stress range according to the relevant S-N curve，

N_L —The total number of stress cycles，

$dn = N_L f_S(S) dS$ — The number of stress cycles between S and S+dS，

$\int_L$ — The integration in the total period of time.

In calculation, the relation between the number of loading cycles to failure and the relevant constant stress amplitude in Eq(6.10) needs to be known and generally is expressed in S-N curves as follows:

$$NS^m = A \tag{6.21}$$

Where

m 、 A — S-N curve constant

Substituting (6.20) into (6.19), then we gets the cumulative fatigue damage formula:

$$D = \frac{N_L}{A} \int_0^{+\infty} S^m f_S(S) dS \tag{6.22}$$

Assuming the voyage time for i-th sea state and j-th sea direction is T_{ij}, then the damage in this period of time may be calculated in the following formula :

$$D_{ij} = \frac{T_{ij} f_{0ij}}{A} \int_0^{+\infty} S^m f_{Sij}(S) dS \tag{6.23}$$

Where

f_{0ij} —Zero-up crossing frequency of the cyclic stress process, which can be obtained by Eq(6.19)；

$T_{ij} \cdot f_{0ij}$ —The number of the stress cycles in the period T_{ij} ;

$f_{Sij}(S)$—The short-term stress range distribution in the period T_{ij}.

Substituting the expression (6.15) for the short-term stress range distribution $f_{Sij}(S)$, we get

$$D_{ij} = \frac{T_{ij} f_{0ij}}{A}\left(2\sqrt{2}\sigma_{Xij}\right)^m \Gamma(1+\frac{m}{2}) = \frac{T_{ij} f_{0ij}}{A}\left(2\sqrt{2m_{0ij}}\right)^m \Gamma(1+\frac{m}{2}) \tag{6.24}$$

Where

σ_{Xij}—Root-mean-square value of the cyclic stress process, given by Eq(6.6)

m_{0ij}—zero order moment of the stress energy spectrum

$\Gamma()$—Gamma function.

Assuming T is the period of the long-term distribution, the relevant long-term stress-range distribution is consisted of n_S sea states and the corresponding occurrence probability is p_i for each sea state. The number of the wave directions is subdivided into n_H and the occurrence probability is p_j for each wave direction, then $T_{ij} = T \cdot p_i \cdot p_j$, we get the total cumulative fatigue damage in the period T as follows:

$$D_T = \sum_{i=1}^{n_S}\sum_{j=1}^{n_H} D_{ij} = \frac{T}{A}\Gamma(1+\frac{m}{2})\sum_{i=1}^{n_S}\sum^{n_H} p_i p_j f_{0ij}\left(2\sqrt{2m_{0ij}}\right)^m \tag{6.25}$$

The cumulative fatigue damage of the structure should satisfy the following demand in the design life,

$$D_T \le 1.0 \tag{6.26}$$

6.4 Selection of S-N curves

The correct S-N curve was selected for each calculated join according to the section 3 of the 《 GUIDE FOR THE FATIGUE ASSESSMENT OF OFFSHORE STRUCTURES》,the results was list in Appendix C.

6.5 The Results of Fatigue Assessment in Coarse Mesh

According to the theory above-mentioned and ABS rules, the fatigue accumulated

damage and fatigue life were calculated when the minimum required service life was taken as 20 years. The results of all the joints were list in **Appendix B**.

It can be seen that most of the joints' fatigue life were longer than 300 years, namely their fatigue strength satisfy the service requirement. But there still have 16 joints whose fatigue lift was less than 300years, and the particular information were list in Table 6.1. All the 16 joints will be fine meshed next section and calculated the fatigue damage and the fatigue life using the hot spot stress method.

Table 6.1 the fatigue strength of the danger joints

Location	Joint Number	Name	Fatigue damage	Fatigue life/year
Stiffener in column	340574	CL25	0.0832	240
Stiffener in column	340578	CL26	0.0748	267
Stiffener in column	43109	CL73	0.0774	258
For. cross pontoon	85063	CPL20	0.0808	247
For. cross pontoon	37142	CPL32	0.0726	276
For. cross pontoon	37702	CPL33	0.1247	160
For. cross pontoon	37700	CPL34	0.2769	72
For. cross pontoon	37594	CPL50	0.0678	295
For. cross pontoon	36960	CPL53	0.2156	93
Aft. cross pontoon	76303	CPL80	0.0676	296
Aft. cross pontoon	3488	CPL93	0.1130	177
Aft. cross pontoon	3490	CPL94	0.0824	243
Aft. cross pontoon	2832	CPL95	0.0716	279
Aft. cross pontoon	3064	CPL110	0.0921	217
Aft. cross pontoon	2645	CPL111	0.1680	119
Aft. cross pontoon	2641	CPL113	0.0970	206
Flange of deck girders	240678	S306	0.0340	588

After analysis, considering geometric symmetry, 10joints were selected to be fine meshed. The number and location were list in Table 6.2.

Table 6.2 location of the fine meshed joints

Location	Joint Number	Name	remark : symmetrical
Stiffener in column	340574	CL25	CL73 and CL25
Stiffener in column	340578	CL26	
For. cross pontoon	37142	CPL32	CPL93 and CPL32 CPL94 and CPL33 CPL95 and CPL34
For. cross pontoon	37702	CPL33	
For. cross pontoon	37700	CPL34	
Aft. cross pontoon	76303	CPL80	CPL20 and CPL80
Aft. cross pontoon	3064	CPL110	CPL50 and CPL110 CPL53 and CPL113
Aft. cross pontoon	2645	CPL111	
Aft. cross pontoon	2641	CPL113	
Flange of deck girders	240678	S306	——

7 Fatigue Assessment in Fine Mesh

The hot spot stress method was adopted to calculate the 10 joints selected in chapter 6 particularly.

7.1 Fine-meshed

The critical location and its adjacent region were modeled with shell elements in term of the ABS rules and the IACS. The element size in way of the hot spot location should be approximately $t \times t$ and extend 10 t away from the weld toe. Then, the aspect ratio should be ideally limited to 1:3, and any element exceeding this ratio should be well away from the area of interest and then should not exceed 1:5. The corner angles of the quadrilateral plate or shell elements should be confined to the range 50 to 130 degree. The fine-meshed model of the critical joins was list following:

1、Fine-meshed FEM of the calculated joint in the main deck(S306)

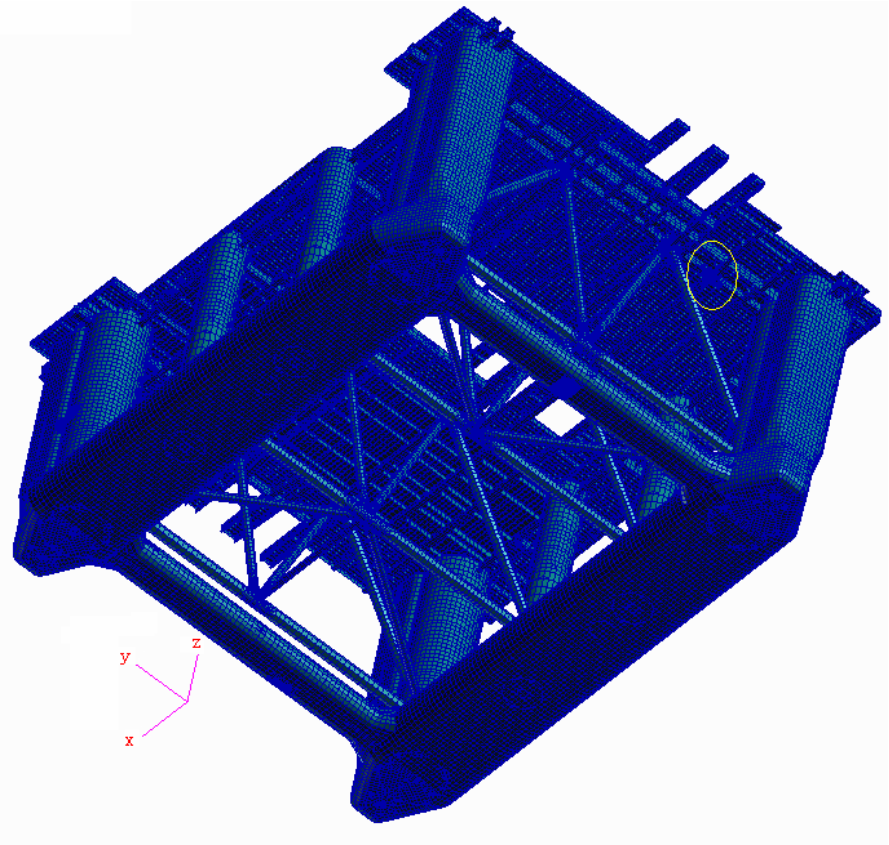

Fig. 7.1 fine-meshed FEM of the calculated joint

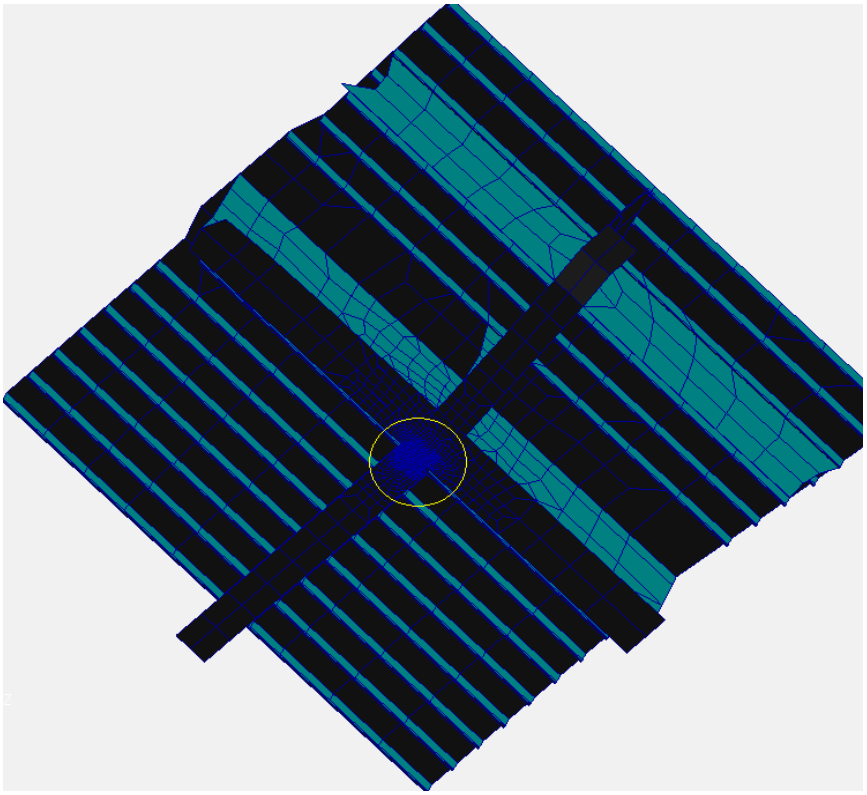

Fig. 7.2 fine-meshed FEM of the calculated joint

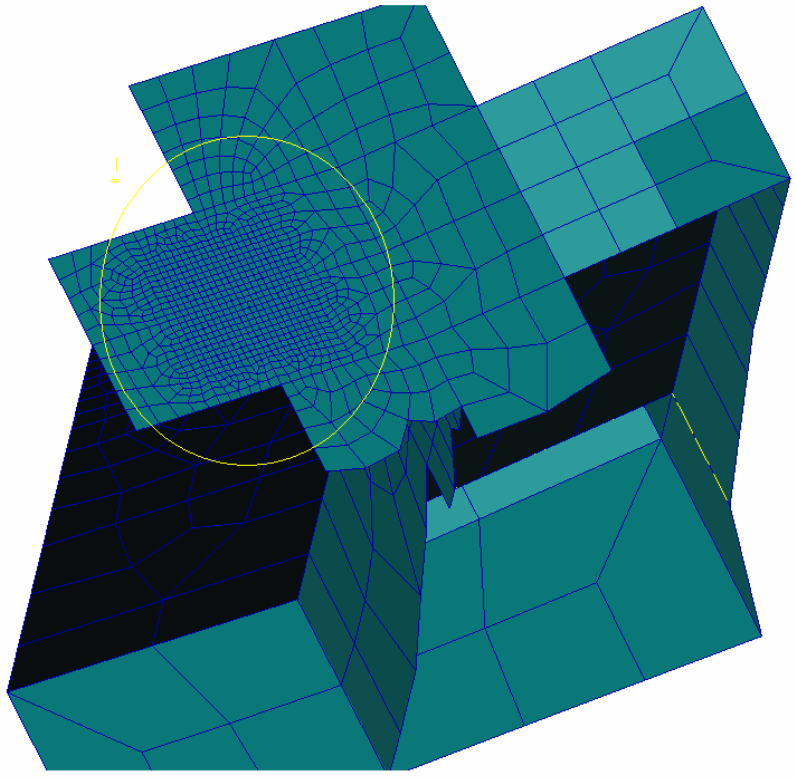

Fig. 7.3 fine-meshed FEM of the calculated joint

2、Fine-meshed FEM of the calculated joints in the middle of the Aft cross pontoon (CPL80)

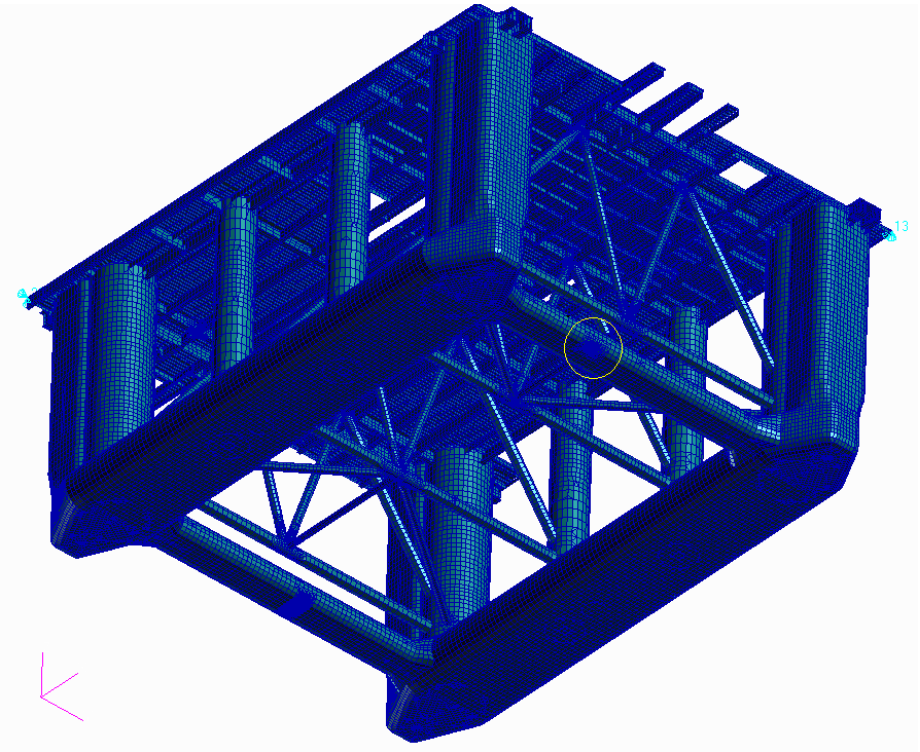

Fig. 7.4 Fine-meshed FEM of the calculated joint

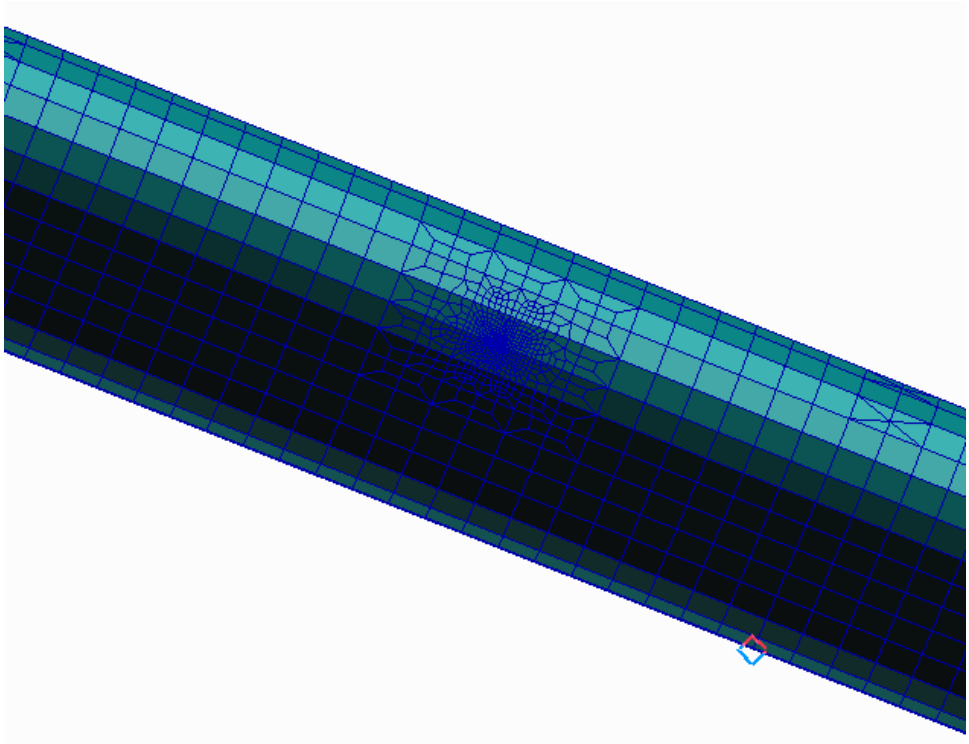

Fig. 7.5 Fine-meshed FEM of the calculated joint

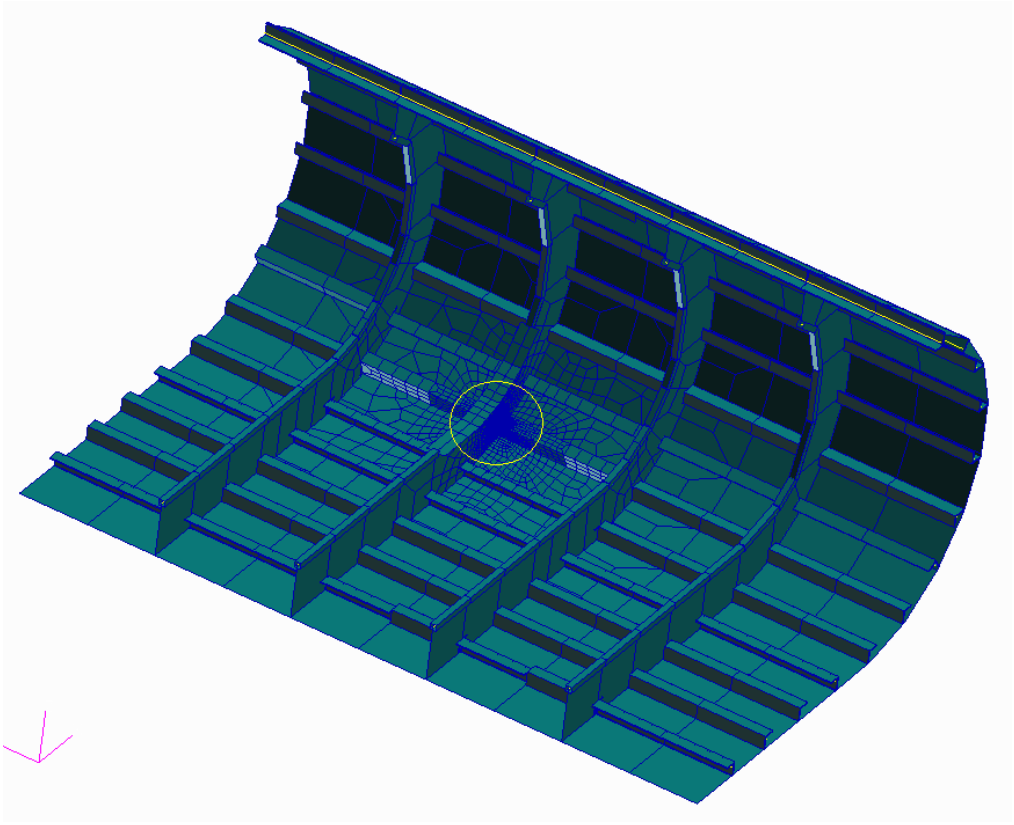

Fig. 7.6 Fine-meshed FEM of the calculated joint

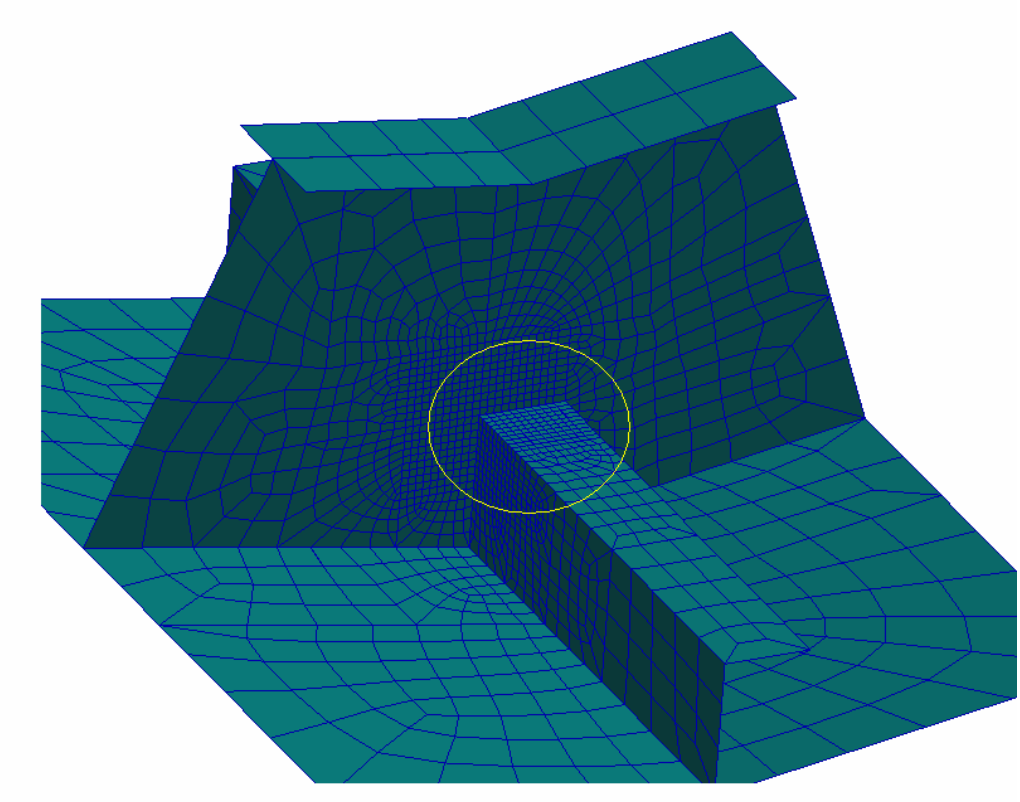

Fig. 7.7 Fine-meshed FEM of the calculated joint

3、Fine-meshed FEM of the calculated joints in the connection between pontoon and cross pontoon（CPL110,CPL111,CPL113）.

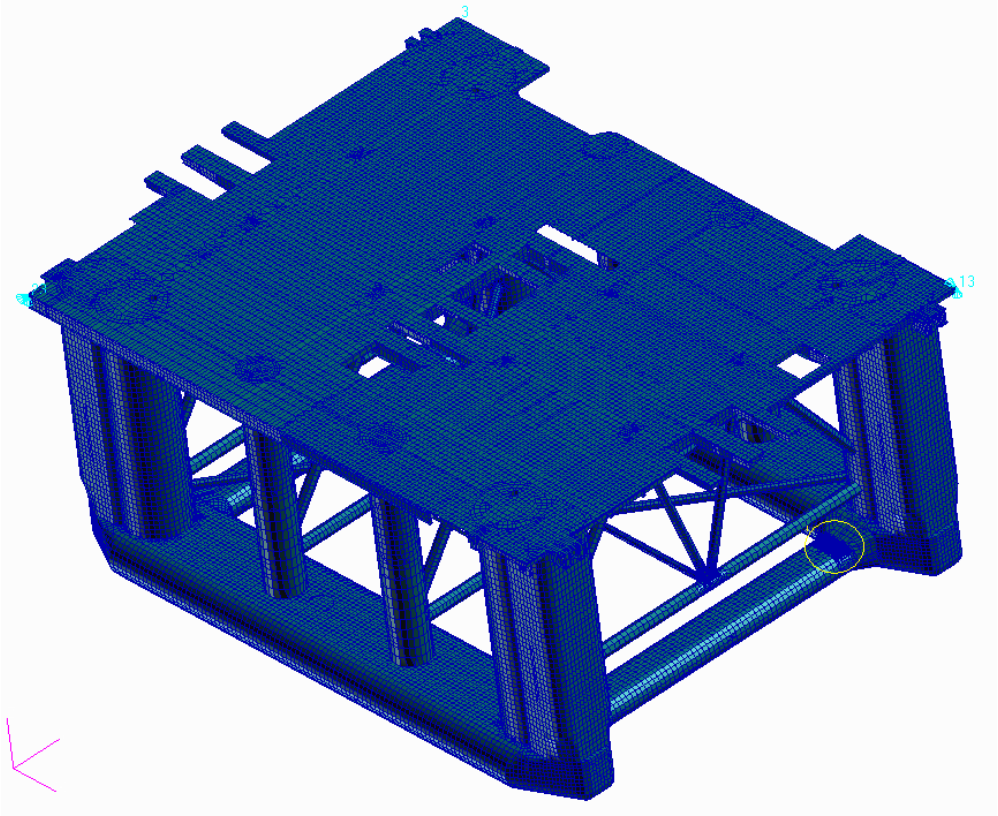

Fig. 7.8 Fine-meshed FEM of the calculated joints

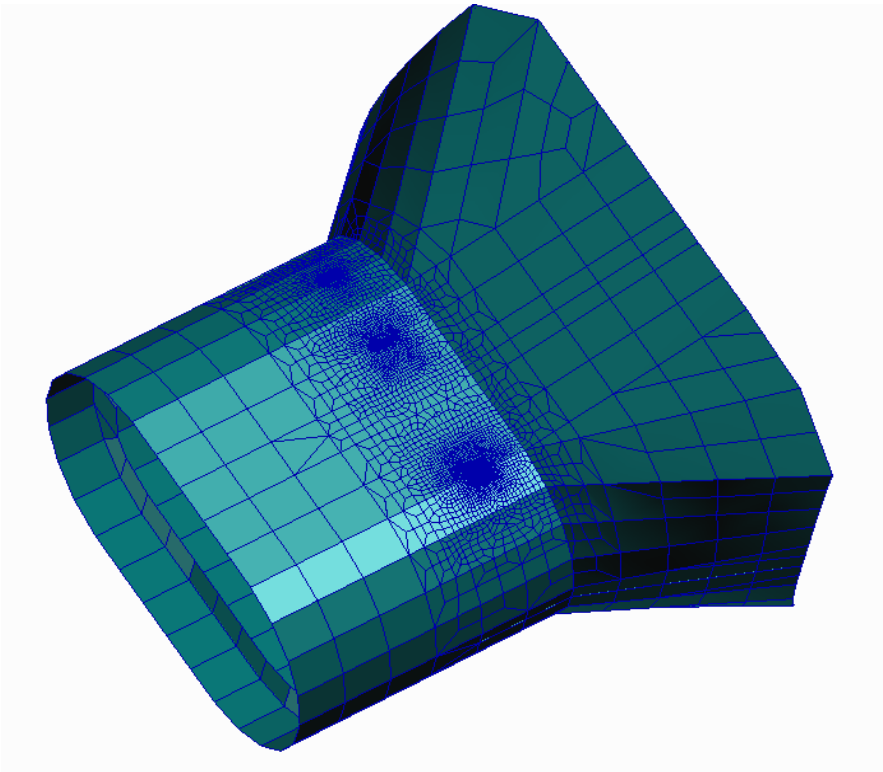

Fig. 7.9 Fine-meshed FEM of the calculated joints

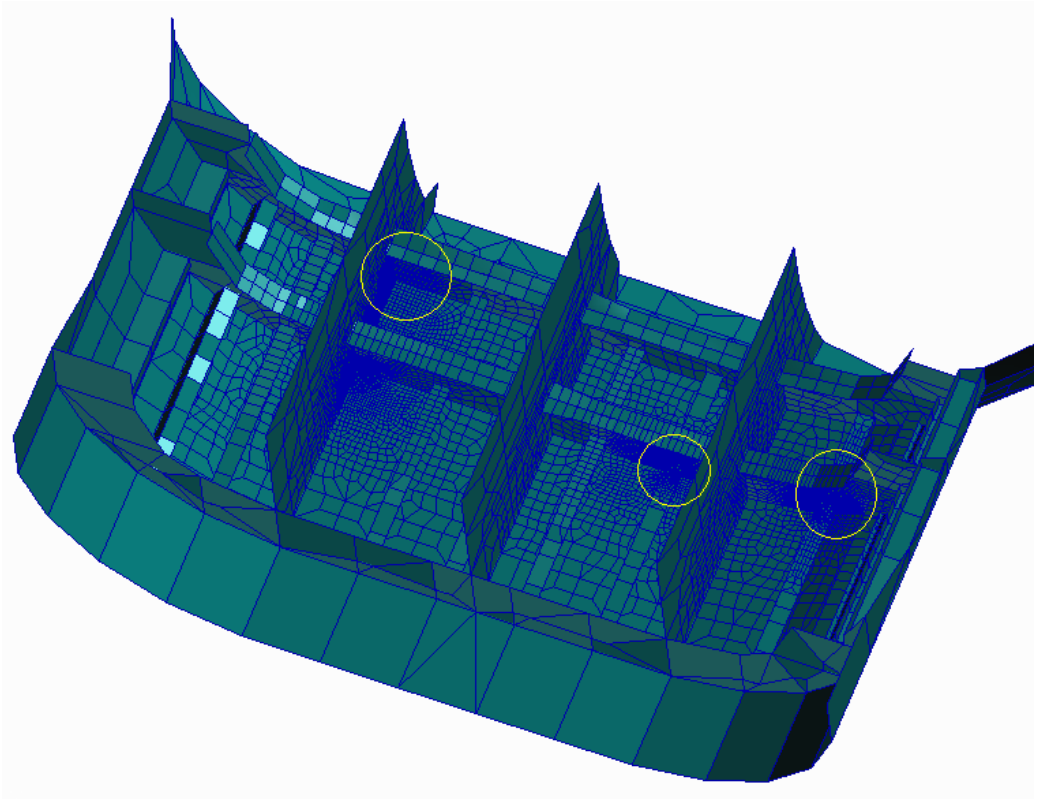

Fig. 7.10 Fine-meshed FEM of the calculated joints

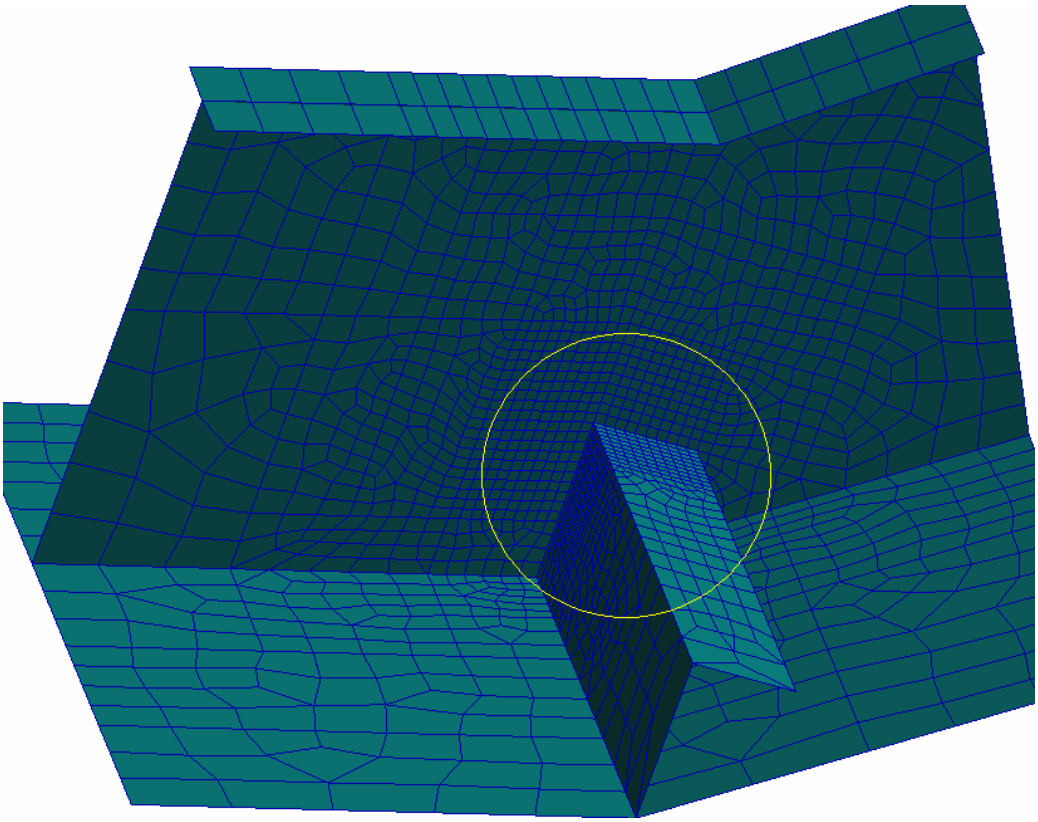

Fig. 7.11 Fine-meshed FEM of the calculated joint (CPL110)

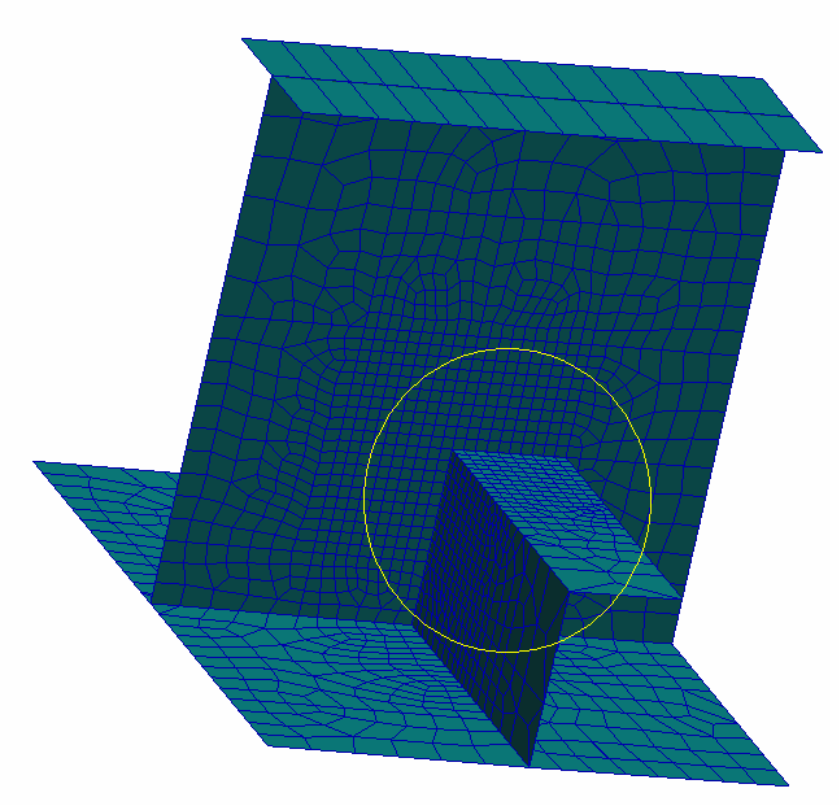

Fig. 7.12 Fine-meshed FEM of the calculated joint（CPL111）

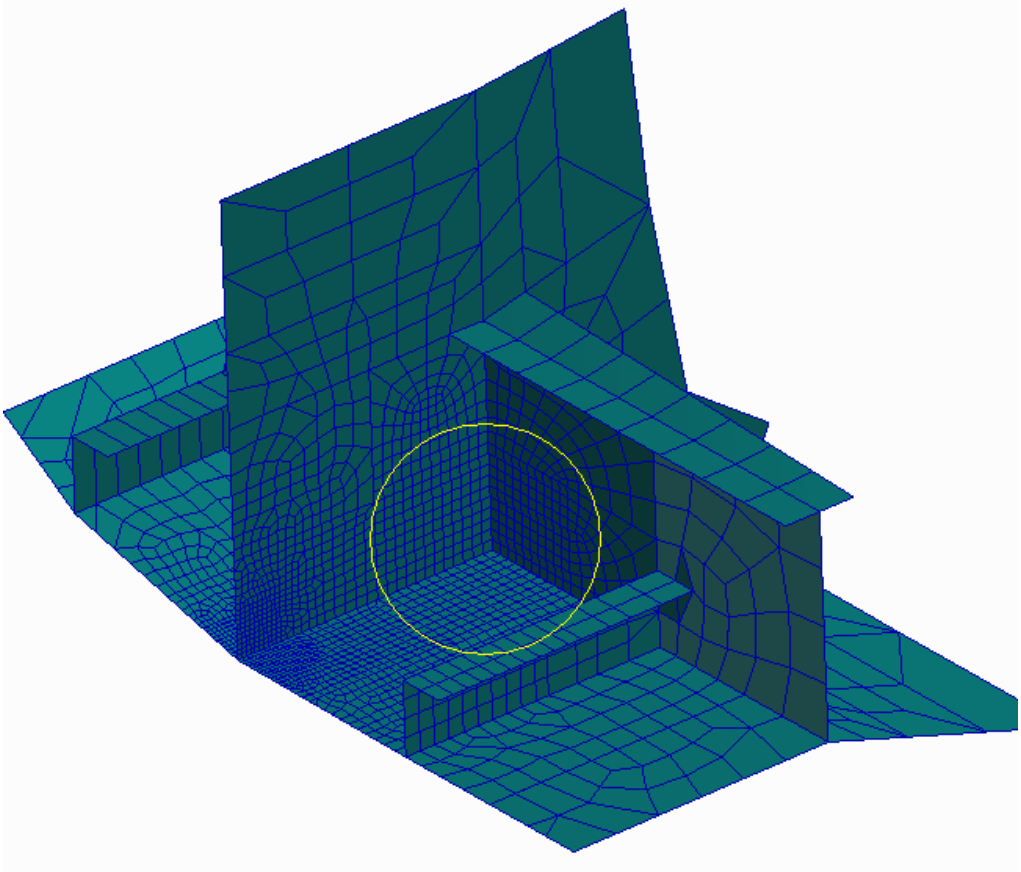

Fig. 7.13 Fine-meshed FEM of the calculated joint（CPL113）

4、Fine-meshed FEM of the calculated joints in the For. Cross pontoon (CPL32, CPL33 and CPL34)

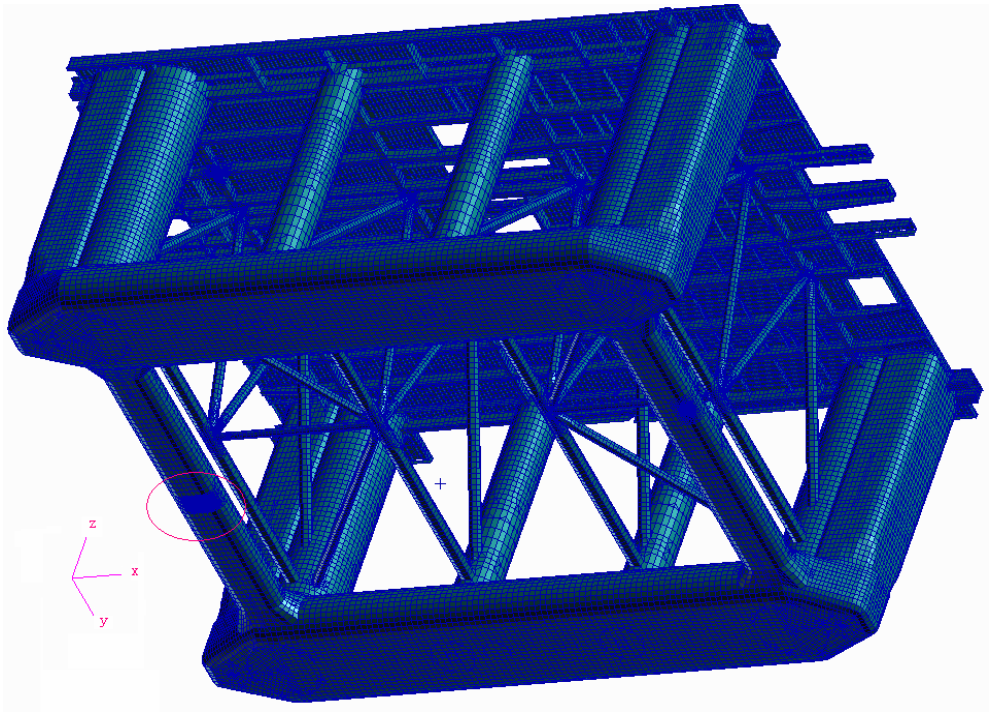

Fig. 7.14 Fine-meshed FEM of the calculated joints

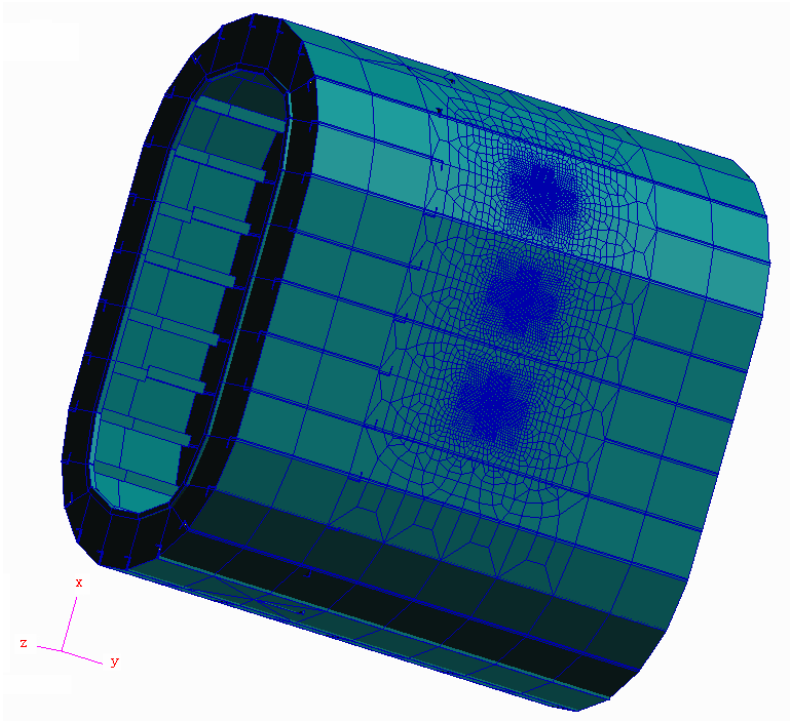

Fig. 7.15 Fine-meshed FEM of the calculated joints

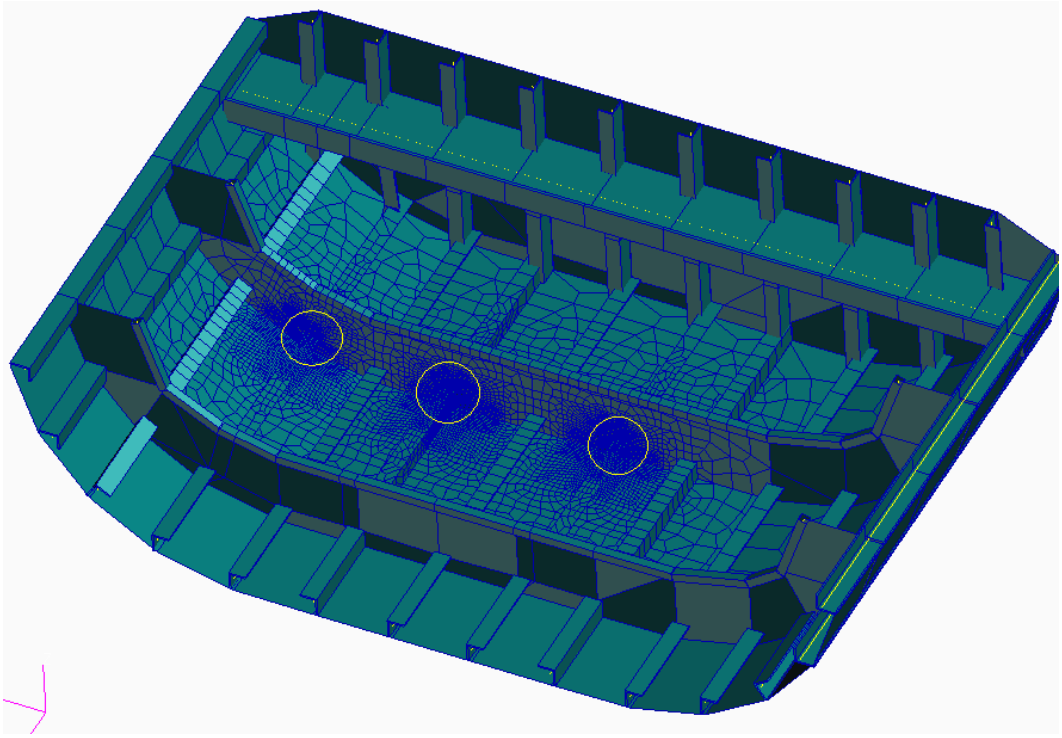

Fig. 7.16 Fine-meshed FEM of the calculated joints

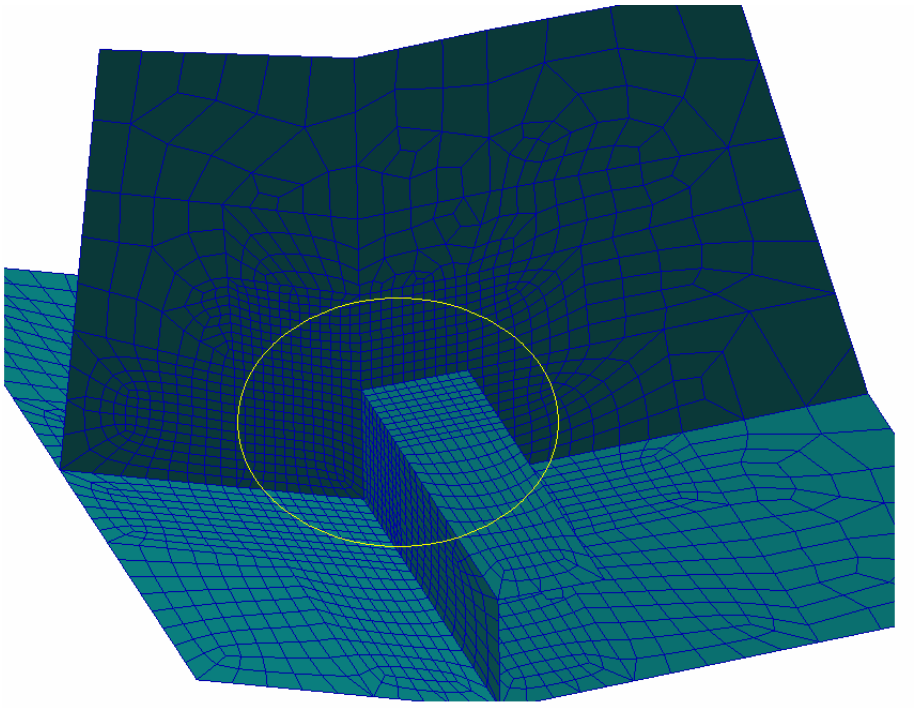

Fig. 7.17 Fine-meshed FEM of the calculated joint (CPL 32)

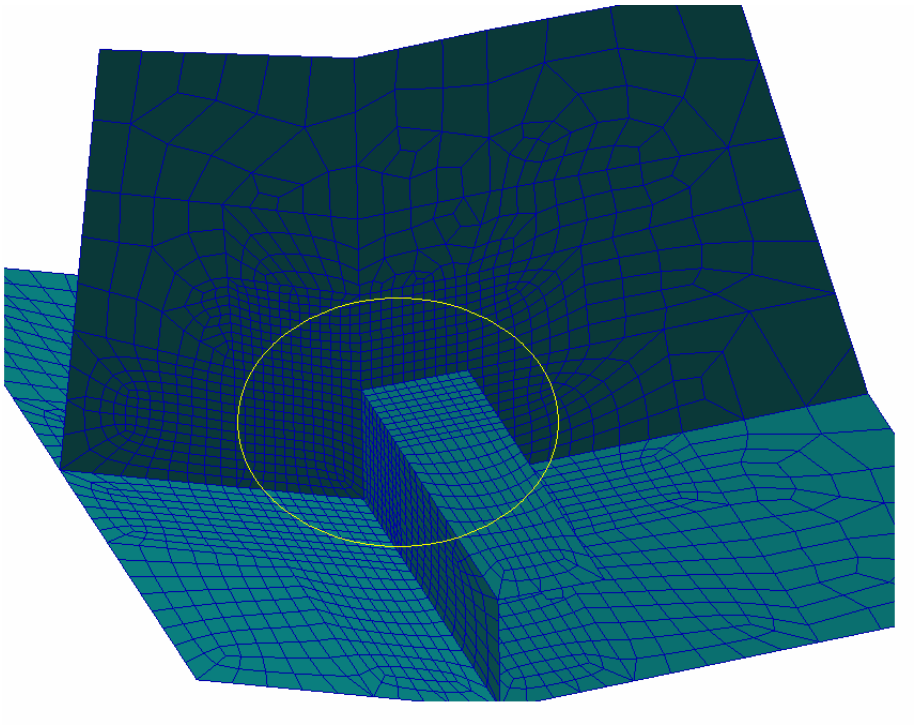

Fig. 7.18 Fine-meshed FEM of the calculated joint (CPL33)

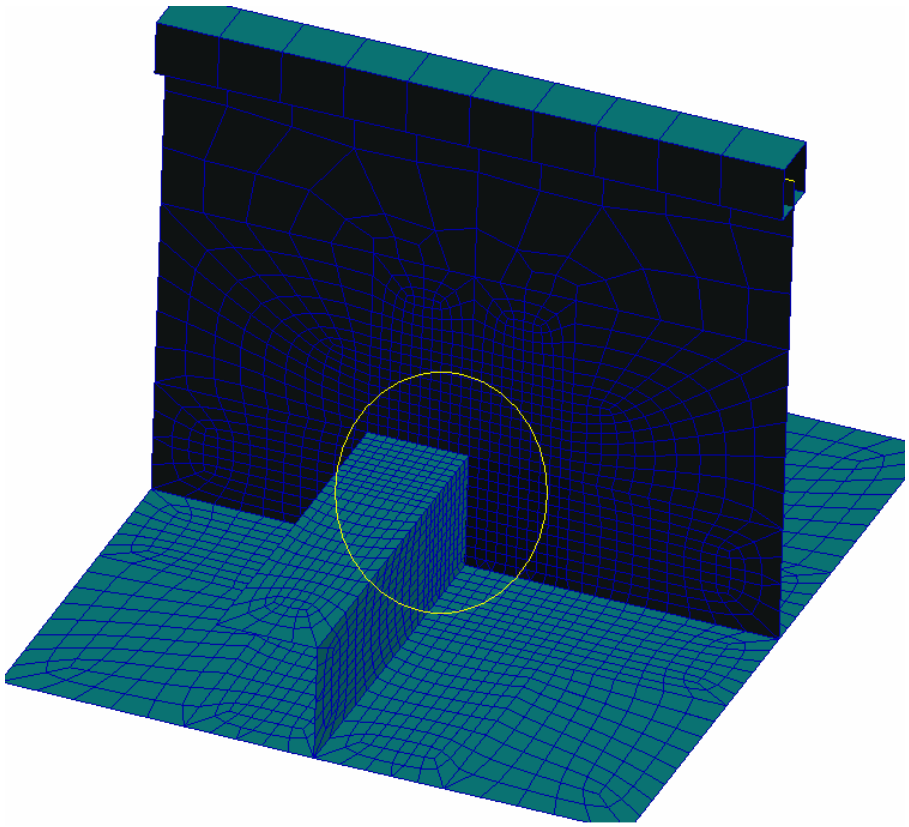

Fig. 7.19 Fine-meshed FEM of the calculated joint (CPL34)

5、Fine-meshed FEM of the calculated joints in the D1 column(CL25,CL26)

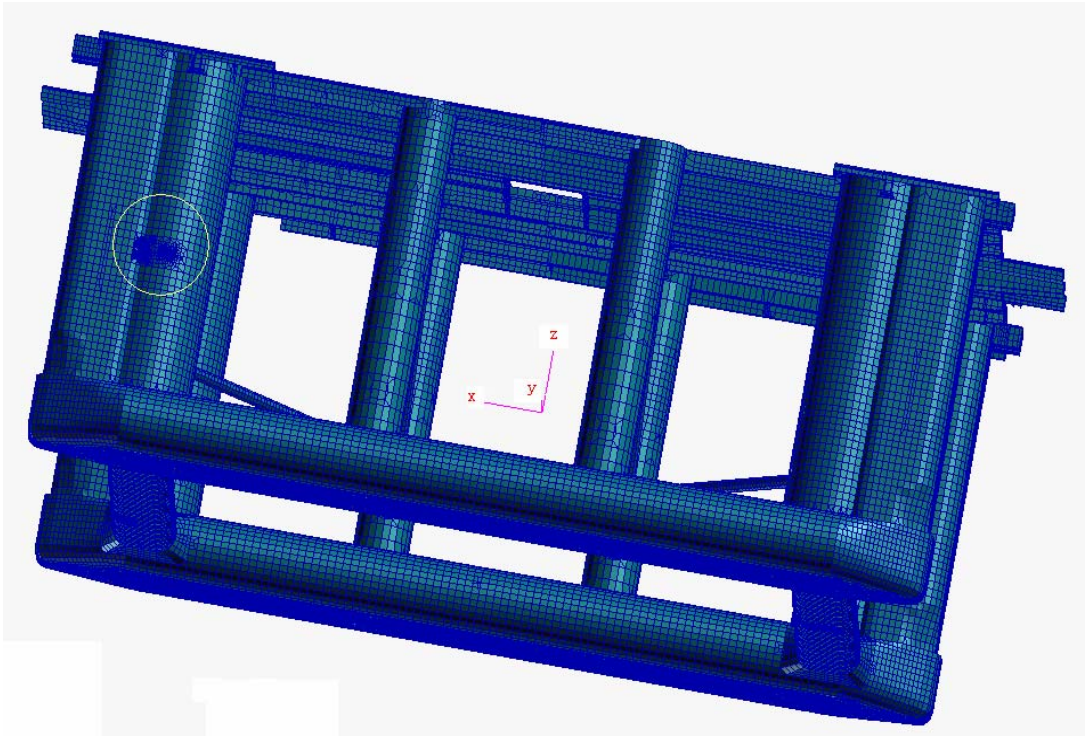

Fig. 7.20 Fine-meshed FEM of the calculated joints

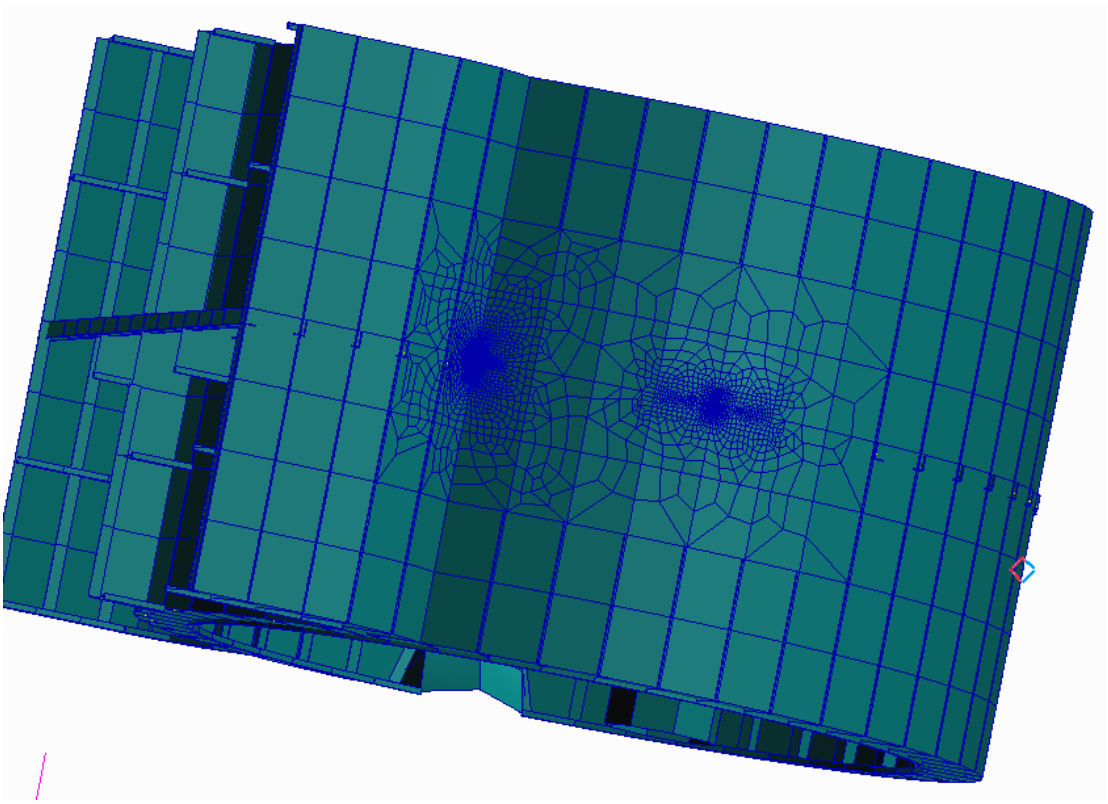

Fig. 7.21 Fine-meshed FEM of the calculated joints

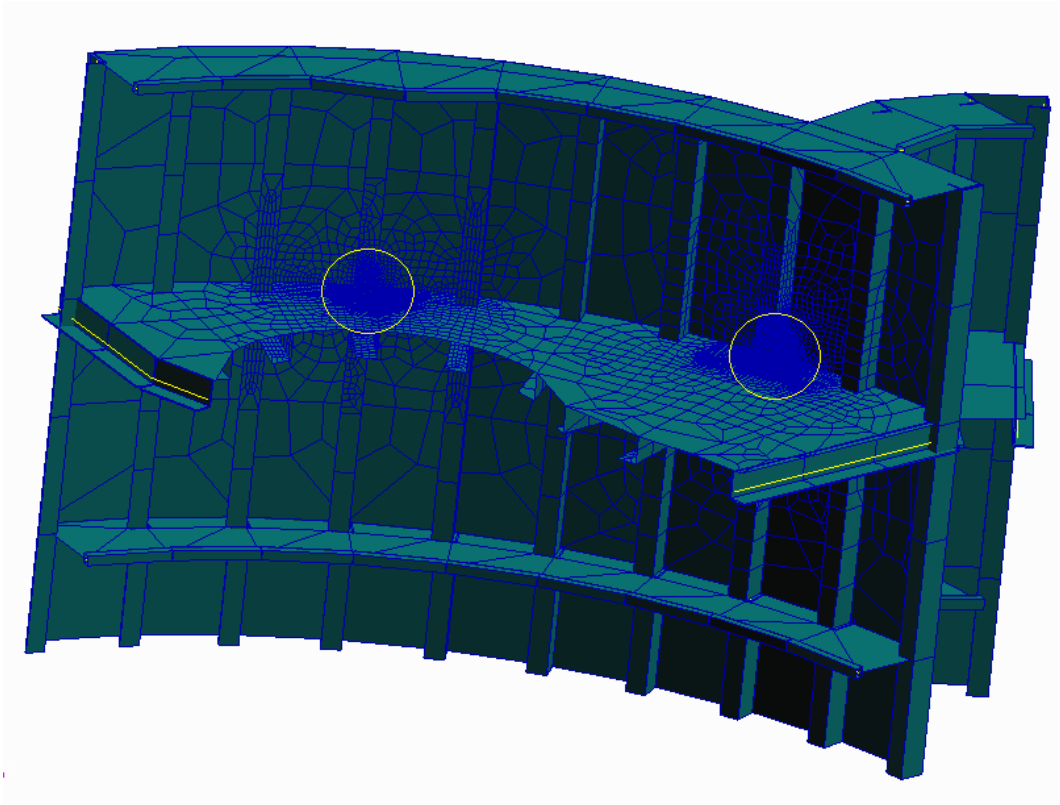

Fig. 7.22 Fine-meshed FEM of the calculated joints

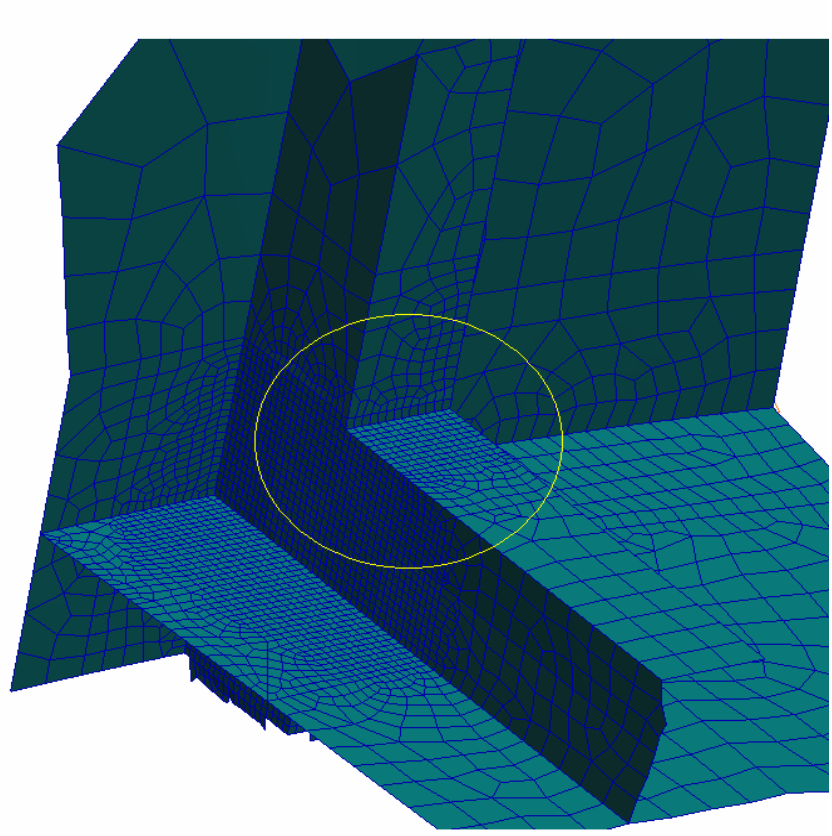

Fig. 7.23 Fine-meshed FEM of the calculated joint (CL25)

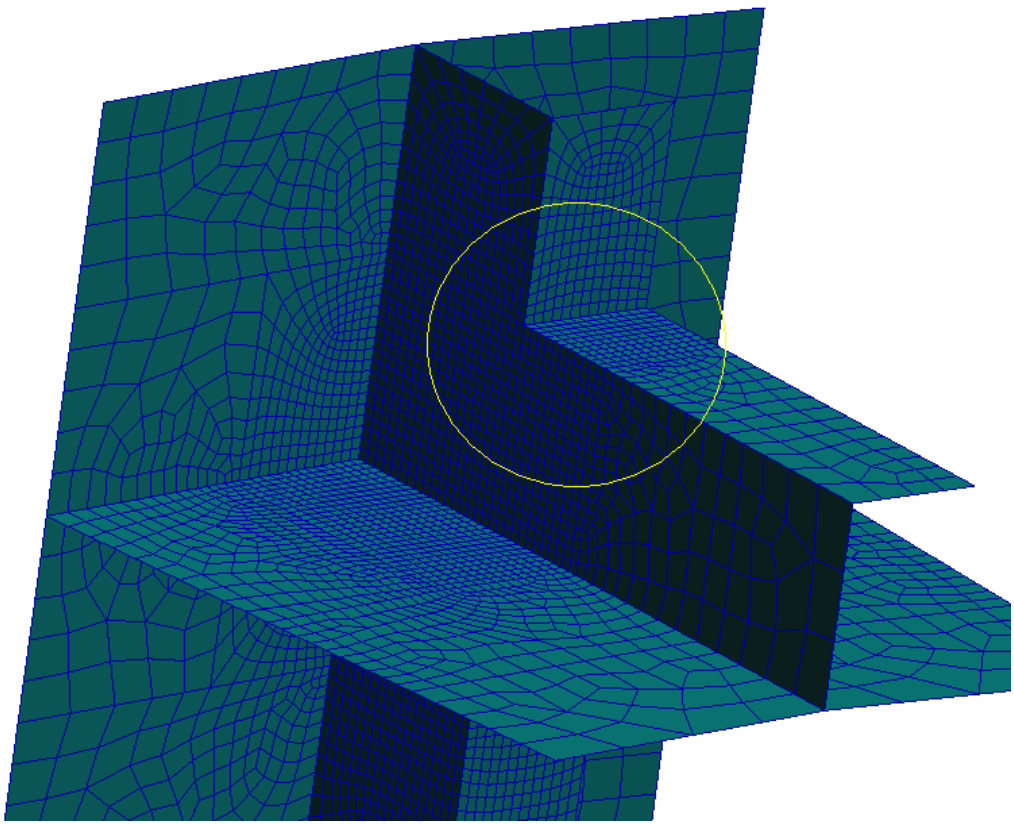

Fig. 7.24 Fine-meshed FEM of the calculated joint (CL26)

7.2 The area of crack likely arising

For fatigue node of stress centralizing, the areas where crack may arise are not sure. A detail explanation for three different structure types of 10 refined nodes will be given.

1) Angle steel perforates round frame or bulkhead，see Figure 7.25. The 9 parts signed in figure all will come forth with crack. By calculation and analysis of node stress, we got that the stresses of NO.2, NO.4, NO.6, NO.7, NO.8 and NO. 9 are smaller than others, so their fatigue damages are relatively small. The stresses of NO.1, NO.2, NO.3, NO.4 and NO.5 are calculated in this assessment.
2) The node on the intersection of two angle steels, which has a 90 degree angle, see Figure 7.26. The stresses of the 4 parts signed in the figure will be calculated.

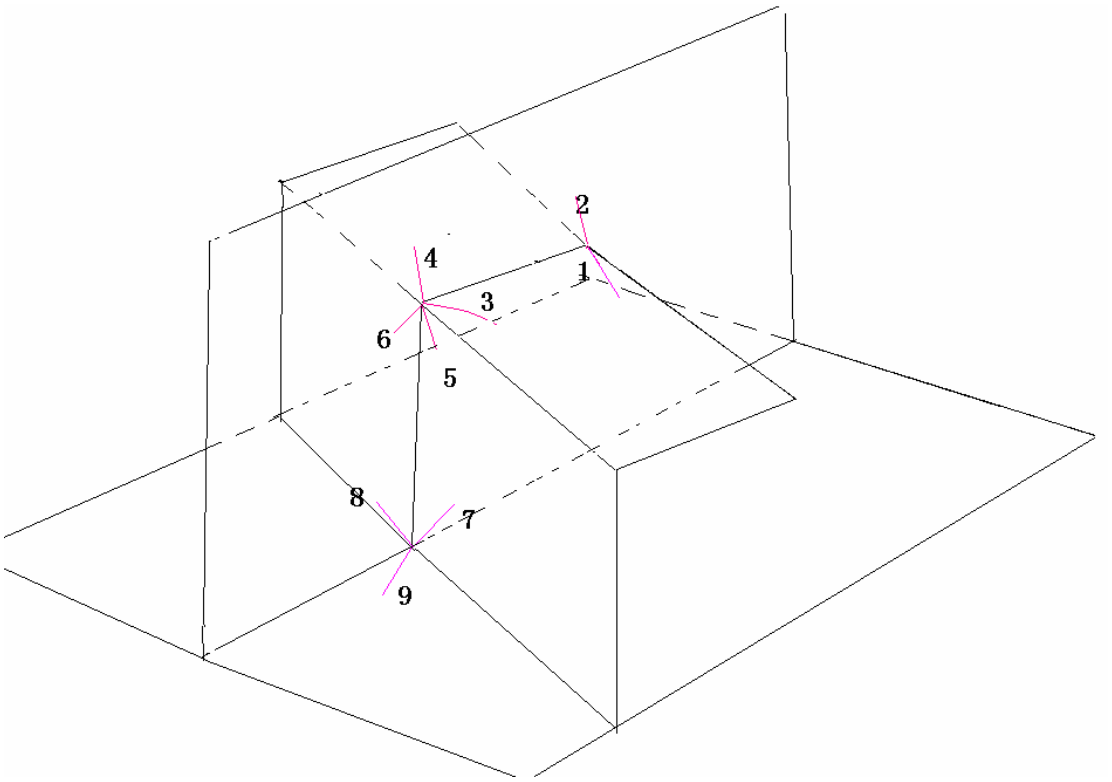

Figure7.25 Figure of crack arising

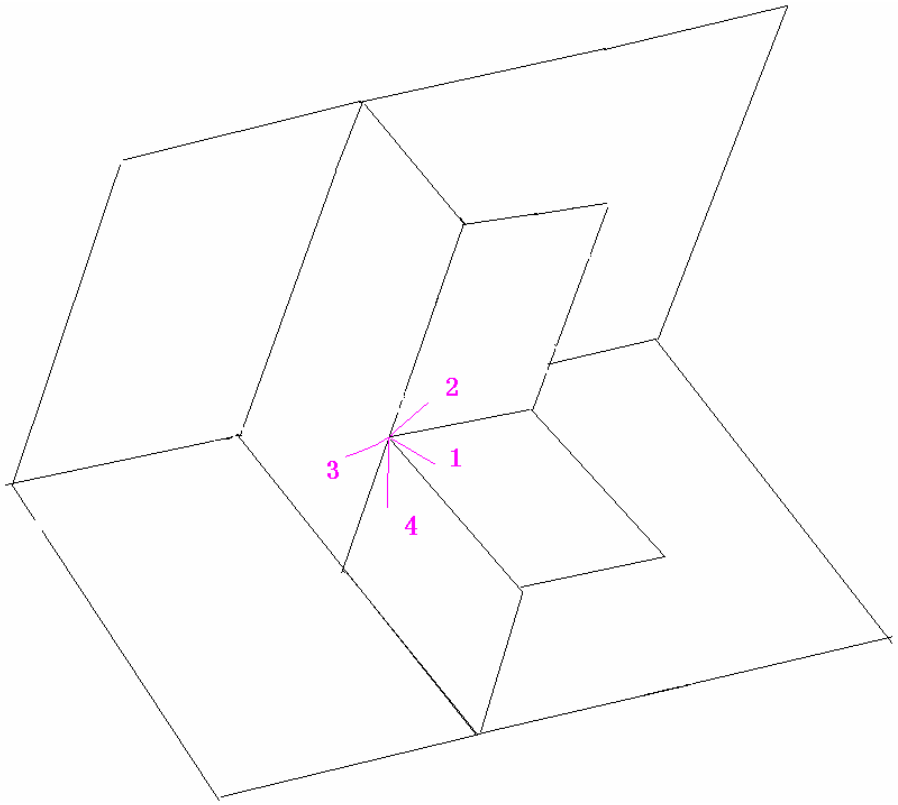

Figure7.26 Figure of crack arising

3）T-bar perforating the bulkhead, see Figure 7.27. For this structural type, the crack will arise at outside shell（1、2、3、4 signed with green line in figure）、web of T-bar（6、8 signed with purple line in figure）or bulkhead（5、7 signed with red line in figure）, so the stresses of these parts are calculated.

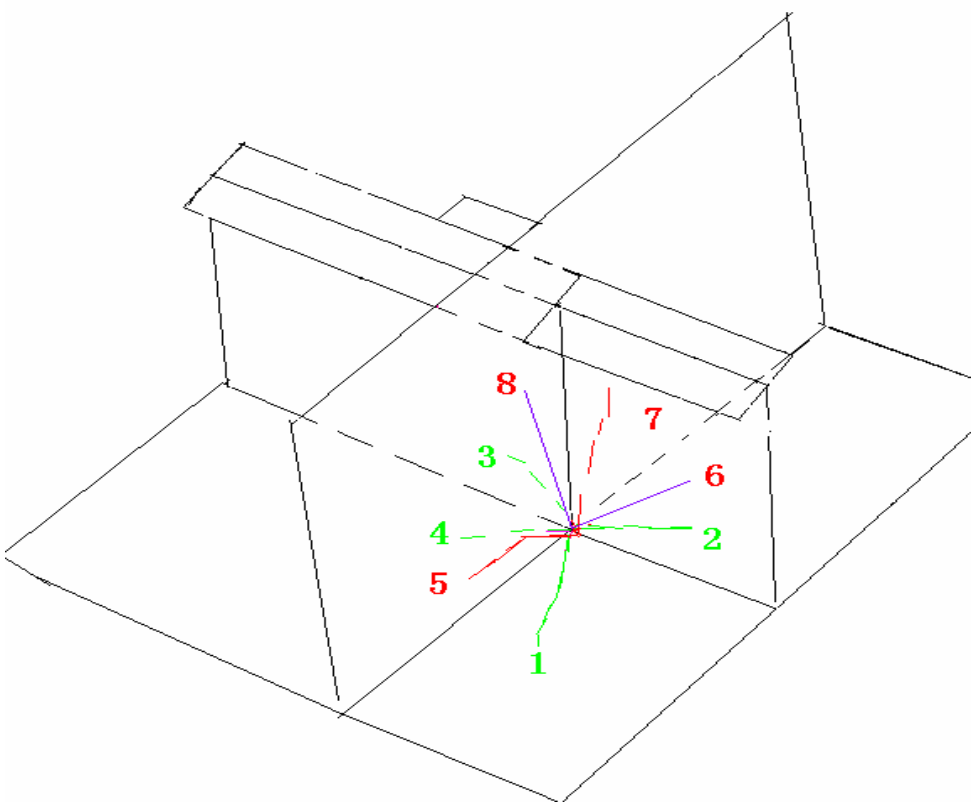

Figure7.27 Figure of crack arising

7.3 The Results of The Fatigue Assessment in Fine Mesh

7.3.1 Hot stress

The fatigue loads were applied to the fine-meshed FEM accordance with the method mention in chapter 6, and fatigue stress would be calculated and pick-up. Figure 7.28 shows an acceptable method, which can be used to extract and interpret the ‘weld toe’ hot spot stress and to obtain a linearly extrapolated stress at the weld toe. According to the figure, the weld’s hot spot stress can be determined by a linear extrapolation to the weld toe using the calculated ‘reference’ stress at t/2 and 3t/2 from weld toe. Then the extrapolated component stresses are used to compute the maximum principal stress at the weld toe and be used in the fatigue assessment.

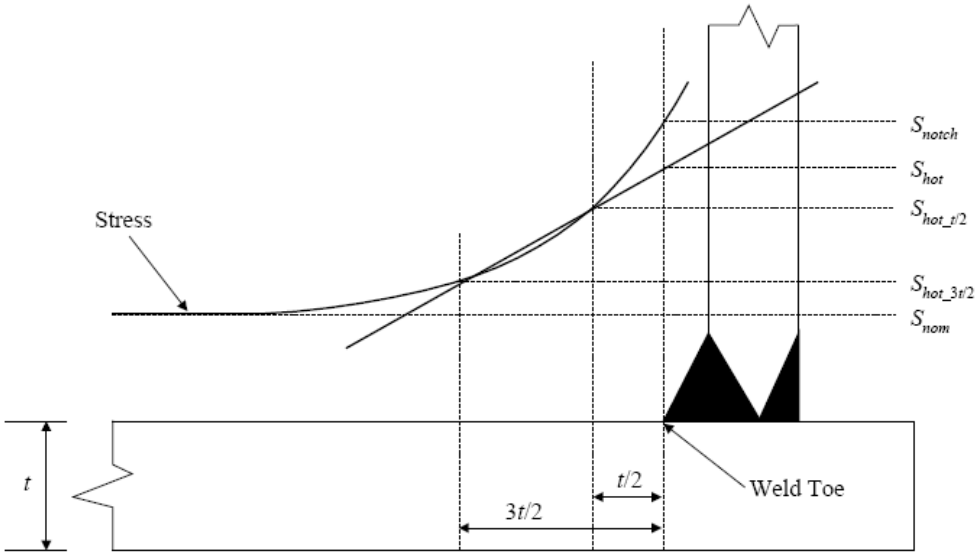

Fig 7.28 stress gradient near the weld

7.3.2 S-N Curve

According to the ABS Rules, the ABS Offshore S-N Curve-Joint Class 'E' is selected for calculation for above-mentioned nodes, the red curve in Table 7.1 和 7.2is the selected curve. The detail information can be seen in ABS《GUIDE FOR THE FATIGUE ASSESSMENT OF OFFSHORE STRUCTURES》SECTION 3/3.3 和 SECTION 2/5.9）.

Table 7.1 Parameters for ABS-(A) Offshore S-N Curves for Non-Tubular Details in Air

Curve Class	*A*		*m*	*C*		*r*	N_Q	S_Q	
	For MPa Units	*For ksi Units*		*For MPa Units*	*For ksi Units*			*For MPa Units*	*For ksi Units*
B	1.01×10^{15}	4.48×10^{11}	4.0	1.02×10^{19}	9.49×10^{13}	6.0	1.0×10^{7}	100.2	14.5
C	4.23×10^{13}	4.93×10^{10}	3.5	2.59×10^{17}	6.35×10^{12}	5.5	1.0×10^{7}	78.2	11.4
D	1.52×10^{12}	4.65×10^{9}	3.0	4.33×10^{15}	2.79×10^{11}	5.0	1.0×10^{7}	53.4	7.75
E	1.04×10^{12}	3.18×10^{9}	3.0	2.30×10^{15}	1.48×10^{11}	5.0	1.0×10^{7}	47.0	6.83
F	6.30×10^{11}	1.93×10^{9}	3.0	9.97×10^{14}	6.42×10^{10}	5.0	1.0×10^{7}	39.8	5.78
F2	4.30×10^{11}	1.31×10^{9}	3.0	5.28×10^{14}	3.40×10^{10}	5.0	1.0×10^{7}	35.0	5.08
G	2.50×10^{11}	7.64×10^{8}	3.0	2.14×10^{14}	1.38×10^{10}	5.0	1.0×10^{7}	29.2	4.24
W	1.60×10^{11}	4.89×10^{8}	3.0	1.02×10^{14}	6.54×10^{9}	5.0	1.0×10^{7}	25.2	3.66

Table 7.2 Parameters for ABS-(CP) Offshore S-N Curves for Non-Tubular Details in Seawater with Cathodic Protection

Curve Class	A		m	C		r	N_Q	S_Q	
	For MPa Units	For ksi Units		For MPa Units	For ksi Units			For MPa Units	For ksi Units
B	4.04×10^{14}	1.79×10^{11}	4.0	1.02×10^{19}	9.49×10^{13}	6.0	6.4×10^{5}	158.5	23.0
C	1.69×10^{13}	1.97×10^{10}	3.5	2.59×10^{17}	6.35×10^{12}	5.5	8.1×10^{5}	123.7	17.9
D	6.08×10^{11}	1.86×10^{9}	3.0	4.33×10^{15}	2.79×10^{11}	5.0	1.01×10^{6}	84.4	12.2
E	4.16×10^{11}	1.27×10^{9}	3.0	2.30×10^{15}	1.48×10^{11}	5.0	1.01×10^{6}	74.4	10.8
F	2.52×10^{11}	7.70×10^{8}	3.0	9.97×10^{14}	6.42×10^{10}	5.0	1.01×10^{6}	62.9	9.13
F2	1.72×10^{11}	5.26×10^{8}	3.0	5.28×10^{14}	3.40×10^{10}	5.0	1.01×10^{6}	55.4	8.04
G	1.00×10^{11}	3.06×10^{8}	3.0	2.14×10^{14}	1.38×10^{10}	5.0	1.01×10^{6}	46.2	6.71
W	6.40×10^{10}	1.96×10^{8}	3.0	1.02×10^{14}	6.54×10^{9}	5.0	1.01×10^{6}	39.8	5.78

7.3.3 The Results of the Fatigue Assessment in Fine Mesh

According to ABS Rules, for those cases where an existing structure is being reused or converted, the basis of the fatigue assessment should be modified to reflect past service or previously accumulated fatigue damage. If D_p denotes the damage from past service, α is a factor to reflect the uncertainty with which the past service data are known, the 'unused fatigue damage', Δ_R, may be taken as:

$$\Delta_R = (1 - D_p \cdot \alpha) / FDF \tag{7.1}$$

Where, FDF is the fatigue design factor. According to the fatigue guide, for the critical structure details above water such as integral deck, FDF was taken as 3, while for the ordinary structure be 2; for the critical structure details in water or submerged such as column stabilized, FDF was taken as 5, while for the ordinary structure be 3. But the minimum Factor to be applied to uninspected 'critical' or uninspected 'ordinary' structure details is 10 or 5, respectively. In this assessment, the FDF was taken as 5.

For the uncertainty factor α, when the past service data are well documented, α may be taken as 1.0, otherwise a higher value should be used. So the assessment formula was taken as

$$D \le \Delta_R \tag{7.2}$$

Where,

D——cumulative fatigue damage

In this assessment, the uncertainty factor α was taken as 1.50 foe the past service data was not well documented. And the past service damage D_p was calculated from analysis,

$$D_p = (D / T_d) \cdot T_p \tag{7.3}$$

Where,

T_P——the past service life，taken as 31 accordance with the data；

T_d——design life，taken as 20 years。

Figure 7.29～7.38 will show the 10 joints' (CPL80、CPL110、CPL111、CPL113、CPL32、CPL33、CPL34、CL25、CL26、S306) RAOs under different wave direction and different frequency, and they are corresponding to the part 1 in Figure 7.25, part 3 in Figure 7.26 and part 8 in Figure 7.27.Other stress transfer function was list in **Appendix D.**

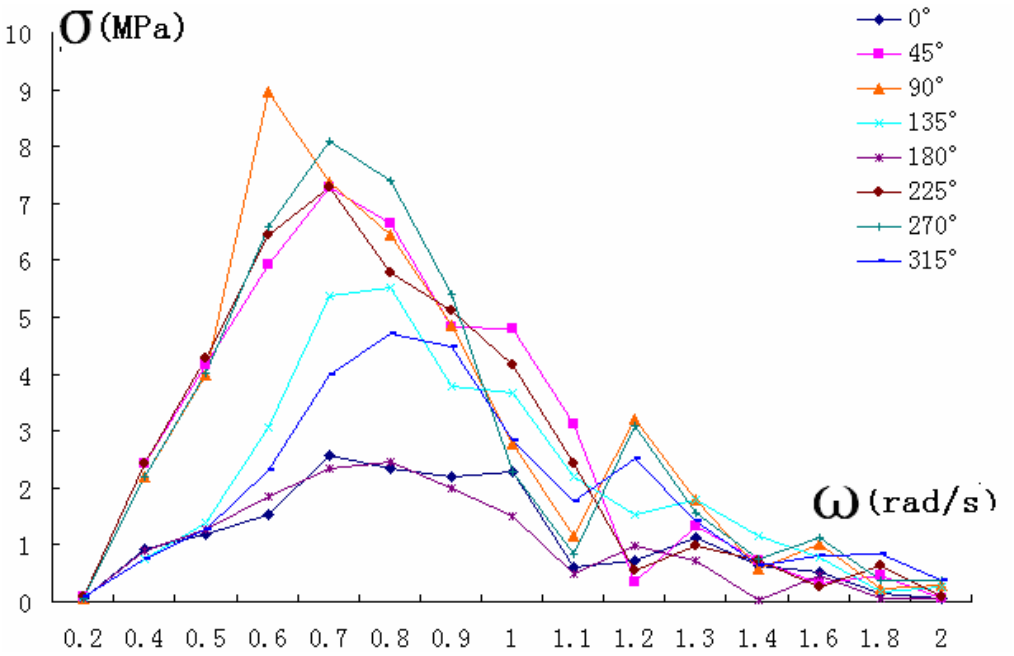

Figure 7.29 the stress transfer function of the calculated joint (CPL80)

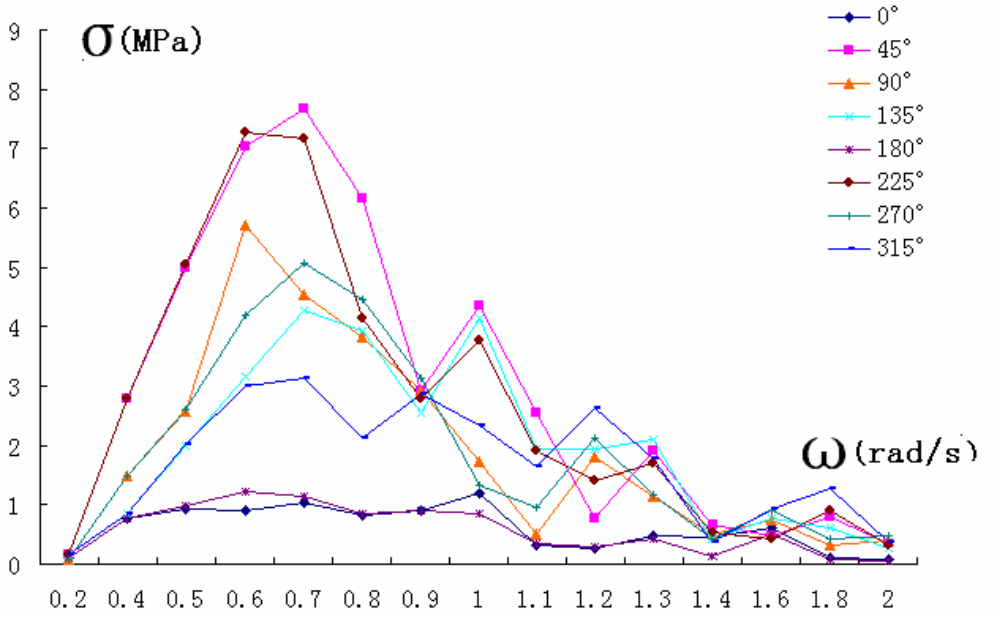

Figure 7.30 the stress transfer function of the calculated joint (CPL110)

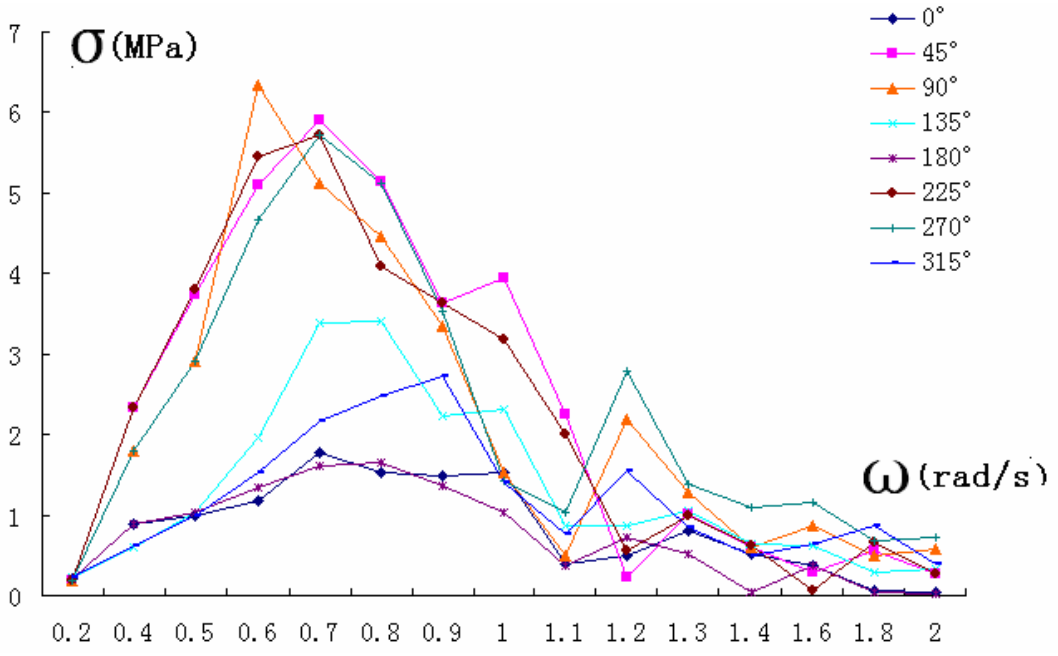

Figure 7.31 the stress transfer function of the calculated joint (CPL111)

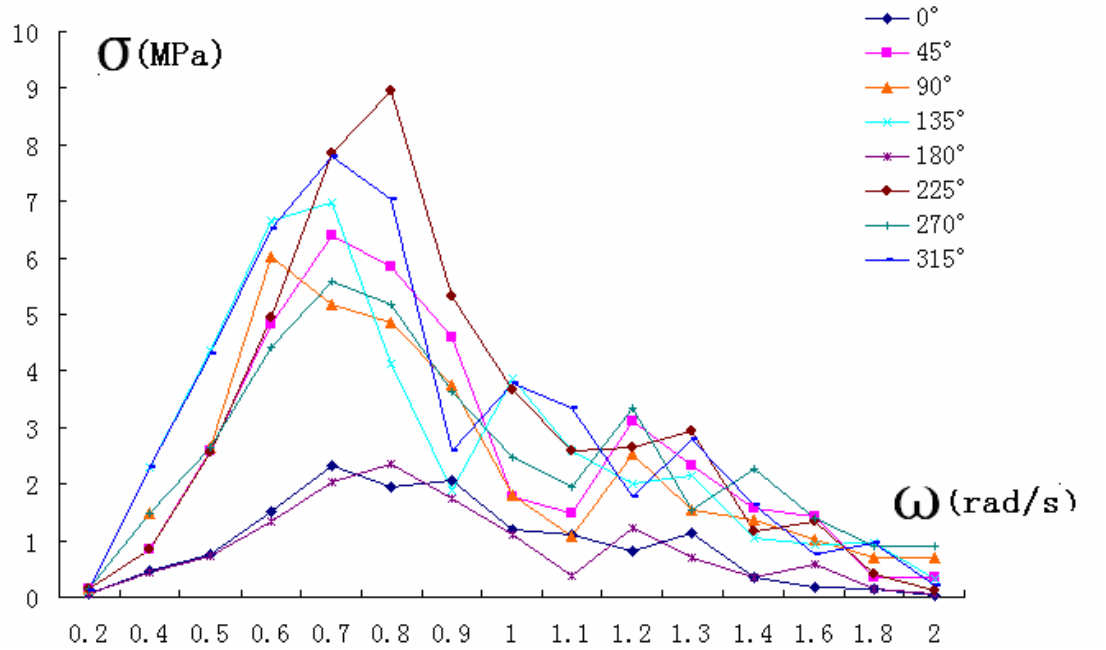

Figure 7.32 the stress transfer function of the calculated joint (CPL121)

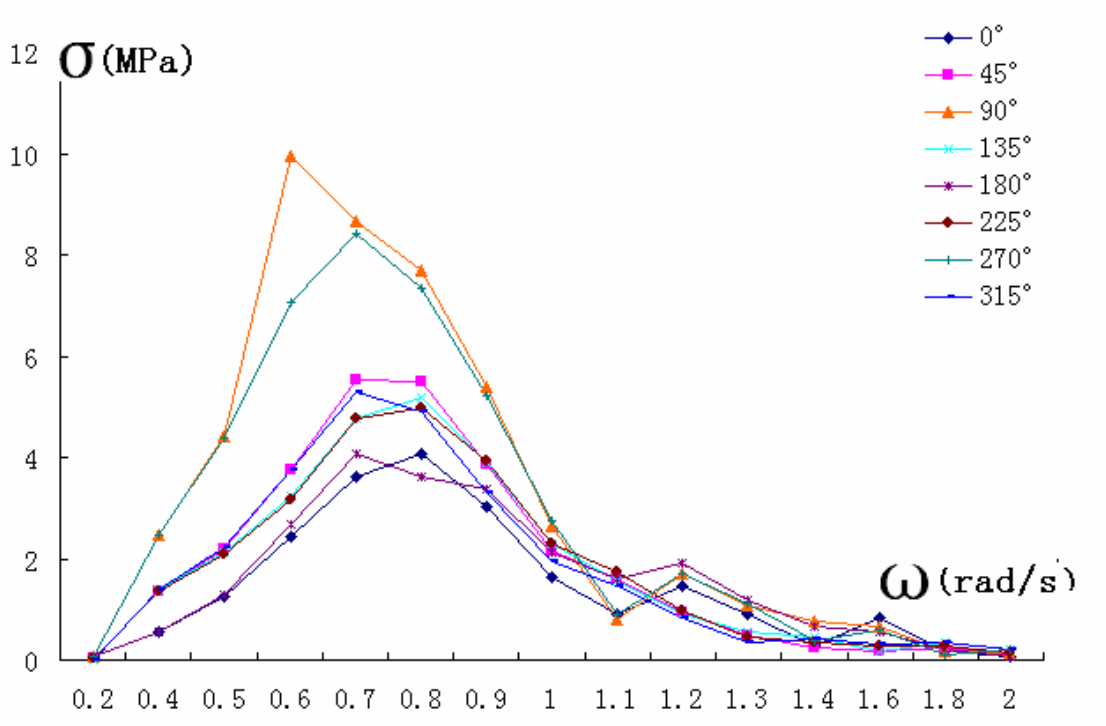

Figure 7.33 the stress transfer function of the calculated joint (CPL32)

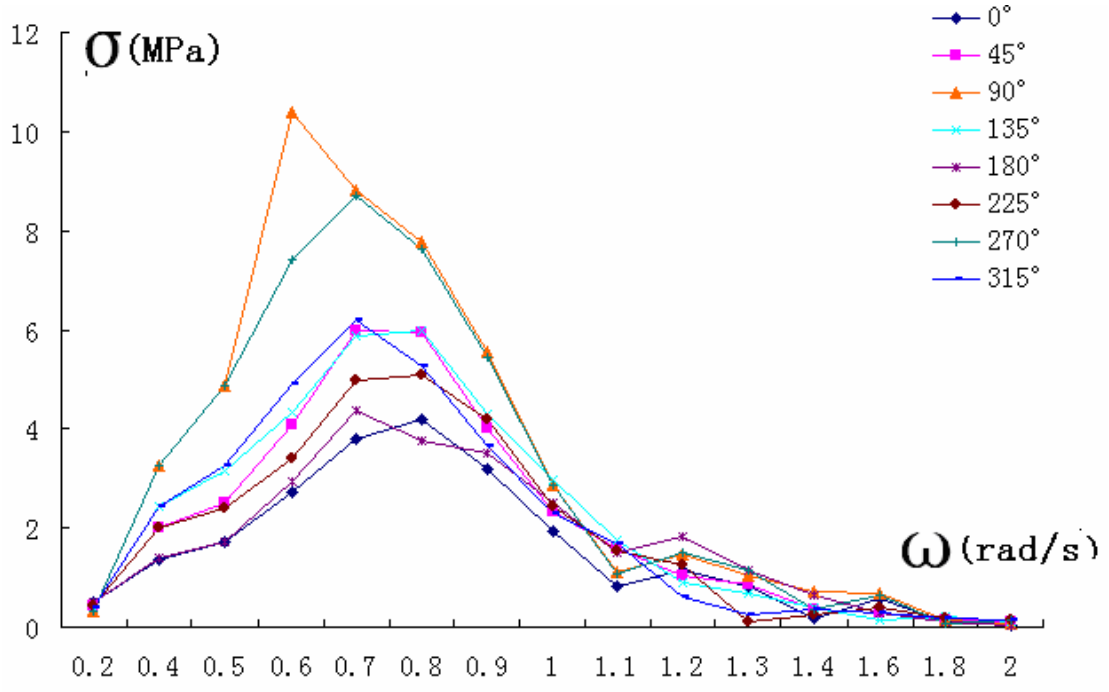

Figure 7.34 the stress transfer function of the calculated joint (CPL33)

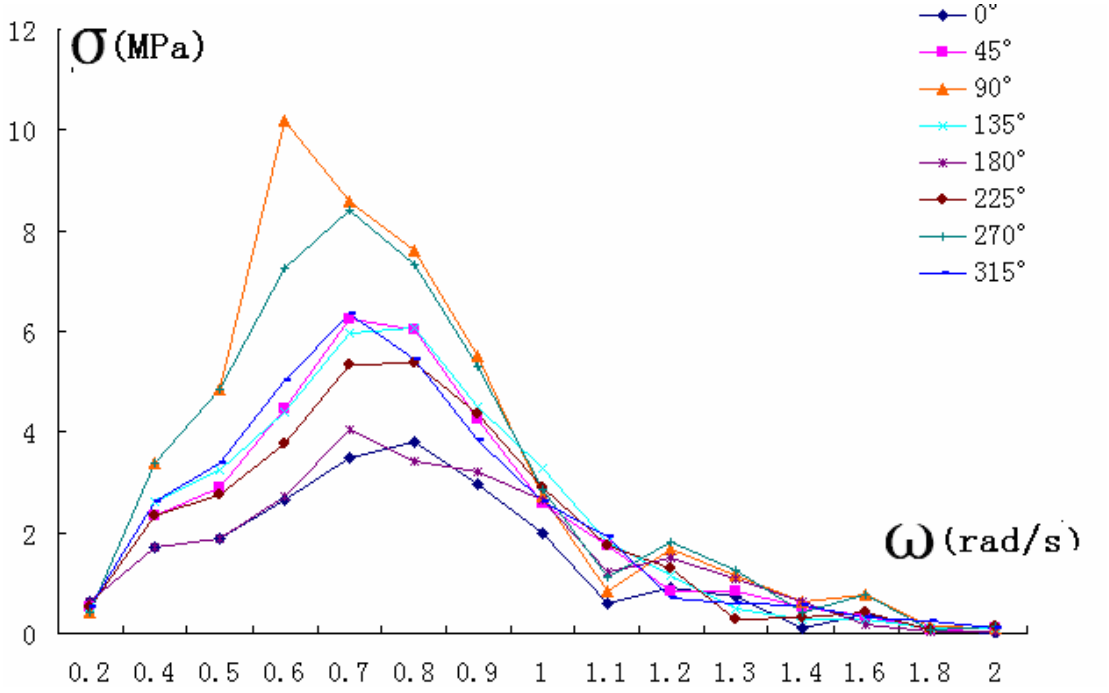

Figure 7.35 the stress transfer function of the calculated joint (CPL34)

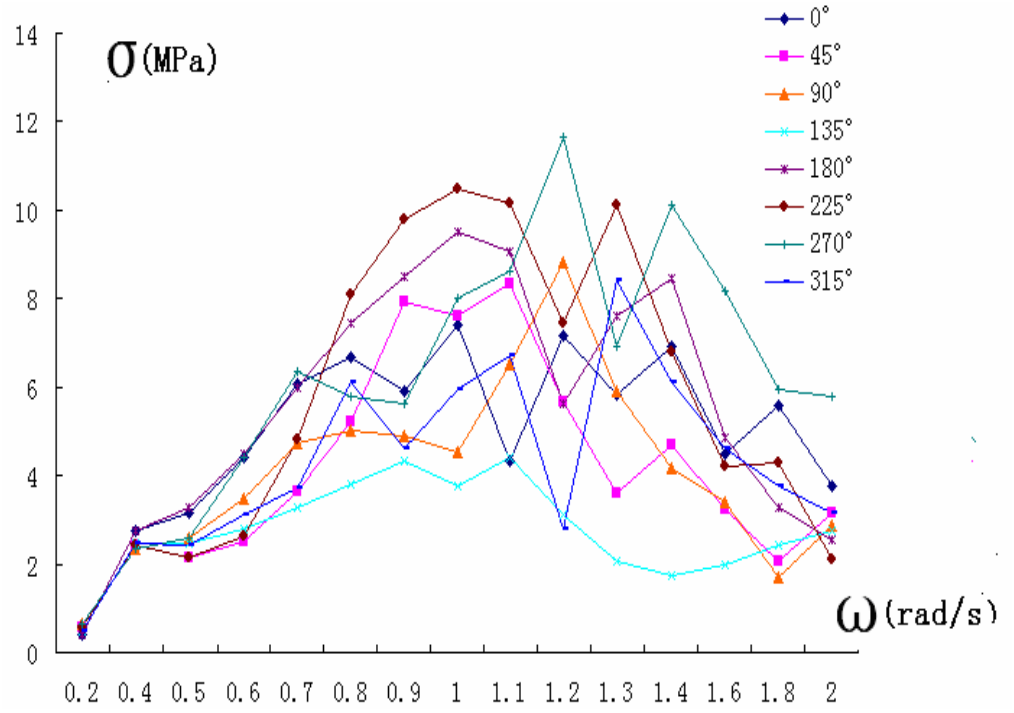

Figure 7.36 the stress transfer function of the calculated joint (CL25)

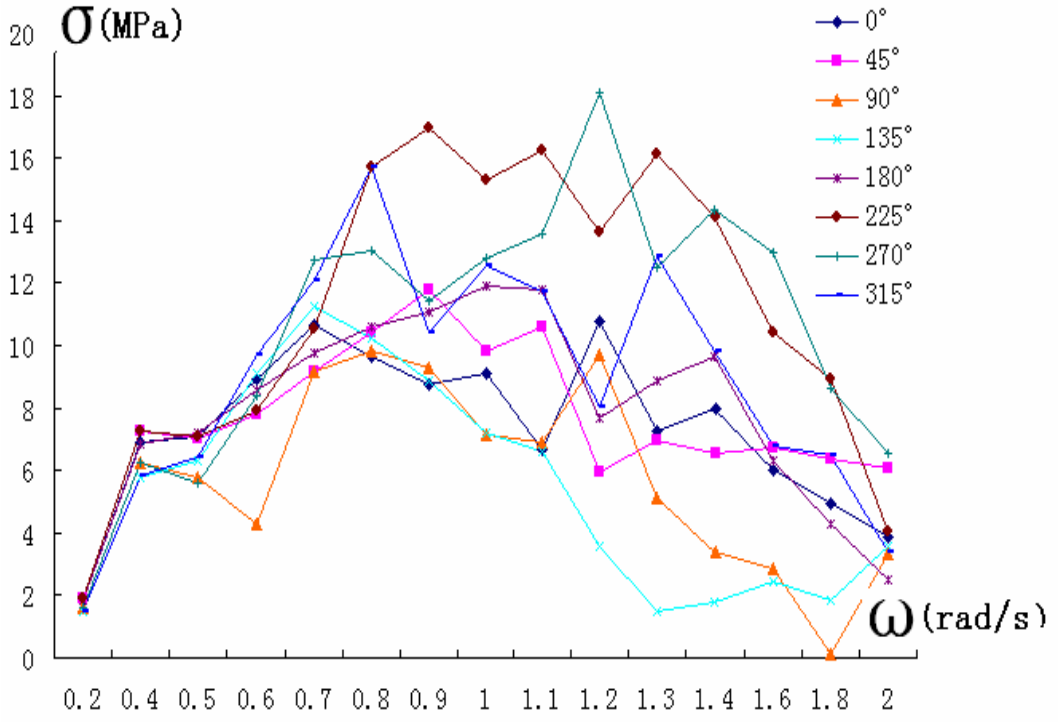

Figure 7.37 the stress transfer function of the calculated joint (CL26)

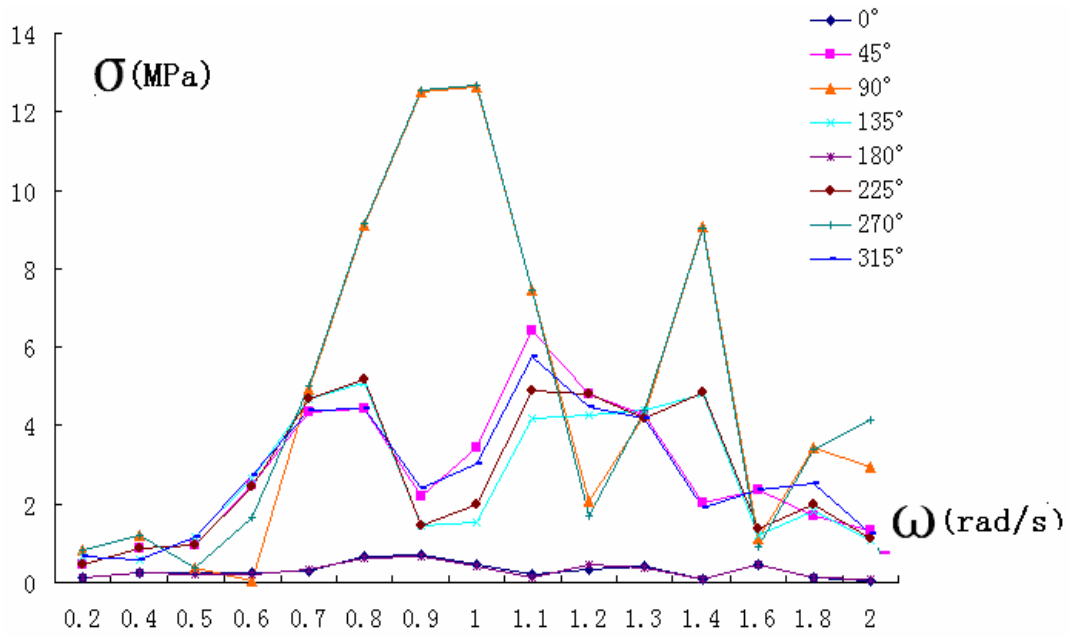

Figure 7.38 the stress transfer function of the calculated joint (S306)

The 10 joints' fatigue damage was calculated in term of the theoretic mentioned above. Due to differences of structures, the results are given respectively. The Table 7.3 is corresponding to the parts given by Figure 7.25, but the CPL121 is corresponding to the part given in Figure 7.27(the limit is 50 years); the Table 7.4 is corresponding to the parts given by Figure 7.26 (the limit is 50 years).

Table 7.3 fatigue accumulated damage of the dangerous joins

Location	Joints Number	Joints Name	Residual fatigue strength	Residual fatigue life (year)	Position of crack
For. cross pontoon (Figure7.14、7.17)	37142	CPL32	0.1114	11.7	1(Figure7.25)
For. cross pontoon (Figure7.14、7.18)	37702	CPL33	0.1639	42.2	3(Figure7.25)
			0.1638	42.1	5(Figure7.25)
For. cross pontoon (Figure7.14、7.19)	37700	CPL34	0.1066	10.6	1(Figure7.25)
			0.1595	36.6	3(Figure7.25)
			0.1591	36.1	5(Figure7.25)

Aft. Cross pontoon (Figure7. 4、7. 7)	76303	CPL80	0.1130	12.1	1(Figure7.25)
Aft. Cross pontoon (Figure7.8、7.11)	3064	CPL110	0.1760	68.1	1(Figure7.25)
Aft. Cross pontoon (Figure7.8、7.12)	2645	CPL111	0.1691	51.0	1(Figure7.25)
			0.1685	49.7	5(Figure7.25)
Aft. Cross pontoon (Figure7.8、7.13)	12338	CPL121	0.136	19.76	8(Figure7.27)
Girders in main deck (Figure7.1、7.3)	240678	S306	0.116	12.84	1(Figure7.25)

Table 7.3 fatigue accumulated damage of the dangerous joins

Location	Joints Number	Joints Name	Residual fatigue strength	Residual fatigue life (year)	Position of crack
Stiffener in A1 column (Figure7.14、7.17)	340574	CL25	0.1741	62.5	1(Figure7.26)
			0.1194	13.8	3(Figure7.26)
			0.1140	12.3	4(Figure7.26)
Stiffener in A1 column (Figure7.14、7.17)	340578	CL26	0.1254	15.6	2(Figure7.26)
			0.15	27.60	3(Figure7.26)
			0.1667	46.5	4(Figure7.26)

8 Conclusions and suggestions of fatigue assessment

The platform for this assessment has been using for 31 years. There are a lot of tubular joints, intersections between girders, nodes of angle plate perforating the bulkhead and so on. Under repeating loads, these nodes are easy to raise fatigue damage, so we do fatigue assessment for these nodes.

According to the results of fatigue assessment, it can be got that the fatigue lives of most nodes are relatively large; only some nodes' fatigue strength in local areas is relatively weak. These nodes are shown as below:

1）The connection between the stringer stiffener and the ring stiffener in For. Crosspontoon and the Aft. Crosspontoon (CPL33, CPL34, CPL94, CPL95), see Figure 8.1; the connection between the stringer stiffener and the ring stiffener in Aft. Cross pontoon and the Aft. Cross pontoon (CPL110, CPL111 and CPL53) and so on. Because the cross pontoons are used as ballast tank and eroded by sea water in service period, these accelerate the fatigue of the structures. Meanwhile, more attention should be paid to other nodes.

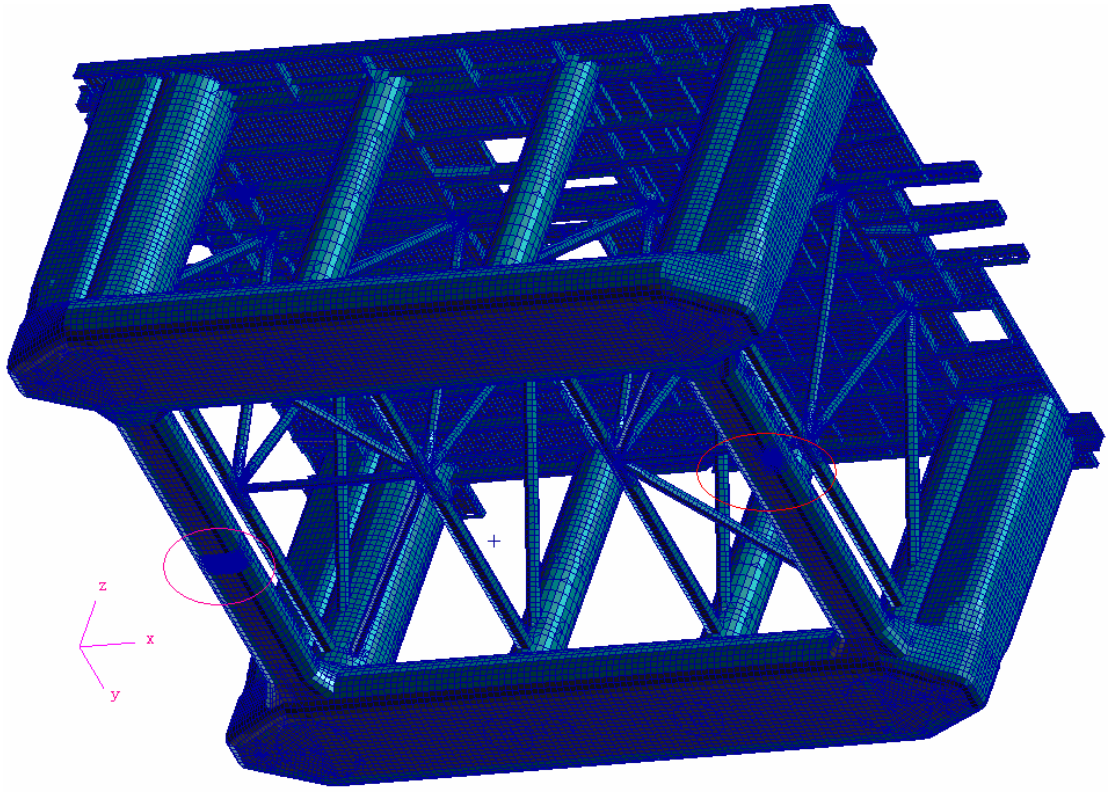

Figure 8.1 the location of the fatigue joints in crosspontoons

2）The joints in D1 and A1 columns (such as CL25,CL26,CL73), see Figure 8.2，because the rigidity of the local structure is relatively strong, the fatigue damage would be great. Therefore, new brackets should be added in order to reduce the stress concentration (see Figure 8.3). The same method can be used to the watertight bulkheads of the 4 corner columns (EL35’、EL51’—2(1/2）”、EL65’、EL100’, see Figure 8.4) in order to reduce the stress concentration.

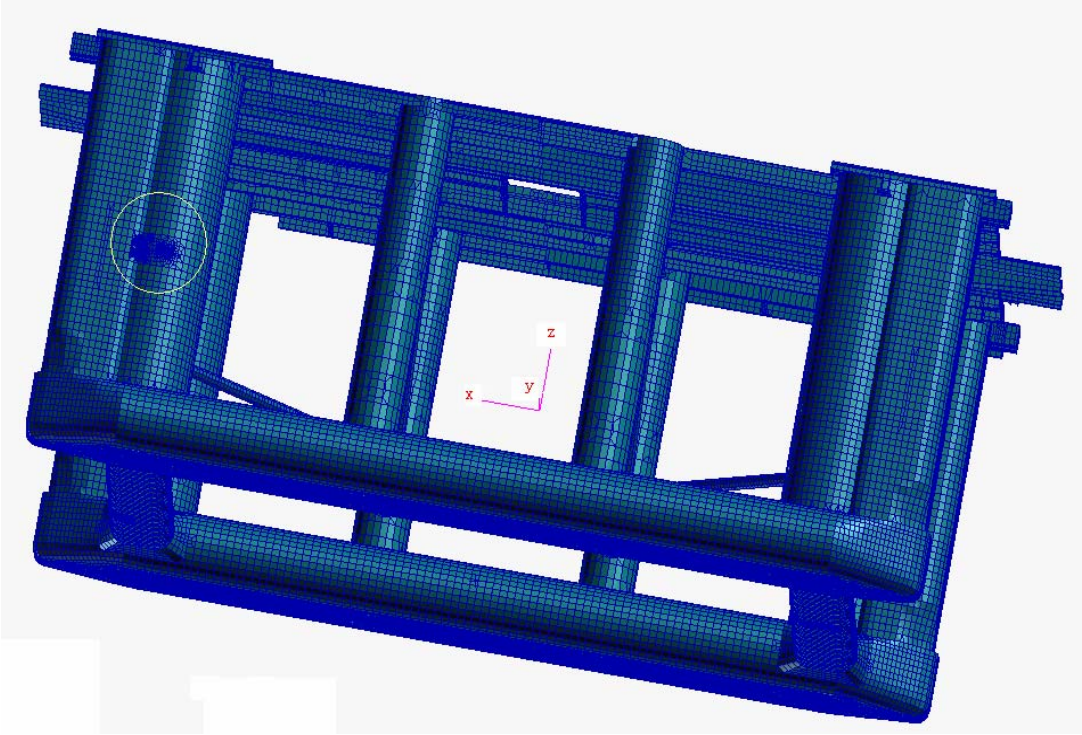

Figure 8.2 the location of the fatigue joints in columns

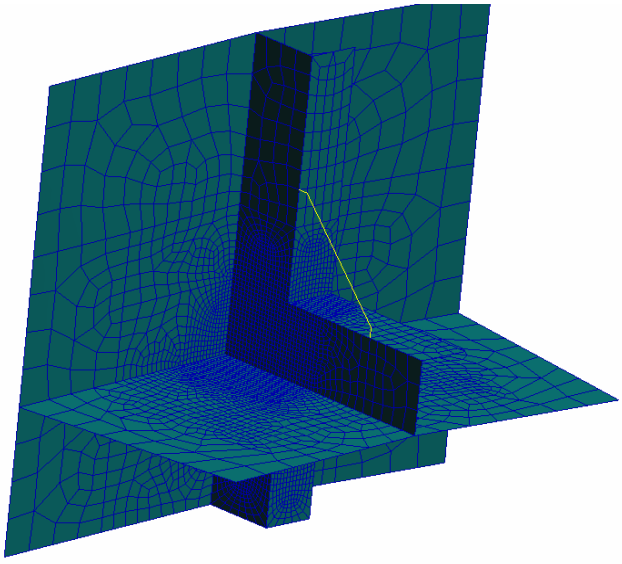

Figure 8.3 weld position of bracket and

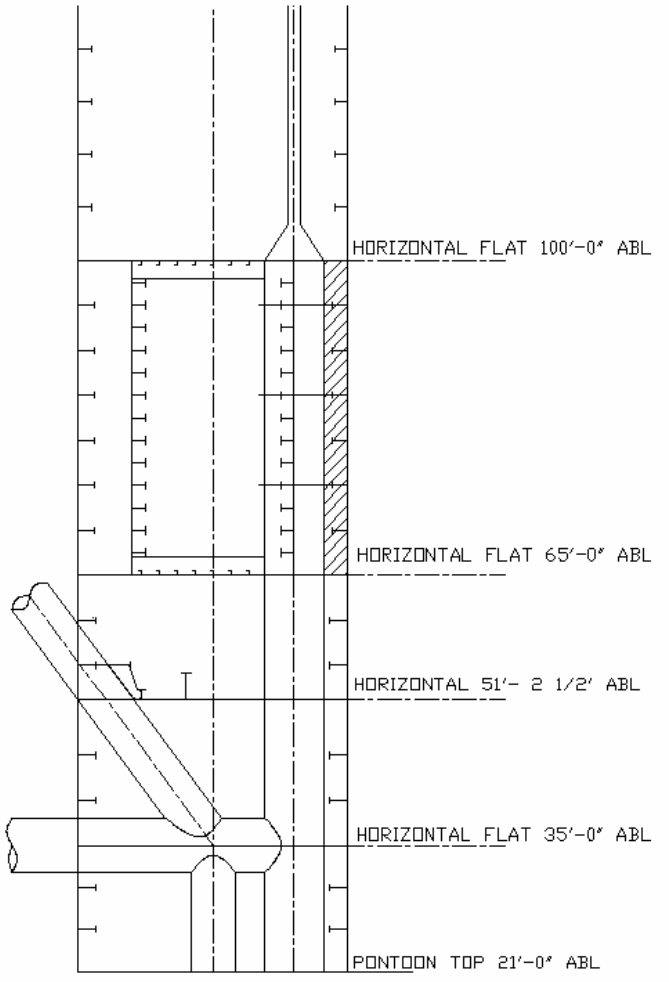

Figure 8.4 Figure of watertight bulkhead of corner columns

3）The structure at the connection between cross and longitudinal pontoon (see Figure 8.5 and 8.6) is complex, the stress concentration is distant and work in seawater, so the fatigue damage is relatively severe. The crack is likely to rise on the outside pontoon shell, so more attention should be paid.

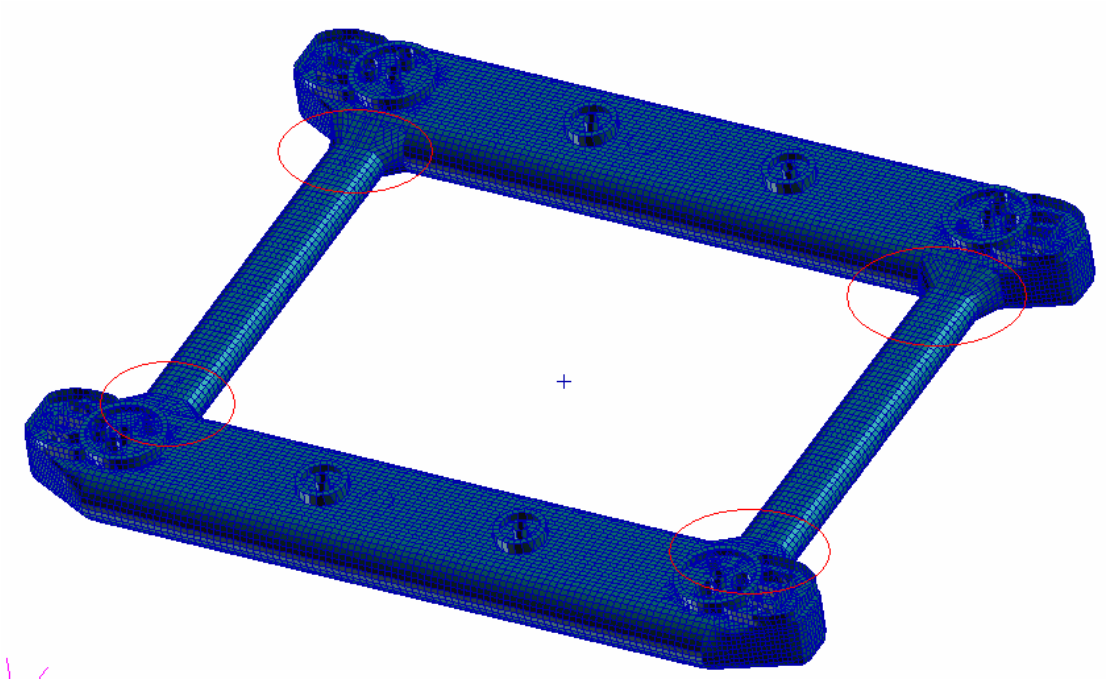

Figure 8.5 the location of fatigue joints in the connection between pontoon and crosspontoon

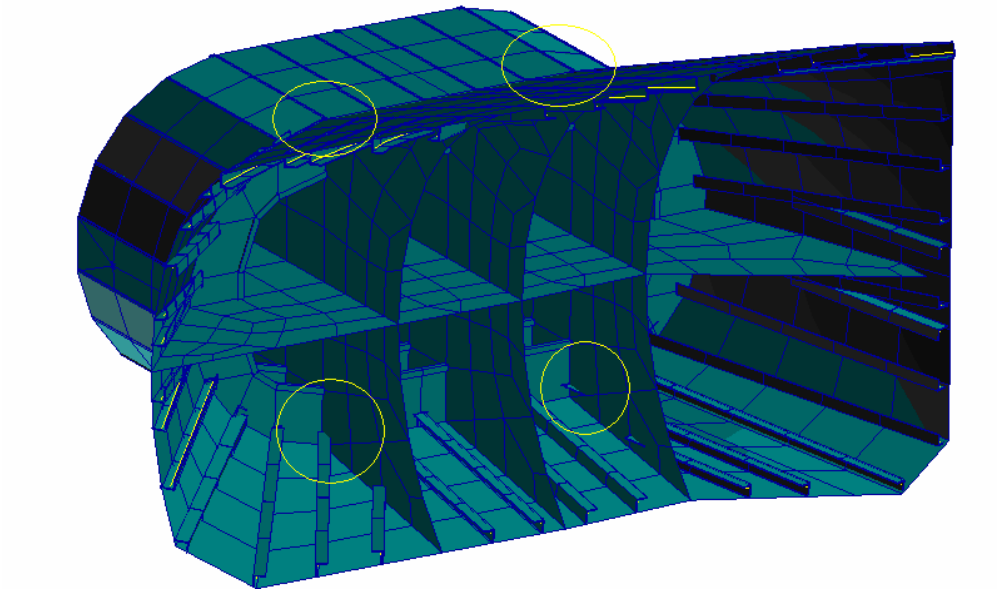

Figure 8.6 Figure of the connection of longitudinal pontoon

4）The stress concentration is distant at the connection between deck girders (see Figure 8.7), so the fatigue damage is relatively severe. Therefore, new brackets should be added in order to reduce the stress concentration (see Figure 8.8) and enhance the fatigue life. During service period, deck structure should be examined regularly.

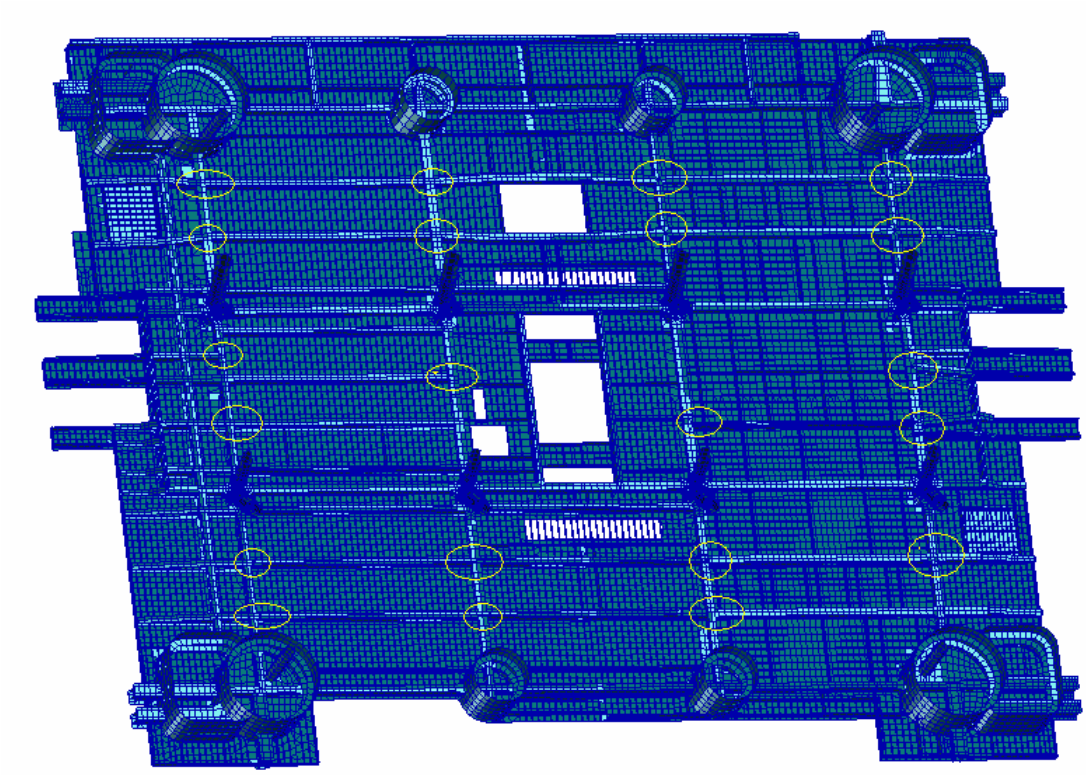

Figure 8.7 location of the connection between deck girders

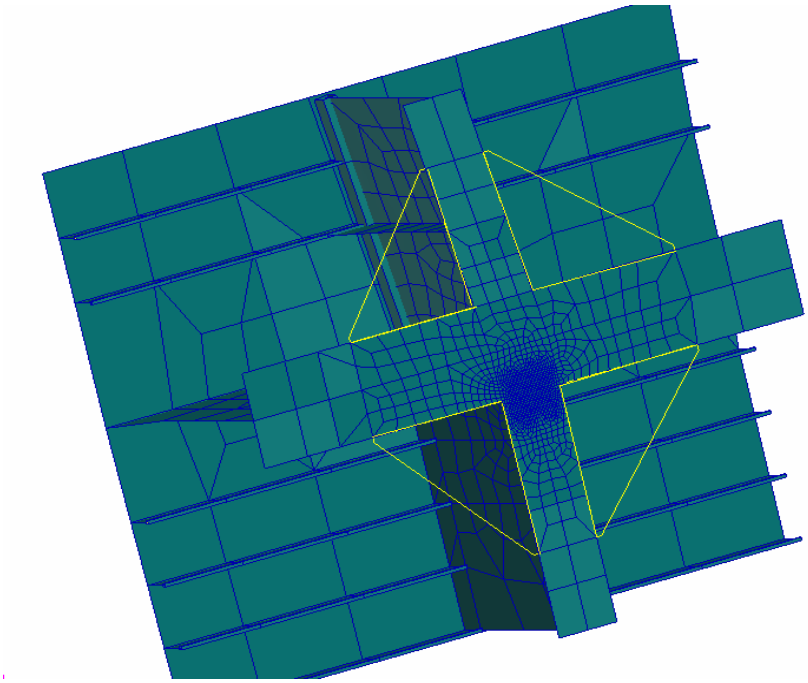

Figure 8.8 Figure of the connection of the deck girders

5）Because of using high strength steel(ABS_AH32) and enhancing the thickness (see Figure 8.9), so the stresses of tubular joints are relatively low. The fatigue performance of the tubular joints satisfies the requirement of the rules during the service life. But the attentions also should be paid to some tubular joints, because

these joints work in seawater.

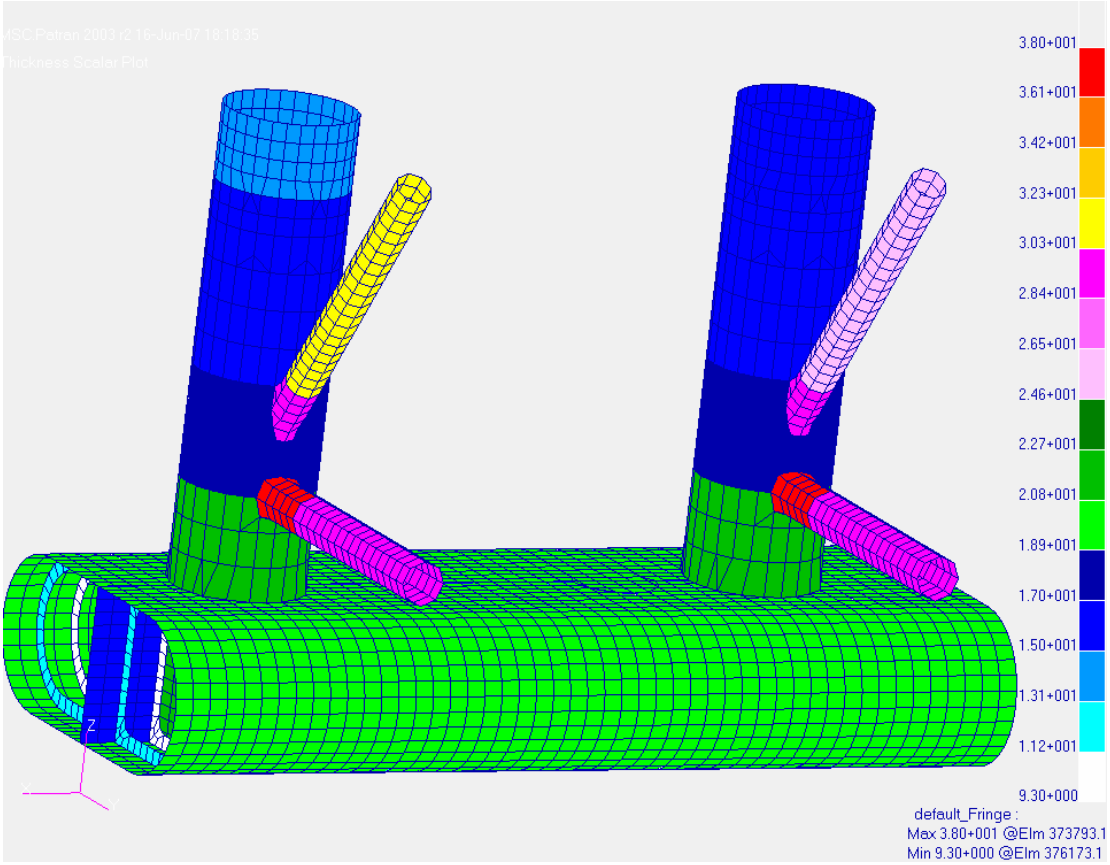

Figure 8.9 Figure of thickness of local area

In conclusion, it is deemed that the fatigue performance of the FPS structures can satisfy the requirement of the rules during the service life. It is necessary that more attention should be paid to these joints with shorter fatigue life in check.